Petroleum Systems and Geologic Assessment of Oil and Gas in the San Joaquin Basin Province, California

Chapter 8

Petroleum Systems Used to Determine the Assessment Units in the San Joaquin Basin Province, California

By Leslie B. Magoon, Paul G. Lillis, and Kenneth E. Peters

Contents

Introduction

For the San Joaquin Basin Province in California (fig. 8.1), six petroleum systems were identified, mapped, and described to provide the basis for the five total petroleum systems (TPS) and ten related assessment units (AU) used in the 2003 U.S. Geological Survey (USGS) National Oil and Gas Assessment (table 8.1; Gautier and others, 2004; Hosford Scheirer, 2007). The petroleum pools in the province were allocated to each petroleum system on the basis of (1) geochemical composition as described by Lillis and Magoon (this volume, chapter 9) and Lillis and others (this volume, chapter 10), (2) reservoir rock nomenclature (fig 8.2; appendix 8.1 and appendix 8.2) as described by Hosford Scheirer and Magoon (this volume, chapter 5), and (3) the volume of oil and gas discovered for each petroleum system by system, flank, and trap type (tables 8.2, 8.3 and 8.4). For this assessment, each petroleum system was determined, followed by the TPS from one or more petroleum systems. For example, the Miocene TPS includes two petroleum systems, the McLure-Tulare(!) and Antelope-Stevens(!) (notation described in Petroleum System Name section, below). Magoon and Schmoker (2000) describe how the TPS is used in this and the USGS world assessments. This chapter describes the six petroleum systems used to make five total petroleum systems in this San Joaquin Basin Province assessment.

The figures and tables for each petroleum system and TPS are as follows: (1) the San Joaquin(?) petroleum system or the Neogene Nonassociated Gas TPS is a natural gas system in the southeast part of the province (figs. 8.3 through 8.8; table 8.5; this volume, chapter 22); (2) the Miocene TPS (this volume, chapters 13, 14, 15, 16, and 17) includes the McLure-Tulare(!) petroleum system north of the Bakersfield Arch (figs. 8.9 through 8.13; table 8.6), and the Antelope-Stevens(!) petroleum system south of the arch (figs. 8.14 through 8.18; table 8.7), and is summarized in figure 8.19; (3) the Eocene TPS (this volume, chapters 18 and 19) combines two petroleum systems, the Tumey-Temblor(.) covering much of the province (figs. 8.20 through 8.24; table 8.8) and the underlying Kreyenhagen-Temblor(!) (figs. 8.25 through 8.29: table 8.9), and is summarized in figure 8.30; (4) the Eocene-Miocene Composite TPS, formed by combining the Miocene and Eocene TPS (this volume, chapter 20); and (5) the Moreno-Nortonville(.) is both a petroleum

system and a TPS consisting mainly of natural gas in the northern part of the province (figs. 8.31 through 8.36: table 8.10; this volume, chapter 21). Oil samples with geochemistry from surface seeps and wells used to map these petroleum systems are listed in table 8.11. Finally, the volume of oil and gas expelled by each pod of active source rock was calculated and compared with the discovered hydrocarbons in each petroleum system (figs. 8.37 through 8.39; tables 8.12 and 8.13).

Method

A petroleum system is the hydrocarbon fluid system that occurs when the essential elements and processes work together to form oil and gas shows, seeps, or accumulations (Magoon and Dow, 1994; Magoon, 2004). The essential elements include the source, reservoir, seal, and overburden rocks that work with the processes of trap formation and generation-migration-accumulation that concentrate migrating petroleum. How petroleum systems were identified, mapped, and named in the San Joaquin Basin Province is described as follows.

Oil-to-oil and to a lesser extent, gas-to-gas, correlations based on geochemical parameters separate the oil and gas samples into distinctive groups. The oil groups are discussed in Lillis and Magoon (this volume, chapter 9) and the gas groups are discussed in Lillis and others (this volume, chapter 10). These groups provide the basis for allocating the oil or gas in a pool to one of five source-rock units: Antelope shale of Graham and Williams (1985; hereafter referred to as Antelope shale), McLure Shale Member of the Monterey Formation, Tumey formation of Atwill (1935; hereafter referred to as Tumey formation), Kreyenhagen Formation, and Moreno Formation. The name, location, and fluid volume for the oil or gas pools to which these petroleum accumulations are allocated came from information provided in appendix 8.1 by publications of the California Department of Conservation, Division of Oil, Gas, and Geothermal Resources (CDOGGR) (1998, 2001a, b). The reservoir rock names used to sort the many producing horizons in appendix 8.2 are from Hosford Scheirer and Magoon (this volume, chapter 5). The geographic distribution, present-day burial depth, and geochemical data for each source rock are discussed by Peters, Magoon, Valin, and Lillis (this volume, chapter 11). The source rock distribution, thickness, and time of thermal maturity are discussed by Peters, Magoon, Lampe, and others (this volume, chapter 12). Our chapter integrates information from chapters 9 through 12 using five figures and a table for each petroleum system as described below.

Petroleum System Name

The petroleum system name includes the source rock and major reservoir rock followed by the level of certainty (Magoon and Dow, 1994), such as McLure-Tulare(!). The existence of petroleum is proof of a system, and it is named according to the convention of Magoon and Dow (1994) and Magoon (2004). If the source rock and the reservoir rock are the same unit, then only one stratigraphic unit is used in the name, such as San Joaquin(?). The level of certainty indicates the confidence that a particular oil or gas type originated from the presumed pod of active source rock. Three levels of certainty are: speculative (?), hypothetical (.), and known (!).

Petroleum System Map

A petroleum system map shows the geographic distribution and burial depth of the source rock unit, pod of active source rock, petroleum accumulations and seeps attributed to that pod, and geographic extent of the system (for example, fig. 8.3). The location of the cross section and burial history chart, described below, are shown. The distribution and thickness of each source rock unit come from maps constructed using well control on regional cross sections and outcrop information, as described in Peters, Magoon, Valin, and Lillis (this volume, chapter 11). The richness of the source rock units is derived from Rock-Eval pyrolysis and total organic carbon (TOC) data, also described in Peters, Magoon, Valin, and Lillis (this volume, chapter 11). The pod of active source rock is determined by modeling the burial history of the source rock, as discussed in Peters, Magoon, Lampe, and others (this volume, chapter 12).

The pod of active source rock is shown on the petroleum system map contoured as four zones of thermal maturity relative to vitrinite reflectance (%R_o): <0.6%R_o is immature or lacks petroleum expulsion; 0.6 to 0.9%R_o is mature and expelled half of its petroleum; 0.9 to 1.2%R_o is mature and expelled the other half of its petroleum; and >1.2%R_o is overmature and the source rock is depleted. The map also shows petroleum accumulations or pools as solid-colored polygons where geochemistry indicates that the oil and/or gas came from the pod of active source rock; these polygons are outlined but not colored where stratigraphic evidence merely suggests that the oil and gas came from the same pod of active source rock. The locations of oil samples from seeps and exploratory wells are included on some petroleum system maps.

Petroleum System Stratigraphic Section

The stratigraphic section for the San Joaquin Basin Province is described in Hosford Scheirer and Magoon (this volume, chapter 5). The petroleum system stratigraphic section shows the stratigraphic relation of each rock unit in the north, central, or south region of the basin (for example, fig. 8.4). The allocation of each producing zone to a reservoir rock is listed in appendix 8.2. The reservoir rock units that contain oil (green) or gas (red) in the petroleum system are shown, as well as the source rock that expelled the hydrocarbons. A rectangle outlines the stratigraphic section of interest.

Petroleum System Cross Section

The petroleum system cross section transects the pod of active source rock at its greatest burial depth, includes the largest accumulations, and the geographic and stratigraphic extent of the system (for example, fig. 8.5). The cross section shows the petroleum window, or the thermal maturity of the source rock, and the fields or accumulations of oil (green) or gas (red) along this transect in their proper stratigraphic interval. This cross section is a present-day, two-dimensional (2D) extract from the San Joaquin Basin four-dimensional (4D) model as described by Peters, Magoon, Lampe, and others (this volume, chapter 12). The number of stratigraphic units shown in the cross section are reduced from the more detailed stratigraphic section to show more easily the relation of the accumulations to the pod of active source rock.

Burial History Chart

Using the rate of deposition and thickness of the overburden rock, the burial history chart provides the temporal basis for the expulsion of petroleum from the source rock (for example, fig. 8.6). The chart represents a one-dimensional (1D) burial and thermal history of the source rock from deposition to its greatest burial depth and is used to determine the time and depth of thermal maturity of the source rock as it passes through the petroleum window. The chart is a 1D extraction taken from the San Joaquin Basin 4D model as described by Peters, Magoon, Lampe, and others (this volume, chapter 12); the location of the extraction is shown on the corresponding petroleum system map. The burial history chart also includes the reservoir and seal rocks.

Events Chart

An events chart summarizes the time for the deposition of the essential elements, such as the source, reservoir, seal, and overburden rocks, and the processes, such as the generation-migration-accumulation of petroleum and trap formation (for example, fig. 8.7; Magoon and Dow, 1994). Also included are the preservation time and critical moment. The nomenclature and age of the rock units comes from Hosford Scheirer and Magoon (this volume, chapter 5), and is used according to the San Joaquin Basin 4D model from Peters, Magoon, Lampe, and others (this volume, chapter 12).

Table of Oil and Gas Volumes

Each petroleum system includes a table that summarizes oil and gas volumes by reservoir rock. This and other tables come from appendix 8.1, which is a compilation of information from several references (CDOGGR, 1998; 2001a; Hosford Scheirer and Magoon, this volume, chapter 5; Lillis and Magoon, this volume, chapter 9; Lillis and others, this volume, chapter 10). This table provides the basis for placing each pool in the six petroleum systems (columns 1 and 2). Columns 7, 11, 12, 13, and 14 are from the California oil and gas field sheets (CDOGGR, 1998). Columns 6 and 8 are the authors' assignments, and columns 9 and 10 are from appendix 8.2. The year 2000 production and reserve data in columns 15 through 20 originate from the Annual Report of the California Division of Oil, Gas, and Geothermal Resources (CDOGGR, 2001a). The oil and gas sample numbers in columns 21 and 22 are from Lillis and Magoon (this volume, chapter 9) and Lillis and others (this volume, chapter 10), respectively.

The authors compiled the last column (23) of appendix 8.1 using the production information and geochemical results from the oil and gas samples. In this column, italic text indicates that the authors interpreted the source rock of the hydrocarbons based on stratigraphic occurrence and location of the pool, whereas plain text indicates a confirmed source rock-hydrocarbon correlation. Where the source rock designation is underlain by a colored rectangle, the oil or gas data were used to indicate its origin. Where only the gas sample number (column 22) but not the source rock name (column 23) is underlain by a colored rectangle, the source rock is based on the following criteria: (1) if the gas is thermogenic in origin and oil also occurs in the pool, then the source rock is based on stratigraphic occurrence and location of the pool; (2) if no oil occurs in the pool, then no source rock can be designated, and the gas can only be classified as thermogenic or biogenic. Tables 8.2 through 8.10 are extracted from appendix 8.1.

The table of oil and gas volumes for each petroleum system is constructed by summing the pools with the same reservoir rock (tables 8.5 through 8.10). The sum of the reservoir rock volumes indicates the size of the petroleum system. The table also shows the complexity of migration paths and reservoir rock that contains the majority of the petroleum. This reservoir rock is used in the petroleum system name. For a given petroleum system, the complexity of a migration path is considered simple when only one reservoir rock is charged with hydrocarbons, whereas it is considered as complex when many reservoir rocks are charged, as is the case for all the San Joaquin Basin petroleum systems.

Regional Setting

The stratigraphic and structural histories of the San Joaquin Basin Province help to determine the evolution and occurrence of each petroleum system. The regional geology is detailed in other chapters and references therein and will not be repeated here (Gautier and others, this volume, chapter 2; Hosford Scheirer and Magoon, this volume, chapter 5; Johnson and Graham, this volume, chapter 6). Regional features that significantly influenced the occurrence of petroleum in

particular areas are summarized (fig. 8.1). The nomenclature for the two depocenters, Buttonwillow and Tejon, come from Ziegler and Spotts (1978). The importance of the Sierra Nevada Batholith that both underlies and borders the east flank of the basin cannot be underestimated—the batholith is the sediment source for quartz-rich, good quality, reservoir rocks; it provides a rigid container for sediments entering from the east; and has low structural dip. It also acts as a buttress for the fold belt on the west flank where the largest oil fields are located.

The bulk of the sedimentation in this basin occurred in a forearc basin prior to the development of the San Andreas Fault in Miocene time. The pre-Miocene section thickens from the Stockton Arch in the northwest to the Tejon depocenter in the southeast, and from the Sierra Nevada Batholith in the northeast to the San Andreas Fault in the southwest. During this time the source rock, reservoir rock, and seal rock were deposited for three petroleum systems. During Miocene time the sedimentary thickness significantly increased in the Buttonwillow and Tejon depocenters and is the time of deposition for the source rock, reservoir rock, and seal rock for the two largest petroleum systems. From Miocene time, tectonic activity associated with movement along the San Andreas Fault created the fold belt on the southwest flank of the basin. From Pliocene time, the greatest thickness of the overburden rock was deposited for all six petroleum systems, especially in the Buttonwillow and Tejon depocenters.

Other areas and structural features referred to in this chapter are as follows (and shown in fig. 8.1). The areas surrounding Chowchilla and Riverdale fields are dominated by gas and oil fields, respectively. The Coalinga Nose is a prominent anticline that plunges to the southeast into the Buttonwillow depocenter and is the focus for migrating petroleum in several important oil fields along its axis. The Pleasant Valley Syncline plunges to the southeast into the Buttonwillow depocenter where the overburden rock is sufficient to thermally mature source rocks. The petroleum generated in the syncline migrated updip into the Coalinga Nose to the northwest, and the fold belt to the southwest.

The volume of oil and gas is markedly different on each basin flank (table 8.3). The west flank traps accumulated 10.6 billion barrels of oil (Gbo), which is almost three times the 4 Gbo in the east flank traps. Proportionally more gas was trapped in the west flank traps (15.9 trillion cubic feet of gas, tcfg) than the east flank traps (2.9 tcfg). Converting gas to barrels of oil equivalent using the relationship of 6,000 cubic feet of gas per barrel of oil, there is still three times more petroleum in the west than in the east flank traps. The number of pools or traps, and whether they trap hydrocarbons primarily structurally or stratigraphically, is given in table 8.4. The west flank is structurally more deformed than the east flank, suggesting that structural traps would be concentrated on the west flank and stratigraphic traps on the east flank. However, our compilation of trap type (appendix 8.1) indicates that a similar percentage of both trap types occurs on each flank, with slightly more structural traps on the west flank (9 percent) than stratigraphic traps on the east flank (7 percent). There are 99 more traps on the west flank (351 traps) than on the east flank (252 traps). In addition, the gas-to-oil ratio (GOR) is two times higher in the west flank traps (table 8.3). This pattern indicates more favorable conditions to trap and retain petroleum on the west flank than the east flank of the San Joaquin Basin Province.

San Joaquin(?) Petroleum System

The San Joaquin(?) is a small petroleum system with an estimated ultimate recovery of 368 billion ft^3 of microbial gas, which represents 2 percent of the natural gas in this basin, or 0.3 percent of the petroleum (table 8.2). The geochemical parameters that indicate biogenic gas are dry hydrocarbn gas composition (100 percent methane) with a methane carbon isotopic composition less than -55 per mil (Lillis and others, this volume, chapter 10). Excluding the noncommercial Los Lobos pool, all commercial gas pools are located on the basin axis (Paloma gas pool), or the east flank (fig. 8.3, table 8.3). Discovered gas pools include 23 structural and 5 stratigraphic traps (appendix 8.1, table 8.4). Seal rock types are fine-grained, low-permeability claystone, mudstone, and tightly cemented sandstone. Depths of discovered accumulations range from less than 1,100 ft to 9,740 ft in the central basin (appendix 8.1). Individual reservoir rocks are mostly less than 30 ft thick (appendix 8.1).

Four accumulations in the Trico, Semitropic, Buttonwillow, and Paloma fields have methane carbon isotopic compositions typical of biogenic gas accumulations so are shown as solid red in figure 8.3. The remaining accumulations are classified as biogenic gas based on the lack of associated liquids and their occurrence in Pliocene and younger rock units (fig. 8.4; table 8.5). Eighty-four percent of this gas occurs in the San Joaquin Formation (table 8.5). The biogenic gas is judged to originate from organic matter in thick Pliocene marine mudstone and claystone that surrounds reservoir quality sandstones (figs. 8.4 and 8.5). Rock-Eval pyrolysis and TOC data are lacking from this interval so the geographic extent of this petroleum system is defined by its accumulations (figs. 8.3 and 8.5).

Occurrences of "dry gas" zones are reported ("dg" in CDOGGR, 2001a) in some oil fields in the Pliocene section outside the geographic extent of the San Joaquin(?) petroleum system, such as at Elk Hills and Buena Vista oil fields. Geochemical analysis of three gas samples (samples 12, 28, and 29 in Lillis and others, this volume, chapter 10) from these zones indicate their origin is thermogenic rather than biogenic—sample 12 is thermogenic and wet, sample 28 is thermogenic and dry, and sample 29 is a mixture of thermogenic dry and biogenic gas. This thermal gas is interpreted to have migrated through the semipermeable seal rock of the underlying oil pool into the overlying reservoir rock that may or may not contain some biogenic gas. Unless the gas accumulations were all

biogenic or interpreted to be biogenic, we did not include them in this petroleum system.

Trap development and gas charge is judged to have occurred near the time of deposition based on the age of the rocks involved and because microbes create methane at low temperatures (figs. 8.6 and 8.7). Biogenic or marsh gas forms from organic matter at low temperatures by microbial action at the surface to a depth of few thousand feet. Typically this gas vents to the atmosphere, but under certain conditions it becomes trapped in sand lenses that become sealed by mudstone and buried to greater depths. Burial can improve seal integrity and increase the pressure of the entrapped gas, setting the stage for a commercial accumulation. Structural traps formed after middle Pliocene time. During this time, burial compacted fine-grained capping beds, gentle folds began to form, and regional southwestward tilting occurred. The events chart summarizes the deposition and timing of the essential elements of the petroleum system (fig. 8.7)

Neogene Nonassociated Gas Total Petroleum System

The Neogene Nonassociated Gas Total Petroleum System includes the San Joaquin(?) petroleum system and the prospective Pliocene section that presently lacks discovered accumulations (fig. 8.8; table 8.1). The maximum extent and geologic rational for the Neogene Nonassociated TPS, including the Neogene Nonassociated Gas Assessment Unit (AU50100501), are discussed by Hosford Scheirer and Magoon (this volume, chapter 22) and the numeric and graphical data are discussed by Klett and Le (this volume, chapter 28).

McLure-Tulare(!) Petroleum System

The McLure-Tulare(!) is a significant petroleum system with an estimated ultimate recovery of 2.9 billion barrels of oil equivalent (Gboe), which represents 16.4 percent of the oil and gas in this basin (table 8.2). This petroleum system is located north of the Bakersfield Arch and straddles the northwest-southeast oriented basin axis (fig. 8.9). The source rock is the McLure Shale Member of the Monterey Formation, as described in Hosford Scheirer and Magoon (this volume, chapter 5, fig. 5.55) and whose source rock distribution and geochemical properties are characterized for the Antelope shale in Peters, Magoon, Valin, and Lillis (this volume, chapter 11). The McLure and Antelope source rock names are used to the north and south of the Bakersfield Arch, respectively, to distinguish two petroleum systems, each with their own pod of active source rock. The reservoir rock name, Tulare, is used because 51 percent of the petroleum occurs in the Tulare Formation (table 8.6). The level of certainty is known, or (!), because there is a positive geochemical correlation between the oil and McLure Shale source rock (Lillis and Magoon, this volume, chapter 9).

The crest of the Bakersfield Arch separates accumulations in the McLure-Tulare(!) petroleum system in the north from accumulations in the Antelope-Stevens(!) petroleum system in the south because of its persistence from Paleocene or late Eocene time (MacPherson, 1978). Migrating oil and gas were unable to migrate across this crest. The McLure-Tulare(!) is defined as an oil-prone system because the GOR (692 ft^3 gas per barrel of oil; table 8.2) of accumulations in the petroleum system is less than the 20,000 ft^3 gas per barrel of oil criterion defined by Klett and others (this volume, chapter 25).

The pod of active source rock for the McLure-Tulare(!) petroleum system is coincident with the Buttonwillow depocenter and the Pleasant Valley Syncline. Comparing the 14,000 ft burial depth contour of the source rock with the 0.6%R_o contour for vitrinite reflectance indicates that the northwest part of the pod has been uplifted by about 2,000 ft (fig. 8.9). The largest accumulations are located near the deepest part of the source rock, or in excess of 22,000 ft. In decreasing volumes, the four largest fields are South Belridge (1,237 million barrels of oil; MMbo), Cymric, (471 MMbo), Lost Hills located on the Coalinga Nose (425 MMbo), and McKittrick (271 MMbo). Except for Lost Hills field, these fields are southwest of the Coalinga Nose on the west flank of the basin, which contains almost 3 Gboe compared to the east flank, which contains about 13 million barrels of oil equivalent (MMboe; table 8.3). On the west flank there are 70 structural and 21 stratigraphic traps, in contrast to only 6 structural traps on the east flank (table 8.4). Zumberge and others (2005) show that the oil at the west end of the Elk Hills field originated from the McLure Shale in the north. East flank stratigraphic traps are the result of a phase change in diatomaceous shale from non-reservoir opal-CT phase to a quartz phase reservoir-rock, as in the Rose and North Shafter oil fields (Sterling and others, 2003).

The large number of reservoir rocks (8) involved in moving petroleum from the pod of active source rock to traps indicates that migration paths are complex (figs. 8.10 and 8.11; table 8.6). All petroleum is found in eight reservoir rocks that range in age from 33.5 Ma to as young as 0.6 Ma, but 91 percent of the oil and gas is in reservoir rocks younger than 6.5 Ma. Only 5.1 percent of the petroleum is contained in the Stevens sand of Eckis (1940; hereafter referred to as Stevens sand) on the Bakersfield Arch. Most McLure petroleum is in the Tulare Formation (51 percent), which is followed by the Reef Ridge Shale Member of the Monterey Formation (30.8 percent). This pattern of petroleum occurrence suggests that the oil and gas were expelled from thermally mature McLure Shale Member of the Monterey Formation source rock starting 5 Ma into the same unit (5.8 percent), and then into the adjacent Reef Ridge Shale Member (fig. 8.12). However, due to inadequate seal rock, the oil and gas migrated through the overlying units into the Tulare Formation (fig. 8.11). Petroleum contained in the remaining reservoir rocks is mostly shows of oil and gas. In the case of the Temblor, Rose, and North Shafter fields, the migration distance is more than about 15 miles (25 km) (fig. 8.9).

The burial history chart for the McLure Shale source rock indicates that the onset of petroleum generation occurred 5 Ma, peak generation or expulsion was at 3.5 Ma, and where buried in excess of 22,000 ft, the source rock was depleted by 1.5 Ma (fig. 8.12) at this location. According to Peters, Magoon, Valin, and Lillis (this volume, chapter 11), only the lower portion of the McLure Shale Member of the Monterey Formation, which overlays the Temblor Formation, is the organic-rich interval. The Temblor Formation has many sandstone units that could act as conduits for migrating petroleum from McLure Shale source rock (Hosford Scheirer and Magoon, this volume, chapter 5, fig. 5.49). The events chart indicates that the traps formed before and during migration of oil and gas (fig. 8.13).

Antelope-Stevens(!) Petroleum System

The Antelope-Stevens(!) is a large petroleum system with an estimated ultimate recovery of 11.5 Gboe, which represents 64.8 percent of the oil and gas in this basin (table 8.2). This petroleum system is located south of the Bakersfield Arch and straddles the east-west basin axis in the Tejon depocenter (figs. 8.1 and 8.14). The source rock name is the Antelope shale, as specified in Hosford Scheirer and Magoon (this volume, chapter 5, fig. 5.56), and whose source rock distribution and geochemical properties are described in Peters, Magoon, Valin, and Lillis (this volume, chapter 11). The reservoir rock name, Stevens, is used because the highest percentage of the petroleum occurs in the Stevens sand (29.3 percent, table 8.7). The level of certainty is known, or (!), because there is a positive geochemical correlation between the oil and Antelope shale source rock (Lillis and Magoon, this volume, chapter 9). The separation of the accumulations related to the Antelope-Stevens(!) to the south from the McLure-Tulare(!) accumulations located to the north occurs at the crest of the Bakersfield Arch because of the persistence of this structural high from Paleocene or late Eocene time (MacPherson, 1978). The gas-to-oil ratio of 1,176 ft^3 gas per barrel of oil is less than 20,000 ft^3, indicating an oil-prone system (table 8.2). On the basis of oil-to-oil comparisons in the Elk Hills Field, Zumberge and others (2005) show that the oil at the east end of the field originated from the Antelope shale to the south.

The pod of active source rock coincides with the Tejon depocenter. Comparing the 14,000 ft burial depth contour of the source rock with the 0.6%R_o contours for vitrinite reflectance indicates that the northwest part of the pod was uplifted by 6,000 ft and the southeast by 10,000 ft. If 14,000 ft of burial is required to create 0.6%R_o, then much of the Antelope pod was uplifted since maximum burial depth. This recent uplift is not reflected in the burial history chart so the very center of the depocenter is at maximum burial depth (fig. 8.17). Three of the four largest accumulations are located at the western extremity of the pod of active source rock, whereas the second largest field is located two-thirds of the way up the Bakersfield Arch. In decreasing volumes, the four largest fields are Midway-Sunset, (3,457 MMbo), Kern River on the Bakersfield Arch (2,078 MMbo), Elk Hills (1,239 MMbo), and Buena Vista (672 MMbo). Midway-Sunset, Elk Hills, and Buena Vista oil fields contain 47 percent of the oil in this petroleum system, indicating the most effective migration path from the pod of active source rock to a trap is in a northwesterly direction (appendix 8.1). There are 316 pools or traps in this system, with the west flank having about twice as many structural compared to stratigraphic traps. The east flank has about the same number of structural and stratigraphic traps (table 8.4).

The large number of reservoir rocks (20) involved in moving petroleum from the pod of active source rock to traps indicates complex migration paths (fig. 8.15; table 8.7). The 311 pools produce from reservoir rocks whose top depth ranges from 200 to 14,100 ft (appendix 8.1). All petroleum is found in reservoir rocks that range in age from 33.5 Ma to as young as 0.6 Ma, but if you include the "undesignated" reservoir rock, then 87 percent of the oil and gas are in reservoir rocks younger than 9.5 Ma. Petroleum in the Stevens sand constitutes 29.3 percent followed by the Kern River Formation (18.1 percent), Etchegoin Formation (7.1 percent), Chanac Formation (4.2 percent), Jewett Sand (3.9 percent) and Vedder Sand (3.9 percent). This pattern of petroleum occurrence suggests that the oil and gas began expulsion from thermally mature Antelope shale source rock at 4 Ma into the adjacent Stevens sand, where it migrated updip to the Kern River oil field to the north and to the Buena Vista, Elk Hills, and Midway-Sunset oil fields to the northwest (figs. 8.16 and 8.17). However, due to inadequate seal rock and erosion, the oil and gas seeped to the surface in many areas, only one of which was analyzed geochemically (fig. 8.14). Petroleum in the remaining reservoir rocks is mostly shows of oil and gas. The petroleum system map suggests that migration distances exceed 30 miles (50 km; fig 8.14).

The burial history chart for the Antelope shale source rock indicates that the onset of petroleum generation was at 4 Ma, peak generation or expulsion was at 2.5 Ma, and where buried in excess of 18,000 ft, it was depleted at 1.5 Ma (fig. 8.17). According to Peters, Magoon, Valin, and Lillis (this volume, chapter 11), only the lower portion of the Antelope shale (overlaying the Temblor Formation) is the organic-rich interval. However, although the Temblor Formation may have acted as a conduit for petroleum expelled from the Antelope shale source rock, it is more likely that the Stevens sand, which overlies the source rock, acted as the most effective carrier bed (Hosford Scheirer and Magoon, this volume, chapter 5, fig. 5.53). The events chart indicates that the traps formed before and during migration of oil and gas (fig. 8.18).

Miocene Total Petroleum System

The Miocene Total Petroleum System includes the Antelope-Stevens(!) petroleum system south of the Bakersfield Arch and the McLure-Tulare(!) petroleum system north

of the arch (fig. 8.19; table 8.1). As discussed above, each petroleum system includes a pod of active source rock and associated petroleum accumulations. Within this TPS, most of the petroleum is in the Stevens sand and related sandstone reservoir rocks from the north flank of the Bakersfield Arch south into the Tejon depocenter. The Miocene TPS includes five assessment units as follows: (1) Southeast Stable Shelf (AU50100401); (2) Lower Bakersfield Arch (AU50100402); (3) Miocene West Side Fold Belt (AU50100403); (4) South of White Wolf Fault (AU50100404); and (5) Central Basin Monterey Diagenetic Traps (AU50100405). The geologic rationale for these assessment units are discussed in Gautier and Hosford Scheirer (this volume, chapter 13 and chapter 14), Tennyson (this volume, chapter 15 and chapter 16), and Hosford Scheirer and others (this volume, chapter 17); the numeric and graphical support for all assessment units is discussed by Klett and Le (this volume, chapter 28).

Tumey-Temblor(.) Petroleum System

The Tumey-Temblor(.) is a significant petroleum system with an estimated ultimate recovery of 966 MMboe, which represents 5.5 percent of the oil and gas in the basin (table 8.2). Except for a small portion of the pod of active source rock south of the Bakersfield Arch, this petroleum system is chiefly located north of the arch (fig. 8.20). The source rock name is the Tumey formation, as identified in Hosford Scheirer and Magoon (this volume, chapter 5, fig. 5.30) and the source rock distribution and geochemical properties are described in Peters, Magoon, Valin, and Lillis (this volume, chapter 11). Because little information was available, the Tumey-Temblor(.) was assumed to have the same geographic distribution as the underlying Kreyenhagen Formation. The reservoir rock name, Temblor, is used because the highest percentage, or 84.3 percent, of the petroleum occurs in the Temblor Formation (table 8.8). The level of certainty is hypothetical, or (.), because the oil-source rock correlation is tentative (Lillis and Magoon, this volume, chapter 9). Unlike the overlying Miocene source rocks and the underlying Eocene Kreyenhagen Formation source rock—for which correlation with produced oil was definite—all that can be said at this time regarding oil correlation with the Tumey formation source rock is that both the source rock and the oil we assume to be associated with it are marine in geochemical character. The Tumey oil type (ET) also occurs in separate accumulations from either the Kreyenhagen Formation oil type (EK) or Miocene oil type (MM; Lillis and Magoon, this volume, chapter 9). The gas-to-oil ratio of 3,455 ft^3 gas per barrel of oil is less than 20,000 ft^3 gas per barrel of oil, so is interpreted as an oil-prone system (table 8.2).

The pod of active Tumey formation source rock coincides with the Buttonwillow depocenter. Comparing the 14,000 ft burial depth contour of the source rock with the 0.6%R_o contour for vitrinite reflectance indicates that the northwest part of the pod has been uplifted by 2,000 ft. If 14,000 ft of burial is required to create 0.6%R_o, then much of the Tumey pod was uplifted since maximum burial depth (fig. 8.23). Kettleman North Dome field (436 MMbo) is updip on the Coalinga Nose from the most mature part of the pod of active source rock and is the largest oil field in this system, so it was fed by the most effective migration path from source rock to trap (fig. 8.20; appendix 8.1). Two other relatively large oil fields, McKittrick (39 MMbo) and McDonald Anticline (23 MMbo), are to the west of the pod of active source rock. Long migration paths in excess of 30 miles (48 km) were required to charge Raisin City (39 MMbo) and Helm (20 MMbo) oil fields. There are 51 pools or traps in this system, with the west and east flanks having similar numbers of structural and stratigraphic traps (table 8.4).

The large number of identified reservoir rocks (10) involved in moving petroleum from the pod of active source rock to traps indicates that the migration paths are complex (fig. 8.21; table 8.8). The 58 pools produce from reservoir rocks whose top depth ranges from 200 to 13,000 ft (appendix 8.1). All of this petroleum occurs in reservoir rocks that range in age from 37 Ma to as young as 6.5 Ma, but 93.6 percent of the oil and gas are in reservoir rocks from 33 to 14 Ma. The Temblor Formation, Zilch formation of Loken (1959), and Vaqueros Formation contain 84.3 percent, 9.3 percent, and 3.7 percent, respectively, of the petroleum. This pattern of petroleum occurrence suggests that the oil and gas began expulsion at 5.5 Ma from thermally mature Tumey formation source rock into the overlying Vaqueros Formation, where it migrated up the Coalinga Nose to the Kettleman North Dome, Guijarral Hills, Pleasant Valley, and finally East Coalinga Extension oil fields (figs. 8.20 and 8.22).

The burial history chart for the Tumey formation source rock indicates that the onset of petroleum generation occurred 5.5 Ma, peak generation or expulsion occurred 4.5 Ma, and where buried in excess of 25,000 ft, depletion occurred 3 Ma (fig. 8.23). The events chart indicates that traps formed before and during migration of oil and gas (fig. 8.24).

Kreyenhagen-Temblor(!) Petroleum System

The Kreyenhagen-Temblor(!) is a significant petroleum system with an estimated ultimate recovery of 2.3 Gboe, which represents 12.9 percent of the oil and gas in this basin (table 8.2). Except for a small portion of the pod of active source rock south of the Bakersfield Arch, this petroleum system is chiefly located north of the arch (fig. 8.25). The source rock name is the Kreyenhagen Formation, as identified in Hosford Scheirer and Magoon (this volume, chapter 5, fig. 5.27), and the source rock distribution and geochemical properties are described in Peters, Magoon, Valin, and Lillis (this volume, chapter 11). The lower portion of the Kreyenhagen Formation contains the organic-rich interval. The reservoir rock name, Temblor, is used because the highest percentage, or 53.5 percent, of the petroleum occurs in the Temblor Formation (table 8.9). The level of certainty is known, or (!),

because there is a positive geochemical correlation between the oil and Kreyenhagen Formation source rock, as discussed by Lillis and Magoon (this volume, chapter 9). The gas-to-oil ratio of 1,700 ft^3 gas per barrel of oil is less than 20,000 ft^3 gas per barrel of oil, so is interpreted as an oil-prone system (table 8.2).

The pod of active source rock coincides with the Buttonwillow depocenter. Comparing the 14,000 ft burial depth contour of the source rock with the 0.6%R_o contour for vitrinite reflectance indicates that the northwest part of the pod was uplifted by 1,000 ft (fig. 8.25). If 14,000 ft of burial is required to create 0.6%R_o, then much of the Kreyenhagen pod is very close to maximum burial depth (fig. 8.28). Coalinga (970 MMbo) and East Extension Coalinga (508 MMbo) oil fields are updip on the Coalinga Nose from the most mature part of the pod of active source rock and are the largest oil fields in this system, indicating the most effective migration path from mature source rock to trap (appendix 8.1). Two other significant oil fields, Belridge North (70 MMbo) and Belgian Anticline (50 MMbo), are to the west of the pod. Long migration paths in excess of 30 miles (48 km) were required to charge Raisin City (4 MMbo) and Riverdale (7 MM bo) oil fields. There are 98 pools or traps in this system with similar numbers of structural (48) and stratigraphic (40) traps on the west flank (88) (table 8.4).

The large number of identified reservoir rocks (14) involved in moving petroleum from the pod of active source rock to traps indicates that the migration paths are complex (fig. 8.26; table 8.9). The 99 pools produce from reservoir rocks whose top depth ranges from 80 ft in Vallecitos field to 18,300 ft in the Paloma field (appendix 8.1). All of this petroleum occurs in reservoir rocks that range from 58.5 Ma to 4.5 Ma. The Temblor Formation contains 53.5 percent of the petroleum followed by the Lodo Formation (36.6 percent). This pattern of petroleum occurrence suggests that the oil and gas began expulsion from thermally mature Kreyenhagen Formation source rock at 5.2 Ma into the underlying Domengine Formation, where it migrated up the Coalinga Nose to the East Coalinga Extension and Coalinga oil fields (figs. 8.25 and 8.27). The most important reservoir rock is the siliciclastic Burbank sand of Sullivan (1966) in the Temblor Formation in the Coalinga field, whose sandstone dikes at the south end of the field act as a migration conduit to move the petroleum from below the Kreyenhagen Formation to above where the Tumey oil type is usually found (B. Bloeser, oral commun.). The Point of Rocks Sandstone Member of the Kreyenhagen Formation is interbedded in such a way that petroleum expelled from the source rock moved directly into the sandstone reservoir with a source rock seal, such as at Cymric and McKittrick oil fields, or to the outcrop such as seep B in figure 8.25.

The burial history chart for the Kreyenhagen source rock shows that the onset of petroleum generation occurred 5.2 Ma, peak generation or expulsion occurred 4.5 Ma, and where buried in excess of 26,000 ft, depletion occurred 3.5 Ma (fig. 8.28). The events chart indicates that traps formed before and during migration of oil and gas (fig. 8.29).

Eocene Total Petroleum System

The Eocene Total Petroleum System includes two petroleum systems—the Tumey-Temblor(.) and Kreyenhagen-Temblor(!) (fig. 8.30; table 8.1). As discussed above, each petroleum system includes a pod of active source rock and associated accumulations. These oil types typically occur in different stratigraphic positions. The Tumey formation is on top, the middle is a nonsource section or seal rock of Kreyenhagen Formation, and the bottom is the organic-rich Kreyenhagen Formation. Thus, the Tumey oil type is expelled from the top and the Kreyenhagen oil type is expelled from the bottom of the source rock section. However, the Temblor Formation is the most important reservoir rock for both petroleum systems because a large volume of Kreyenhagen oil type moved up into the Temblor Formation through sandstone dikes at the south end of the Coalinga field. The Eocene TPS includes two assessment units—(1) Eocene West Side Fold Belt (AU50100301), and (2) North and East of Eocene West Side Fold Belt (AU50100302). The geologic rationale of these assessment units is discussed in Tennyson (this volume, chapter 18) and Gautier and Hosford Scheirer (this volume, chapter 19), respectively; the numeric and graphical support are discussed by Klett and Le (this volume, chapter 28).

Eocene-Miocene Composite Total Petroleum System

The Eocene-Miocene Composite Total Petroleum System is undifferentiated for the Deep-Fractured Pre-Monterey Assessment Unit (AU50100201) (table 8.1). The geologic rationale for this assessment unit is discussed by Tennyson and Hosford Scheirer (this volume, chapter 20) and the numeric and graphical support are discussed by Klett and Le (this volume, chapter 28).

Moreno-Nortonville(.) Petroleum System

The Moreno-Nortonville(.) is a small gas-prone system with an estimated ultimate recovery of 31 MMboe, which represents 0.2 percent of the oil and gas in this basin (table 8.2). This petroleum system is the farthest north, stretching from Chowchilla gas field on the north to further south than Oil City oil pool in the Coalinga field (fig. 8.31). The source rock name is the Moreno Formation as identified in Hosford Scheirer and Magoon (this volume, chapter 5, fig. 5.17) and source rock distribution and geochemical properties are described in Peters, Magoon, Valin, and Lillis (this volume, chapter 11). The reservoir rock name, Nortonville sand of Frame (1950; hereafter referred to as Nortonville sand), is used because the highest percentage, or 40.3 percent, of the petroleum occurs in this rock unit (fig. 8.32;

table 8.10). The Nortonville sand is in the basal part of the Kreyenhagen Formation (Frame, 1950). The level of certainty is hypothetical, or (.), because previous correlation studies were inconclusive, and we have been unable to find an oil-prone thermally mature source rock sample to compare with the Oil City oil sample (Lillis and Magoon, this volume, chapter 9; Peters, Magoon, Valin, and Lillis, this volume, chapter 11; and Peters, Magoon, Lampe, and others, chapter 12). The gas-to-oil ratio of 1,156,797 ft^3 gas per barrel of oil is more than 20,000 ft^3 gas per barrel of oil, indicating a gas-prone system (table 8.2).

The pod of active source rock for this petroleum system is located northwest of the Buttonwillow depocenter (fig. 8.31). Comparing the 14,000 ft burial depth contour of the source rock with the 0.6%R_o contour for vitrinite reflectance indicates that none of the pod corresponds with this burial depth. If 14,000 ft of burial is required to create 0.6%R_o, then much of the Moreno pod has been uplifted such that present-day burial depths cut across lines of equal vitrinite reflectance (fig. 8.31). Oil City pool near Coalinga has an API gravity of 33 to 40 degrees, and the Cheney Ranch gas field produced 118,000 barrels of 50.5 degrees API gravity oil. Both samples are relatively light crude oil and represent small volumes (CDOGGR, 1998). The largest gas field in this system is at Gill Ranch (93 billion cubic feet of gas; bcfg) followed by Chowchilla (25 bcfg) and Merrill Avenue (20 bcfg). Of the 16 identified trap types, all three stratigraphic traps are on the west flank, whereas the others are structural traps on the east flank (table 8.4).

Seven reservoir rocks are involved in moving petroleum from the pod of active source rock to traps, indicating complex migration paths (fig. 8.33; table 8.10). The 21 pools produce from reservoir rocks that range in depth from 700 to 9,300 feet deep (appendix 8.1). Reservoir rocks that contain gas and oil generated from the Moreno Formation range from 83.5 Ma to as young as 14 Ma. Gas in the Nortonville sand constitutes 40.3 percent of the total known gas in the petroleum system, followed by the Panoche Formation (32.6 percent), Blewett sands of Hoffman (1964) (19 percent), and other reservoir rocks (table 8.10).

The onset of petroleum generation started 37.5 Ma with peak generation at 10 Ma and depletion of the source rock at 4 Ma (fig. 8.34). The small amount of expelled oil moved a short distance into the Oil City pool and Cheney Ranch field, whereas the gas migrated a much longer distance to at least as far as the Chowchilla field, a minimum of 35 miles (57 km). The events chart summarizes the deposition of the essential elements and the time over which the processes took place (fig. 8.35). This chart indicates that this gas system is the oldest petroleum system in the basin and that traps formed before petroleum migrated.

Winters-Domengine Total Petroleum System

The Winters-Domengine Total Petroleum System (fig. 8.36) includes only the Northern Nonassociated Gas Assessment Unit (AU50100101). The geologic rationale for this assessment unit is discussed by Hosford Scheirer and Magoon (this volume, chapter 21), and the numeric and graphical support are discussed by Klett and Le (this volume, chapter 28). Chapter 21 provides the rationale as to why the assessment of this unit assumed that the natural gas came from north of the Stockton Arch. However, work since the assessment indicated that the discovered gas and minor oil originated from the Moreno Formation in the San Joaquin Basin Province as discussed in the Moreno-Nortonville(.) above.

Volumetric Estimate of Generated Petroleum

Estimates of the volume of petroleum generated from thermally mature source rocks require information on the distribution, thickness, richness, and thermal maturity of each source rock (Peters, Magoon, Valin, and Lillis, this volume, chapter 11) and how petroleum expulsion changes in accordance with these four variables. The expulsion factor is the ratio of the grams of carbon expelled as petroleum from thermally mature source rock to the original total organic carbon (TOC_o) in the immature source rock (Lewan and others, 1995; Peters and others, 2006). Two laboratory pyrolysis methods used to determine expulsion factors include Rock-Eval pyrolysis and hydrous pyrolysis.

Rock-Eval pyrolysis data were used in calculations by Cooles and others (1986), Schmoker (1994), and Peters and others (2006; these calculations are referred to herein as "Cooles," "Schmoker," and "Peters" methods, respectively). In Rock-Eval pyrolysis, approximately 100 mg of rock powder is heated from 300° to 600°C at 25°C/min under atmospheric pressure and flowing inert carrier gas (Peters, 1986). The Cooles method assumes that some portion of the organic carbon in each source-rock sample consists of inert material that cannot be vaporized as volatile or cracked hydrocarbon products (S1 and S2, respectively; mg hydrocarbon/g rock) and that this inert organic carbon content remains constant as each source rock thermally matures. The Schmoker method assumes that expelled petroleum represents the difference between the original hydrogen index and measured hydrogen index (HI_o and HI, respectively, in milligrams of hydrocarbon per gram TOC; mg HC/g TOC). The Peters method to determine expulsion factors does not assume constant inert carbon with thermal maturation. However, the amount of petroleum that can be expelled is constrained by the petroleum generative potential of the starting organic matter (HI_o), the extent of fractional conversion of the organic matter to pyrolyzate, and a mass-balance constraint based on the amount of carbon in the pyrolyzed product (83.33 weight percent TOC).

Hydrous pyrolysis experiments by Lewan and others (2002; referred to herein as "Lewan" method) gave expulsion factors for oil at different thermal maturity levels for the Devonian-Mississippian New Albany Shale source rock from the Illinois Basin. This organic-rich source rock sample (14.34

weight percent TOC) contains thermally immature (Tmax = 425°C, PI = 0.03), Type I (HI_O = 604 mg HC/g TOC) organic matter. Each hydrous pyrolysis experiment heated 300 g of gravel-sized chips of New Albany Shale with 400 g of distilled water in 1 L pressure vessels for 72 hours at a constant temperature in the range 270° to 365°C.

This chapter compares expulsion factors determined by the three Rock-Eval pyrolysis methods with those determined using data from hydrous pyrolysis experiments by Lewan and others (2002). We calculated the petroleum charge in barrels supplied by the thermally mature Antelope shale, McLure Shale Member of the Monterey Formation, Kreyenhagen Formation, and Moreno Formation source rocks within the study area using the following equation:

(8.1)

Petroleum Charge = [(Area, m^2)(Thickness, m)(Shale Density, g/cm^3)(TOC_O/100)(Expulsion Factor)(6.29 barrels/m^3)]/(Oil Density, g/cm^3)

The present-day thickness for each source rock (figs. 11.8 to 11.10 in Peters, Magoon, Valin, and Lillis, this volume, chapter 11) was converted to meters for the calculation. For simplicity, we used a constant shale density of 2.5 g/cm^3, although we are aware that shale density increases with burial depth (compaction) and decreases with increasing TOC. Reconstruction of TOC_O from measured TOC using the method in Peters and others (2005) was required in those source rock intervals that were mature or spent (figs. 11.11 to 11.13 in Peters, Magoon, Valin, and Lillis, this volume, chapter 11). We assigned oil densities of 0.8984, 0.8762, and 0.8448 g/cm^3 in equation 8.1 assuming 26, 30, and 36 degrees API oil was expelled from the McLure-Antelope, Kreyenhagen, and Moreno source rocks, respectively. We calculated expulsion factors using the three-step approach of Lewan and others (1995; 2002), which determines (1) the fraction of TOC that occurs as inert organic carbon, (2) the original immature TOC (TOC_O), and (3) the amount of organic carbon expelled from thermally mature source rock. The expulsion factor is the ratio of the grams of carbon expelled from a thermally mature source rock as petroleum compared to the TOC_O of immature source rock. Expulsion factors increase with decreasing hydrogen index of the maturing source rock (fig 8.37; see also fig. 17 in Lewan and others, 2002).

The area term in equation 8.1 was determined by using Arc/Info® (v. 8.1) to generate polygons by intersecting contoured line coverage of mapped thickness (figs. 8.38, 11.8 to 11.10), TOC_O (figs. 11.11 to 11.13), and measured hydrogen index (table 8.12 obtained from table 11.5 in Peters, Magoon, Valin, and Lillis, this volume, chapter 11) for each of the four source rocks. The polygons were constructed only within thermally mature or spent regions of the distribution of each source rock as determined by the 0.6% vitrinite reflectance contour calculated from the 4-D model (Peters, Magoon, Lampe, and others, this volume, chapter 12). Figure 8.38 is a schematic depiction of how these polygons were constructed. Expulsion factors (g Carbon/g TOC, fig. 8.37) were linked to these polygons in an attribute table according to the midpoint for each of the measured hydrogen index maturity intervals. For example, expulsion factors corresponding to a hydrogen index of 150 mg HC/g TOC in figure 8.37 were linked to all polygons having measured hydrogen indices in the range 100 to 200 mg HC/g TOC. The Arc/Info® polygons and their characteristics were exported to an Excel spreadsheet for computation of petroleum volumes using equation 8.1 and expulsion factors determined by the Rock-Eval pyrolysis ("Cooles," "Peters," and "Schmoker") and hydrous pyrolysis ("Lewan") methods.

Figure 8.37 shows expulsion factors calculated by the Rock-Eval and hydrous pyrolysis methods (solid and open symbols, respectively). The "Lewan HP" and "Lewan Actual" curves (open circles and open squares, respectively) are based on twelve hydrous pyrolysis experiments on New Albany Shale samples (Lewan and others, 2002). In the hydrous pyrolysis experiments, increased reactor temperatures resulted in hydrogen indices that progressively decreased from that of the unheated sample (HI_O = 604 mg HC/g TOC, expulsion factor = 0) to as low as 88 mg HC/g TOC (expulsion factor = 0.343). The "Lewan Actual" curve in figure 8.37 (open squares) has expulsion factors that were corrected by multiplying the hydrous pyrolysis curve by 58.9 percent. The 58.9 percent factor is based on data from a well-constrained catchment area within the Illinois Basin with no erosional or leakage losses of oil generated from the thermally mature New Albany Shale (Lewan and others, 2002). This area contained only 58.9 percent of the petroleum charge that was predicted on the basis of the hydrous pyrolysis experiments (open circles in fig. 8.37).

Unlike the Antelope shale, McLure Shale Member of the Monterey Formation, and Kreyenhagen Formation source rocks, which contain mainly oil-prone type II kerogen, the Moreno Formation source rock contains mainly oil and gas-prone type II/III kerogen. We corrected the measured HI used to estimate expulsion efficiency in figure 8.37 by assuming HI_O of 300 mg HC/g TOC for the Moreno source rock rather than the higher HI of 600 mg HC/g TOC assumed for the other source rocks. This was accomplished by a linear interpolation of HI values from 50 to 600 for type II compared to 50 to 300 mg HC/g TOC for the Moreno Formation, where HI400 = (1.3987*HI300) - 19.6172.

The large range in calculated volumes of petroleum charge within and between source rocks (fig. 8.39; table 8.13) reflects differences in calculated expulsion factors based on the Rock-Eval pyrolysis and hydrous pyrolysis methods (fig. 8.37). The "uncorrected" volume of expelled petroleum determined by the Rock-Eval pyrolysis method assumes that no threshold value of TOC is required for expulsion (Lewan, 1987; Peters and others, 2005), and the "corrected" volume assumes (1) a threshold TOC value of 2.0 weight percent, and (2) 55 weight percent of the pyrolyzate consists of NSO-compounds (Behar and others, 1997) swept out of the rock by carrier gas. These NSO-compounds would otherwise cross-link to form pyrobitumen and thus fail to contribute to expelled petroleum (table 8.13). The

volumes of expelled petroleum determined by hydrous pyrolysis ("HP") were corrected using a factor of 0.5 as recommended by Lewan and others (1995; 2002) and are actual calculated volumes (table 8.13). In all cases, calculated volumes decrease from left to right in table 8.13.

The richness of the source rock, the size and thermal maturity of the pod of active source rock, the distance of the migration path, trap size, leakage, and loss are some of the factors that affect the efficiency of these four petroleum systems. The generation-accumulation efficiency (GAE) was calculated for each of the "corrected" volumes for each pod of active source rock (Magoon and Valin, 1994). The in-place barrel of oil equivalent was calculated assuming that the estimated ultimate recoverable oil equivalent represents 25 percent of the oil and gas in the accumulation—a GAE of 20 percent indicates that for every 100 barrels of oil-equivalent generated, 20 reached the trap. In these four pods of active source rock the efficiencies range from a low of 0.8 percent to an unlikely high of 97.7 percent. Because actual efficiency cannot be corroborated by another method, the discussion of absolute numbers is meaningless, but relative efficiencies can be subjectively evaluated relative to other geologic factors. Assuming most accumulations have been discovered in this province, then the relative migration efficiencies can be ranked as follows—Antelope-Stevens(!)>McLure-Tulare(!)>Kreyenhagen-Temblor(!)>Moreno-Nortenville(.). The most efficient petroleum system, the Antelope-Stevens(!), has the Stevens sand interbedded with the source rock, so its efficiency is expected. The other three petroleum systems have greater distances of migration from source rock to trap. The least efficient system, the Moreno-Nortonville(.), involves gas that may dissipate more during migration, or alternatively, the entire system may be underexplored.

Acknowledgments

The authors acknowledge Ian Kaplan, George Claypool, Zenon Valin, Keith Kvenvolden, Elisabeth Rowen, Tom Lorenson, and the numerous field operators who helped acquire oil and gas samples. We thank Occidental Oil Company and Chevron Oil Company for providing oil samples from their archives. We also acknowledge Ron Hill and Tony Reid for reviewing an early draft of this paper, and Wally Dow, Debra Higley, and Tony Reid, all of whom reviewed the most recent draft.

References Cited

Atwill, E.R., 1935, Oligocene Tumey Formation of California: Bulletin of the American Association of Petroleum Geologists, v. 19, no. 8, p. 1192-1204.

Behar, F., Vandenbroucke, M., Tang, Y., Marquis, F., and Espitalie, J., 1997, Thermal cracking of kerogen in open and closed systems—Determination of kinetic parameters and stoichiometric coefficients for oil and gas generation: Organic Geochemistry, v. 26, no. 5-6, p. 321-339.

Bishop, C.C., 1970, Upper Cretaceous stratigraphy on the west side of the Northern San Joaquin Valley, Stanislaus and San Joaquin Counties, California: Sacramento, Calif., California Division of Mines and Geology Special Report 104, 29 p.

Callaway, D.C., 1964, Distribution of uppermost Cretaceous sands in the Sacramento-Northern San Joaquin Basin of California: Selected Papers Presented to San Joaquin Geological Society, v. 2, p. 5-18.

CDOGGR, 1998, California oil and gas fields: Sacramento, Calif., California Department of Conservation, Division of Oil, Gas, and Geothermal Resources Publication No. CD-1, 1472 p.

CDOGGR, 2001a, 2000 Annual Report of the State Oil and Gas Supervisor: Sacramento, Calif., California Department of Conservation, Division of Oil, Gas, and Geothermal Resources, Publication No. PR06, 255 p. [also available at ftp://ftp.consrv.ca.gov/pub/oil/annual_reports/2000/].

CDOGGR, 2001b, Oil, gas, and geothemal fields in California: California Department of Conservation, Division of Oil, Gas, and Geothermal Resources, scale 1:1,500,000 [also available at ftp://ftp.consrv.ca.gov/pub/oil/maps/Map_S-1.pdf].

Cole, F., Magoon, L.B., Hodgson, S.F., Lillis, P., and Stanley, R.G., 1999, Natural oil and gas seeps in California: U.S. Geological Survey [http://seeps.wr.usgs.gov].

Cooles, G.P., Mackenzie, A.S., and Quigley, T.M., 1986, Calculation of petroleum masses generated and expelled from source rocks: Organic Geochemistry, v. 10, p. 235-245.

Eckis, R., 1940, The Stevens sand, southern San Joaquin Valley, California [abs.]: Bulletin of the American Association of Petroleum Geologists, v. 24, no. 12, p. 2195-2196.

Edwards, E.C., 1943, Kern Front area of the Kern River oil field, in Jenkins, O.P., ed., Geologic formations and economic development of the oil and gas fields of California: San Francisco, Calif., State of California, Department of Natural Resources, Division of Mines Bulletin No. 118, p. 571-574.

Frame, R.G., 1950, Helm oil field, in Summary of operations, California oil fields: San Francisco, Calif., Annual Report of the State Oil and Gas Supervisor, v. 36, no. 1, p. 5-14 [also available in California Division of Oil and Gas, Summary of Operations, 1915-1999: California Division of Conservation, Division of Oil, Gas, and Geothermal Resources, Publication No. CD-3, and at ftp://ftp.consrv.ca.gov/pub/oil/Summary_of_Operations/1950/].

Gautier, D.L., Hosford Scheirer, A., Tennyson, M.E., Peters, K.E., Magoon, L.B., Lillis, P.G., Charpentier, R.R., Cook, T.A., French, C.D., Klett, T.R., Pollastro, R.M., and Schenk, C.J., 2004, Assessment of Undiscovered Oil and Gas Resources of the San Joaquin Basin Province of California, 2003: U.S. Geological Survey Fact Sheet FS-2004-0343

[also available at URL http://pubs.usgs.gov/fs/2004/3043/].

Goudkoff, P.P., 1943, Correlation of oil field formations on west side of San Joaquin Valley, *in* Jenkins, O.P., ed., Geologic formations and economic development of the oil and gas fields of California: San Francisco, Calif., State of California, Department of Natural Resources, Division of Mines Bulletin No. 118, p. 247-252.

Graham, S.A., and Williams, L.A., 1985, Tectonic, depositional, and diagenetic history of Monterey Formation (Miocene), central San Joaquin Basin, California: American Association of Petroleum Geologists Bulletin, v. 69, no. 3, p. 385-411.

Hoffman, R.D., 1964, Geology of the northern San Joaquin Valley: Selected Papers Presented to San Joaquin Geological Society, v. 2, p. 30-45.

Hosford Scheirer, A., ed., 2007, Petroleum systems and geologic assessment of oil and gas in the San Joaquin Basin Province, California: U.S. Geological Survey Professional Paper 1713 [available at http://pubs.usgs.gov/pp/pp1713/].

Kasline, F.E., 1942, Edison oil field, in Summary of operations, California oil fields: San Francisco, Calif., Annual Report of the State Oil and Gas Supervisor, v. 26, p. 12-18 [also available in California Division of Oil and Gas, Summary of Operations, 1915-1999: California Division of Conservation, Division of Oil, Gas, and Geothermal Resources, Publication No. CD-3, and at ftp://ftp.consrv.ca.gov/pub/oil/Summary_of_Operations/1940/].

Kirby, J.M., 1943, Upper Cretaceous stratigraphy of the west side of Sacramento Valley south of Willows, Glenn County, California: Bulletin of the American Association of Petroleum Geologists, v. 27, no. 3, p. 279-305.

Klemme, H.D., 1994, Petroleum systems of the world involving Upper Jurassic source rocks, *in* Magoon, L.B., and Dow, W.G., eds., The petroleum system—From source to trap: Tulsa, Okla., American Association of Petroleum Geologists Memoir 60, p. 51-72.

Lewan, M.D., 1987, Petrographic study of primary petroleum migration in the Woodford Shale and related rock units, *in* Doligez, B., ed., Migration of hydrocarbons in sedimentary basins: Paris, Éditions Technip, p. 113-130.

Lewan, M.D., Comer, J.B., Hamilton-Smith, T., Hasenmueller, N.R., Guthrie, J.M., Hatch, J.R., Gautier, D.L., and Frankie, W.T., 1995, Feasibility study of material-balance assessment of petroleum from the New Albany Shale in the Illinois Basin: U.S. Geological Survey Bulletin 2137, 31 p.

Lewan, M.D., Henry, M.E., Higley, D.K., and Pitman, J.K., 2002, Material-balance assessment of the New Albany-Chesterian petroleum system of the Illinois basin: American Association of Petroleum Geologists Bulletin, v. 86, p. 745-777.

Loken, K.P., 1959, Gill Ranch gas field, in Summary of operations, California oil fields: San Francisco, Calif., Annual Report of the State Oil and Gas Supervisor, v. 45, no. 1, p. 27-32 [also available in California Division of Oil and Gas, Summary of Operations, 1915-1999: California Division of Conservation, Division of Oil, Gas, and Geothermal Resources, Publication No. CD-3, and at ftp://ftp.consrv.ca.gov/pub/oil/Summary_of_Operations/1959/].

MacPherson, B.A., 1978, Sedimentation and trapping mechanism in upper Miocene Stevens and older turbidite fans of southeastern San Joaquin Valley, California: American Association of Petroleum Geologists Bulletin, v. 62, p. 2243-2274.

Magoon, L.B., 2004, Petroleum system—Nature's distribution system of oil and gas, *in* Cleveland, C., and Ayres, R.U., eds., Encyclopedia of Energy: Amsterdam, Elsevier Academic Press, p. 823-836.

Magoon, L.B., and Dow, W.G., 1994, The petroleum system, *in* Magoon, L.B., and Dow, W.G., eds., The petroleum system—From source to trap: Tulsa, Okla., American Association of Petroleum Geologists Memoir 60, p. 3-24.

Magoon, L.B., and Schmoker, J.W., 2000, The total petroleum system—The natural fluid network that constrains the assessment unit, *in* U.S. Geological Survey World Energy Assessment Team, ed., U.S. Geological Survey world petroleum assessment 2000—Description and results: U.S. Geological Survey Digital Data Series DDS-60.

Magoon, L.B., and Valin, Z.C., 1994, Overview of petroleum system case studies, *in* Magoon, L.B., and Dow, W.G., eds., The petroleum system—From source to trap: Tulsa, Okla., American Association of Petroleum Geologists Memoir 60, p. 251-260.

McMasters, J.H., 1948, Oceanic sand [abs.]: Bulletin of the American Association of Petroleum Geologists, v. 32, no. 12, p. 2320.

Miller, R.H., and Bloom, C.V., 1939, Mountain View oil field, in Summary of operations, California oil fields: San Francisco, Calif., Annual Report of the State Oil and Gas Supervisor, v. 22, no. 4, p. 5-36 [also available in California Division of Oil and Gas, Summary of Operations, 1915-1999: California Division of Conservation, Division of Oil, Gas, and Geothermal Resources, Publication No. CD-3, and at ftp://ftp.consrv.ca.gov/pub/oil/Summary_of_Operations/1937/].

Noble, E.B., 1940, Rio Bravo oil field, Kern County, California: Bulletin of the American Association of Petroleum Geologists, v. 24, no. 7, p. 1330-1333.

Peters, K.E., 1986, Guidelines for evaluating petroleum source rock using programmed pyrolysis: American Association of Petroleum Geologists Bulletin, v. 70, p. 318-329.

Peters, K.E., Magoon, L.B., Bird, K.J., Valin, Z.C., and Keller, M.A., 2006, North Slope, Alaska—Source rock distribution, richness, thermal maturity, and petroleum charge: American Association of Petroleum Geologists Bulletin, v. 90, p. 1-31.

Peters, K.E., Walters, C.C., and Moldowan, J.M., 2005, The biomarker guide: Cambridge, U.K., Cambridge University Press, 1155 p.

Schmoker, J.W., 1994, Volumetric calculation of hydrocarbons generated, *in* Magoon, L.B., and Dow, W.G., eds., The petroleum system—From source to trap: Tulsa, Okla., American Association of Petroleum Geologists Memoir 60, p. 323-326.

Sterling, R., Grau, A., Kidney, R., Ganong, B., Pendleton, P., Drennan, L., and Bosse, A., 2003, The North Shafter and Rose oil fields—A seismically defined, diagenetic stratigraphic trap in the Miocene McLure Shale, San Joaquin Basin, CA [abs.]: Annual Meeting Expanded Abstracts—American Association of Petroleum Geologists, v. 12, p. 163.

Sullivan, J.C., 1963, Guijarral Hills oil field, in Summary of operations, California oil fields: San Francisco, Calif., Annual Report of the State Oil and Gas Supervisor, v. 48, no. 2, p. 37-51 [also available in California Division of Oil and Gas, Summary of Operations, 1915-1999: California Division of Conservation, Division of Oil, Gas, and Geothermal Resources, Publication No. CD-3, and at ftp://ftp.consrv.ca.gov/pub/oil/Summary_of_Operations/1962/].

Sullivan, J.C., 1966, Kettleman North Dome oil field, in Summary of operations, California oil fields: Sacramento, Calif., Annual Report of the State Oil and Gas Supervisor, v. 52, no. 1, p. 6-21 [also available in California Division of Oil and Gas, Summary of Operations, 1915-1999: California Division of Conservation, Division of Oil, Gas, and Geothermal Resources, Publication No. CD-3, and at ftp://ftp.consrv.ca.gov/pub/oil/Summary_of_Operations/1966/].

Wilkinson, E.R., 1960, Vallecitos field, in Summary of operations, California oil fields: San Francisco, Calif., Annual Report of the State Oil and Gas Supervisor, v. 45, no. 2, p. 17-33 [also available in California Division of Oil and Gas, Summary of Operations, 1915-1999: California Division of Conservation, Division of Oil, Gas, and Geothermal Resources, Publication No. CD-3, and at ftp://ftp.consrv.ca.gov/pub/oil/Summary_of_Operations/1959/].

Williams, R.N., Jr., 1938, Recent developments in the North Belridge oil field, in Summary of operations, California oil fields: San Francisco, Calif., Annual Report of the State Oil and Gas Supervisor, v. 21, no. 4, p. 5-16 [also available in California Division of Oil and Gas, Summary of Operations, 1915-1999: California Division of Conservation, Division of Oil, Gas, and Geothermal Resources, Publication No. CD-3, and at ftp://ftp.consrv.ca.gov/pub/oil/Summary_of_Operations/1936/].

Zieglar, D.L., and Spotts, J.H., 1978, Reservoir and source-bed history of Great Valley, California: American Association of Petroleum Geologists Bulletin, v. 62, p. 813-826.

Zumberge, J.E., Russell, J.A., and Reid, S.A., 2005, Charging of Elk Hills reservoirs as determined by oil geochemistry: American Association of Petroleum Geologists Bulletin, v. 89, no. 10, p. 1347-1371.

This page intentionally left blank

Figures 8.1–8.39

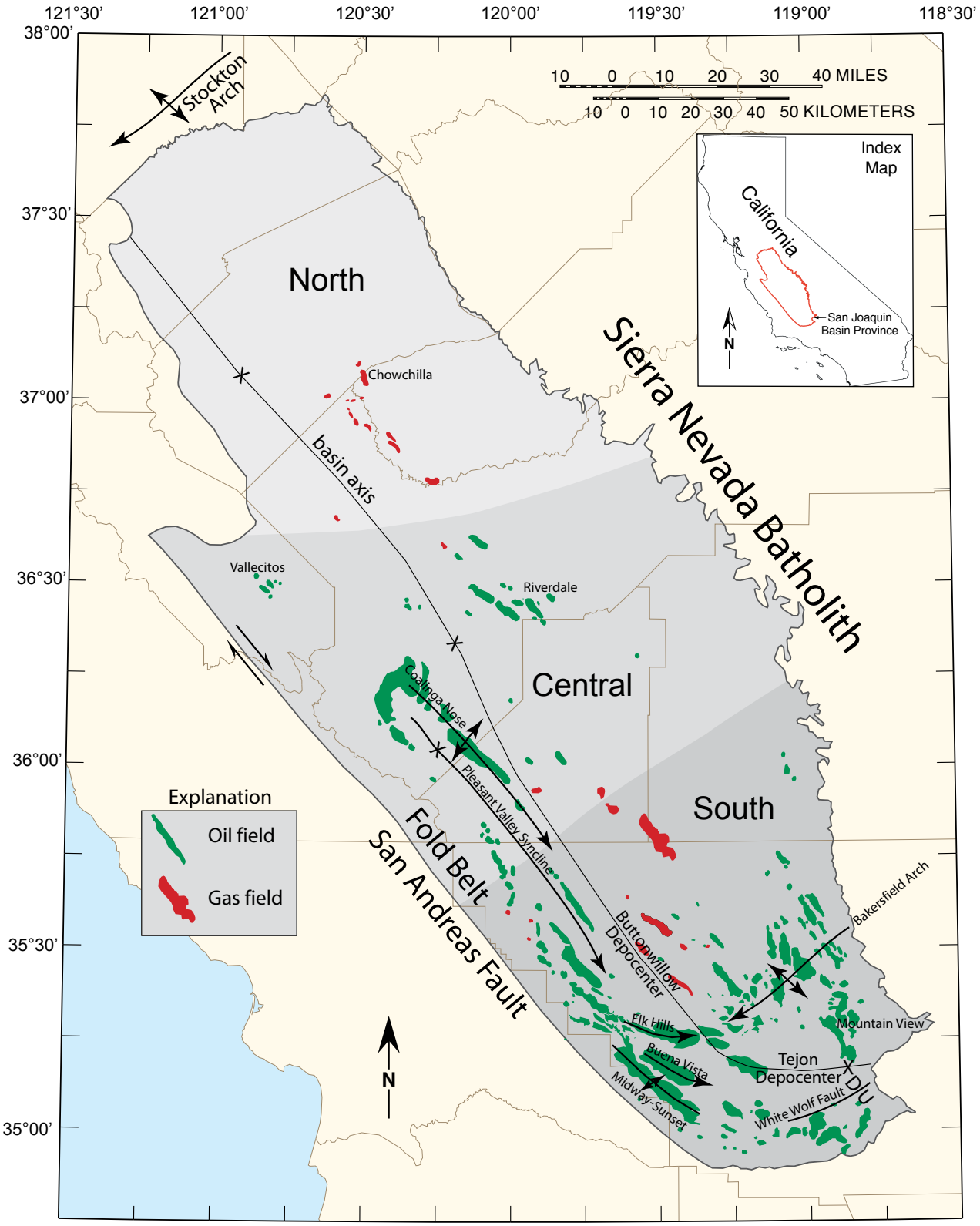

Figure 8.1. Index map of the San Joaquin Basin Province divided into the north, central, and south subregions (three shades of gray). Thin brown lines are county boundaries. Oil and gas fields are shown in green and red colored polygons, respectively. Inset shows location of study area in California.

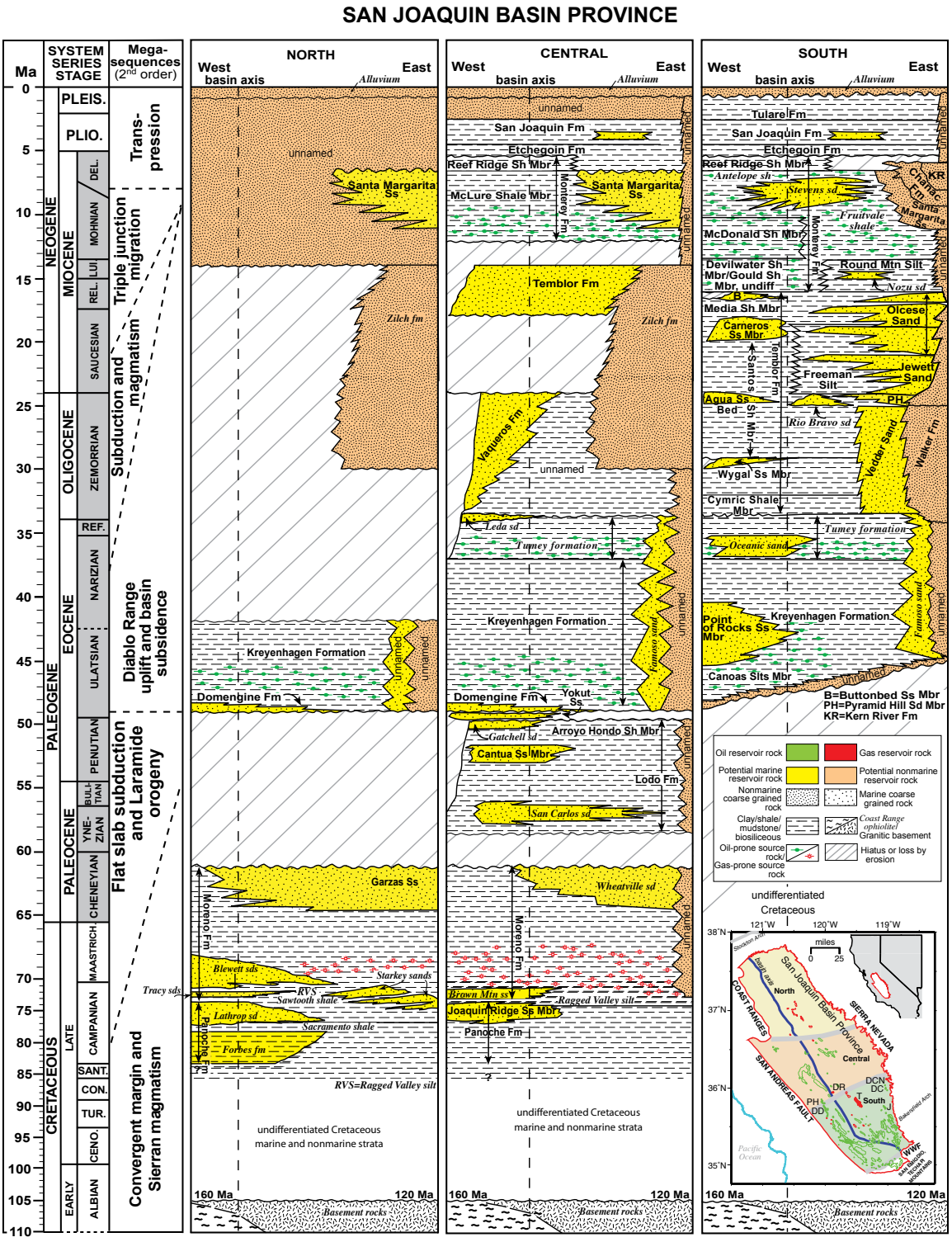

Figure 8.2. San Joaquin Basin Province stratigraphy showing hydrocarbon reservoir rocks and potential hydrocarbon source rocks. See Hosford Scheirer and Magoon (this volume, chapter 5) for complete explanation of the figure. Formation names in italics are informal and are defined as follows (in approximate age order): Forbes formation of Kirby (1943), Sacramento shale and Lathrop sand of Callaway (1964), Sawtooth shale and Tracy sands of Hoffman (1964), Brown Mountain sandstone of Bishop (1970), Ragged Valley silt, Starkey sands, and Blewett sands of Hoffman (1964), Wheatville sand of Callaway (1964), San Carlos sand of Wilkinson (1960), Gatchell sand of Goudkoff (1943), Oceanic sand of McMasters (1948), Leda sand of Sullivan (1963), Tumey formation of Atwill (1935), Famoso sand of Edwards (1943), Rio Bravo sand of Noble (1940), Nozu sand of Kasline (1942), Zilch formation of Loken (1959), Stevens sand of Eckis (1940), Fruitvale shale of Miller and Bloom (1939), and Antelope shale of Graham and Williams (1985).

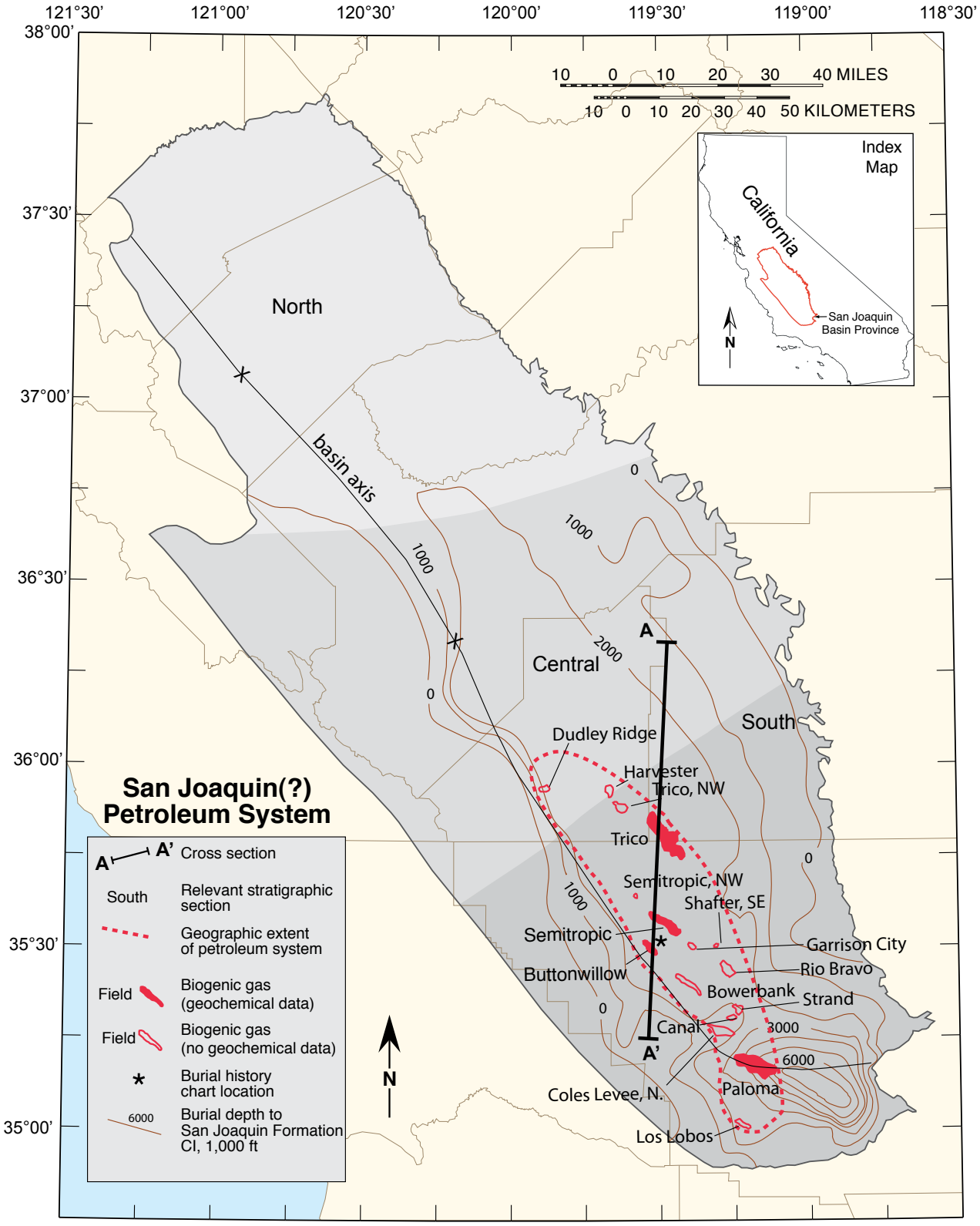

Figure 8.3. San Joaquin(?) petroleum system map showing the present-day burial depth of the speculative source rock—the San Joaquin Formation (brown contours)—as well as location of cross section A-A', location(*) of burial history chart, and a red dashed line indicating the geographic extent of the system. Gas accumulations in this petroleum system are shown in red; solid polygons indicate biogenic gas accumulations based on geochemical analysis, whereas outlines indicate suspected biogenic accumulations from stratigraphic proximity. In this and in all other geographic maps, the three geographic regions illustrated in the stratigraphy chart (such as fig. 8.2) are shown in shades of gray. CI, contour interval.

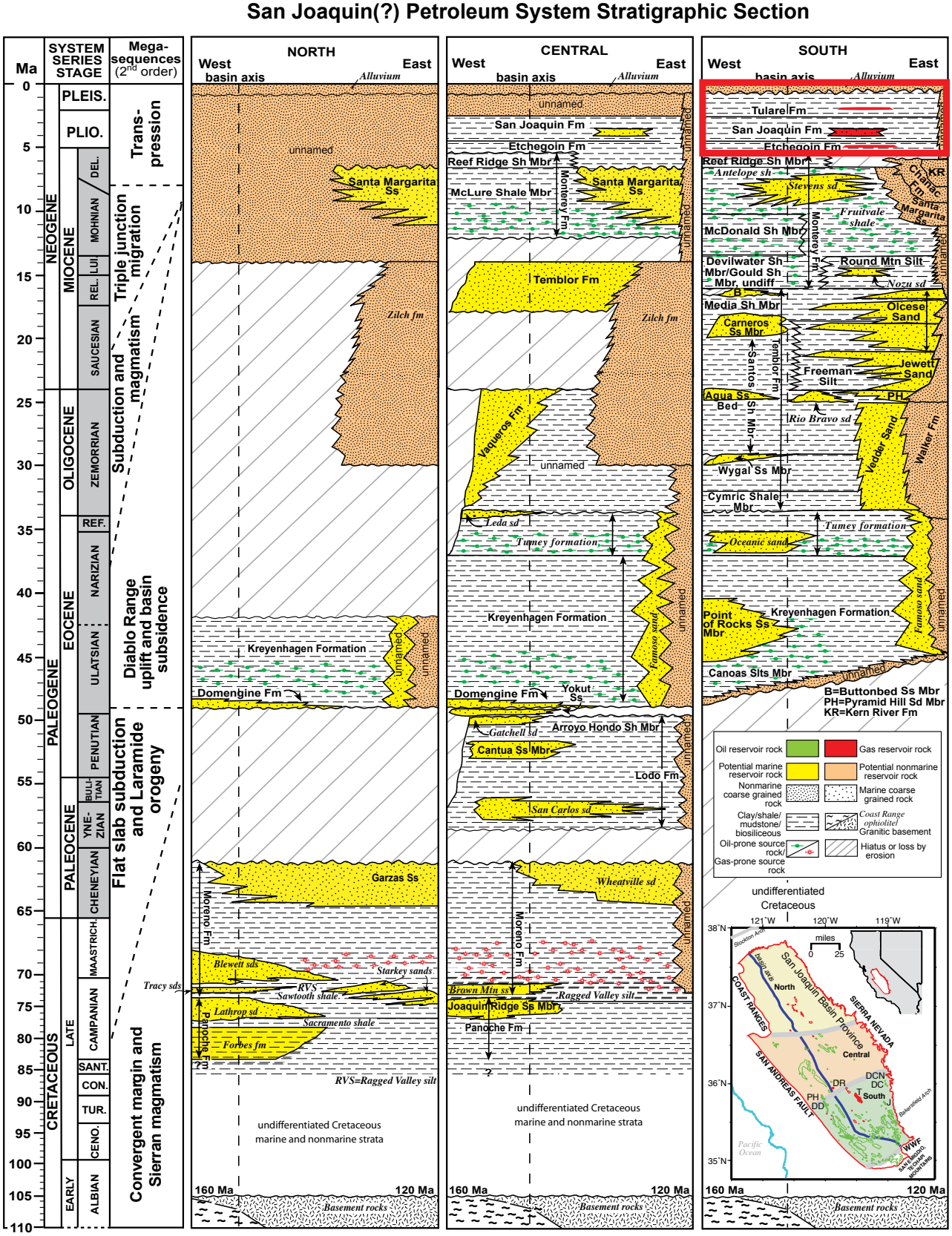

Figure 8.4. Stratigraphic column shown in figure 8.2, but with gas reservoir rocks for the San Joaquin(?) petroleum system (red outline) shown on the south region of the stratigraphic section.

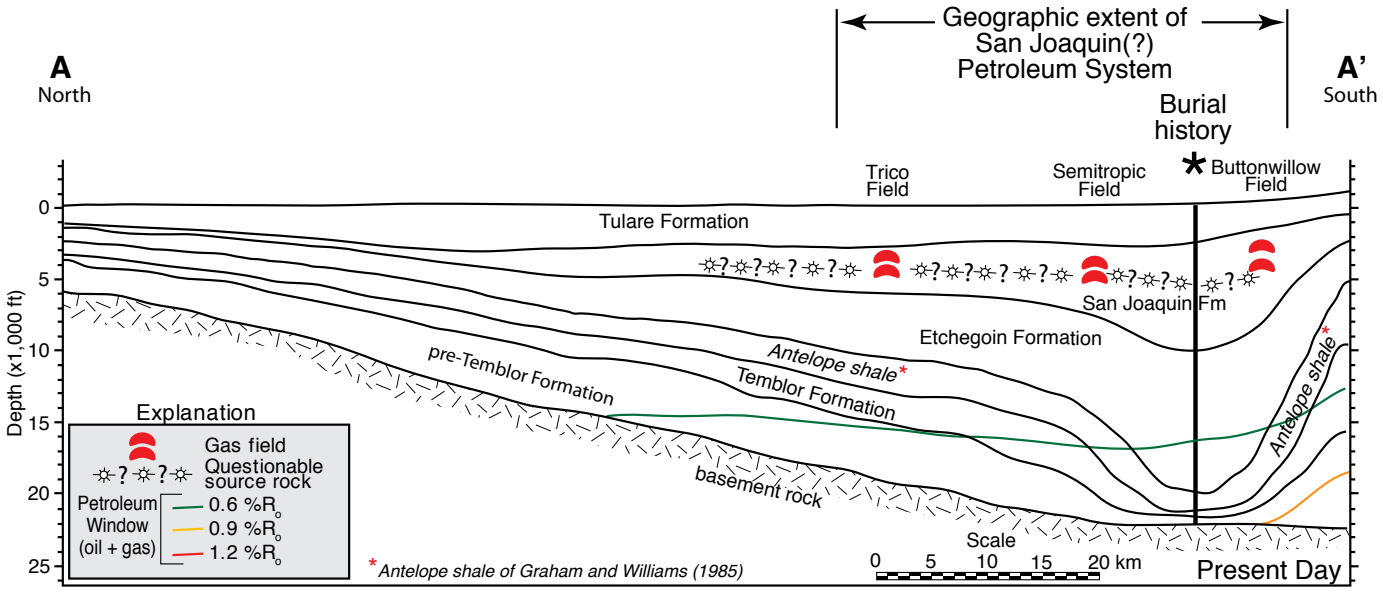

Figure 8.5. Cross section A-A' showing geographic extent of the San Joaquin(?) petroleum system, the location of the burial history chart (vertical line; location also shown on map in fig. 8.3 and chart shown in fig. 8.6), the questionable source rock interval for the biogenic gas (open stars), and the stratigraphic unit that contains the gas accumulations in known fields (red blobs). Stratigraphic depth contours and vitrinite reflectance contours (%R_o) are derived from the San Joaquin Basin model of Peters, Magoon, Lampe, and others (this volume, chapter 12). Formation names in italics are informal. Fm, Formation.

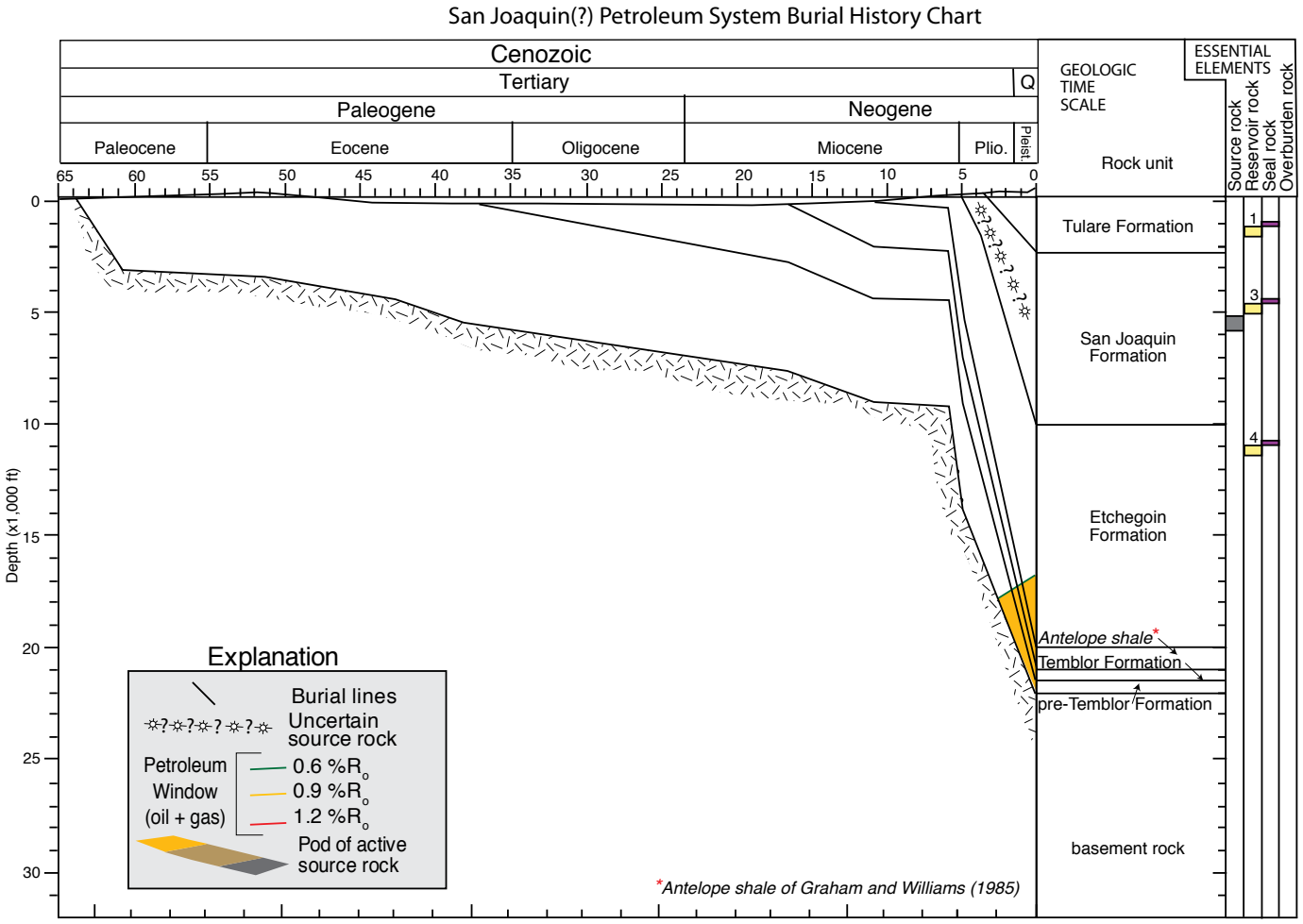

Figure 8.6. Burial history chart for the San Joaquin(?) petroleum system shows that the speculative source rock interval, the San Joaquin Formation, is immature for petroleum generation; only the Antelope shale has a pod of active source rock (yellow shading). The numbers overlying yellow rectangles in the reservoir rock column refer to the reservoir rock numbers in table 8.5 and appendix 8.2. If relevant, in this and all other burial history charts, gray rectangles indicate source rocks, yellow rectangles indicate reservoir rocks, purple rectangles indicate seal rocks, and orange rectangles indicate overburden rocks. Note that there is no overburden in this system. Formation names in italics are informal. Pleist., Pleistocene; Plio., Pliocene; Q, Quaternary; $\%R_o$, percent vitrinite reflectance.

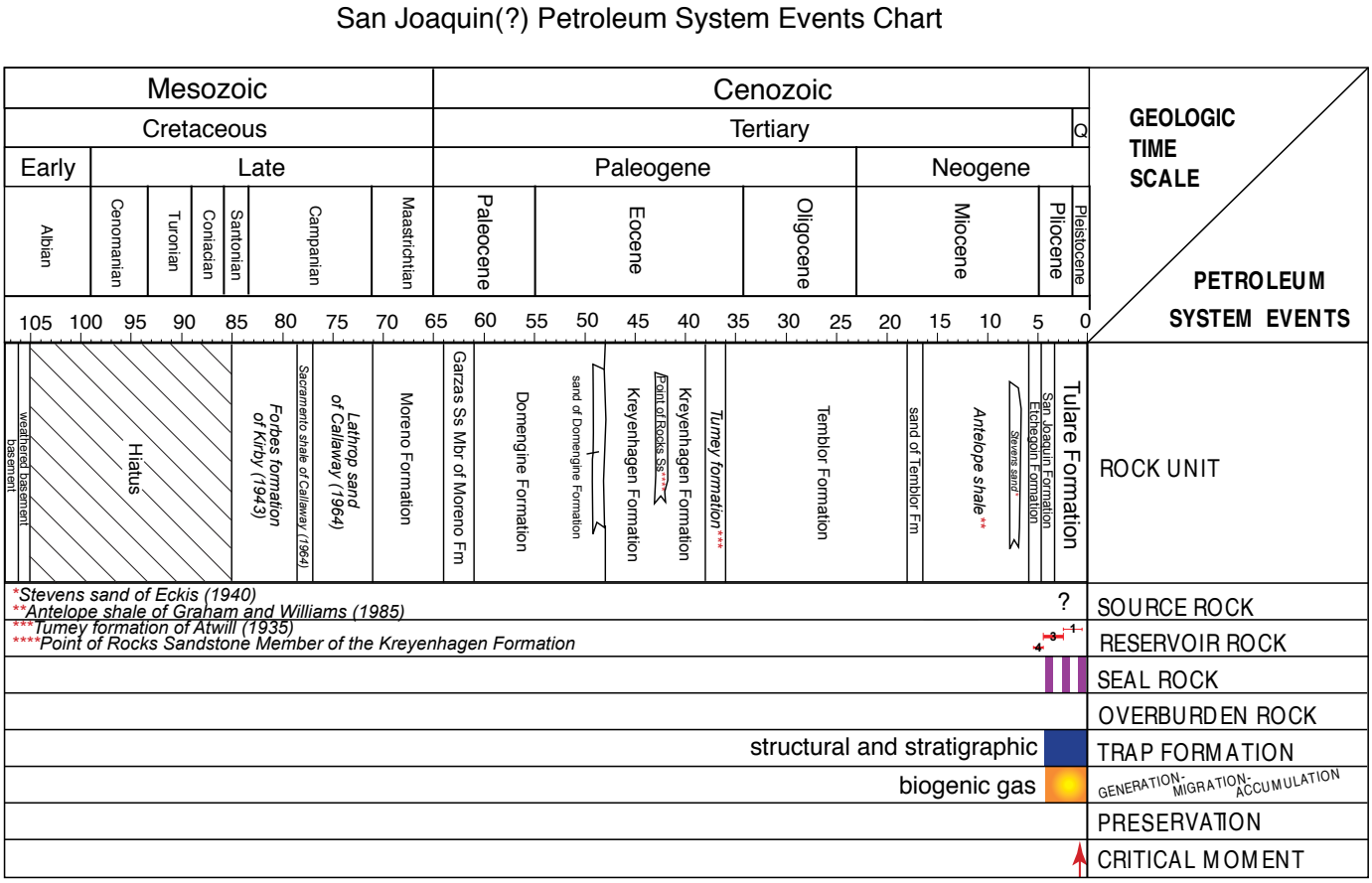

Figure 8.7. Events chart for the San Joaquin(?) petroleum system shows the timing of the essential elements, processes, and critical moment (see Magoon and Dow, 1994, for more information). In this system, petroleum generation-migration-accumulation is microbial, rather than thermal, in origin as in the other petroleum systems. The numbers on the lines in the reservoir rock item refer to the reservoir numbers in table 8.5; the relative thickness of the lines is proportional to the volume of gas in known pools. If relevant, in this and all other events charts, gray rectangles indicate source rocks, purple rectangles indicate seal rocks, orange rectangles indicate overburden rocks, and blue rectangles indicate traps. Formation names in italics are informal. Fm, Formation; Mbr, Member; Q, Quaternary; Ss, Sandstone.

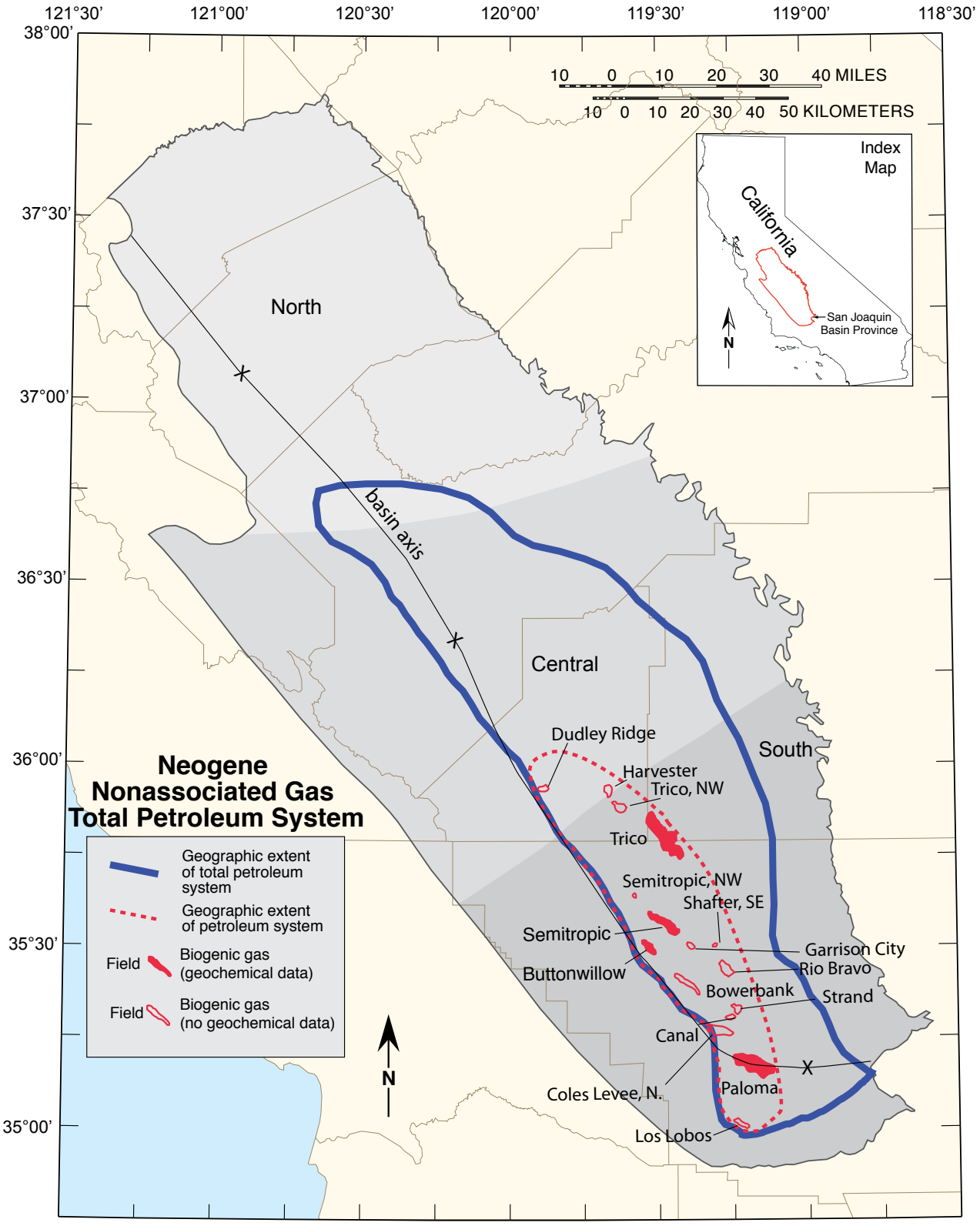

Figure 8.8. Neogene Nonassociated Gas Total Petroleum System map shows the area beyond the geographic extent of the San Joaquin(?) petroleum system, shown by the dashed red line, where undiscovered biogenic gas accumulations may be found. As in figure 8.3, gas accumulations in this petroleum system are shown in red; solid polygons indicate biogenic gas accumulations based on geochemical analysis, whereas outlines indicate suspected biogenic accumulations from stratigraphic proximity.

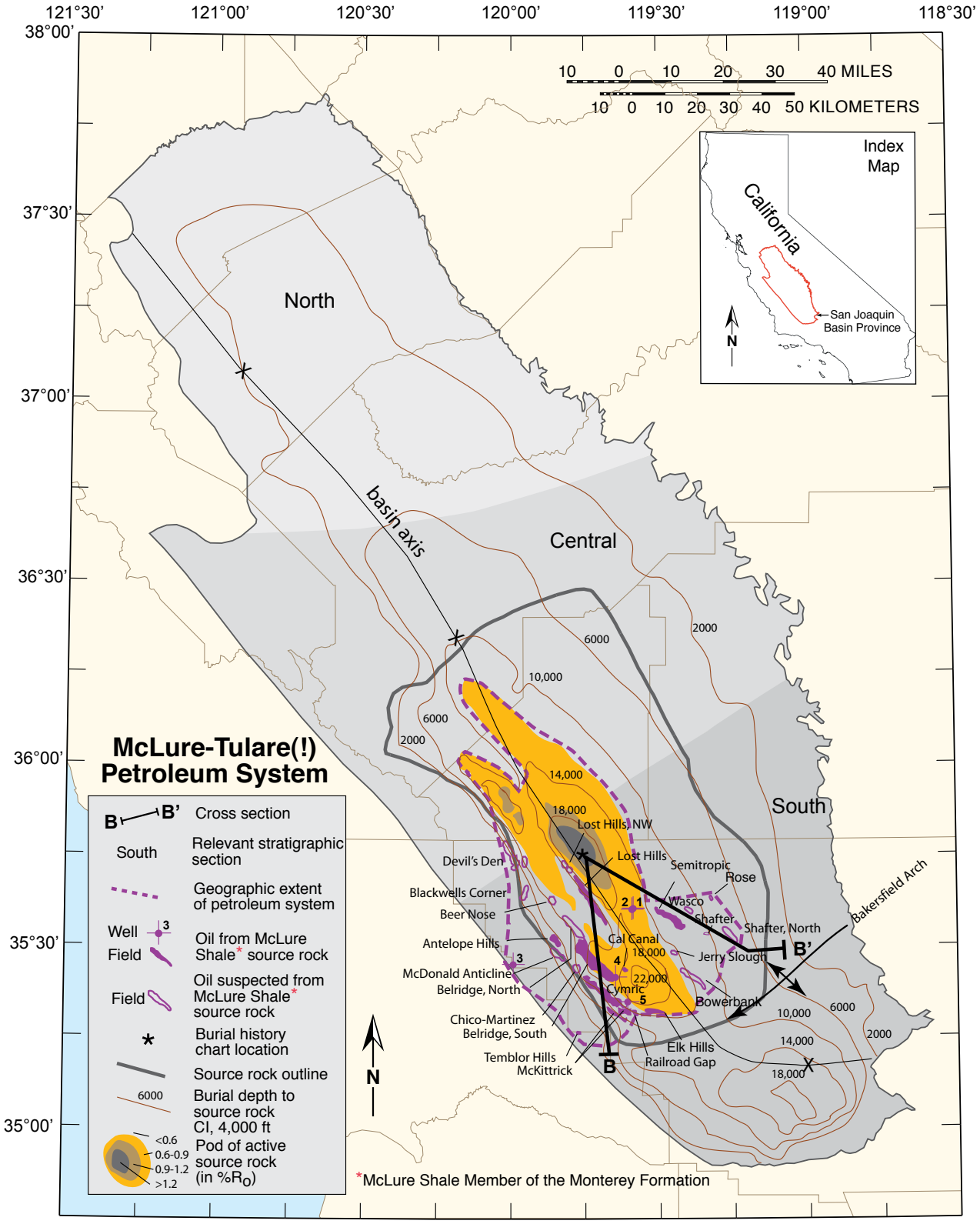

Figure 8.9. The McLure-Tulare(!) petroleum system map shows the present-day burial depth of the known source rock—the McLure Shale Member of the Monterey Formation (brown contours)—as well as the extent of the source rock thought to have good source rock qualities (such as facies, hydrogen index, and total organic carbon; gray line), location of cross section B-B', location(*) of burial history chart, and a purple dashed line indicating the geographic extent of the system. Petroleum accumulations in this system are shown in purple; solid polygons indicate accumulations based on geochemical analysis, whereas outlines indicate suspected accumulations based on stratigraphic proximity. CI, contour interval; $\%R_o$, percent vitrinite reflectance.

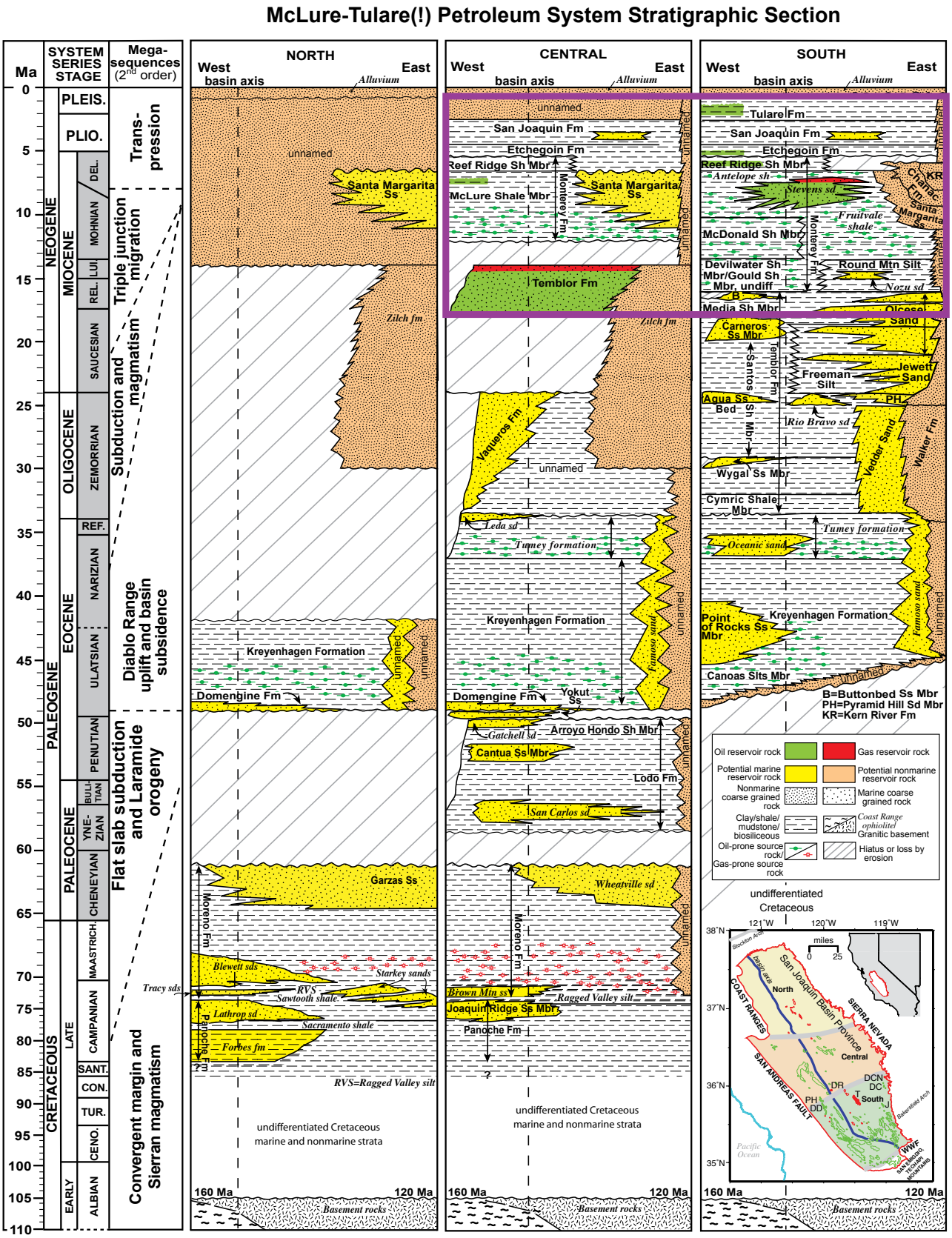

Figure 8.10. Stratigraphic column shown in figure 8.2, but with petroleum source rock and reservoir rocks for the McLure-Tulare(!) petroleum system (purple outline) on the central and south regions of the stratigraphic section.

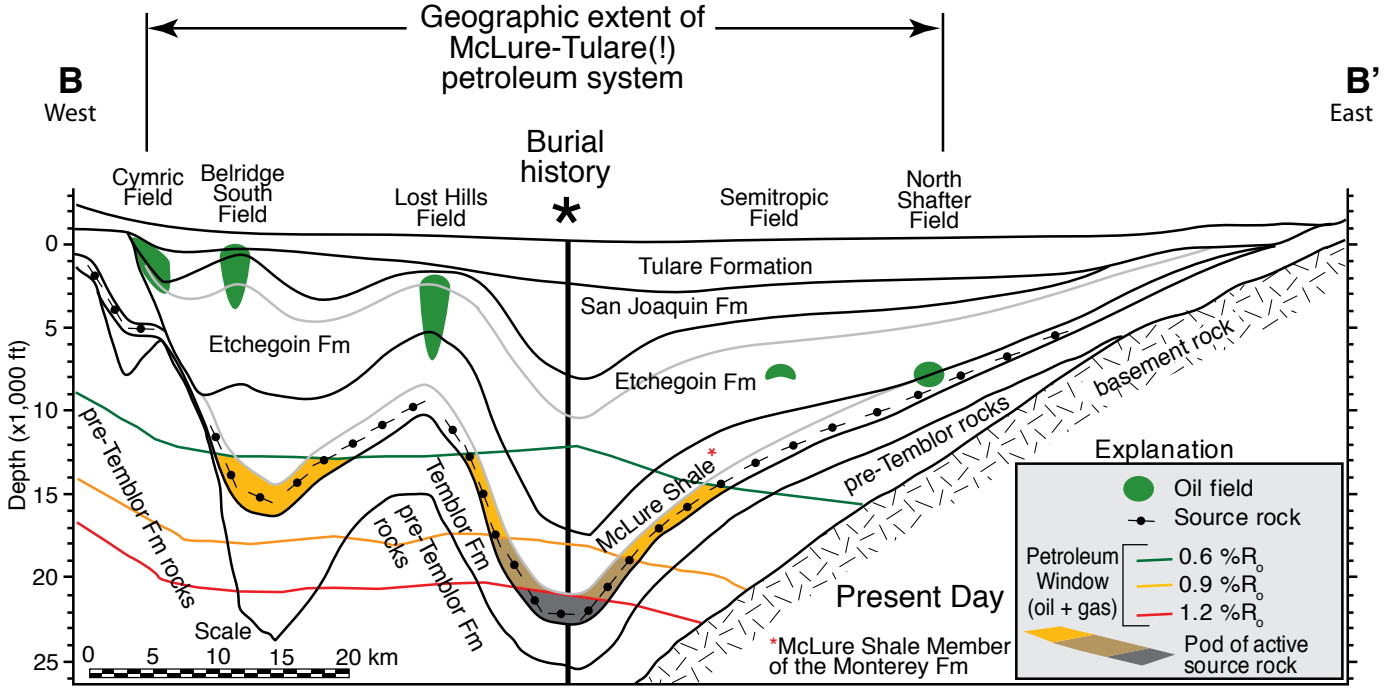

Figure 8.11. Cross section B-B' showing geographic extent of the McLure-Tulare(!) petroleum system, the location of the burial history chart (vertical line; location also shown on map in fig. 8.9 and chart shown in fig. 8.12), the McLure Shale source rock interval (circle-bar pattern), the petroleum window, pod of active source rock (warm shading), and the stratigraphic units that contains the petroleum accumulations in known fields (green blobs). Stratigraphic depth contours and vitrinite reflectance contours (%R_o) are derived from the San Joaquin Basin model of Peters, Magoon, Lampe, and others (this volume, chapter 12). Fm, Formation.

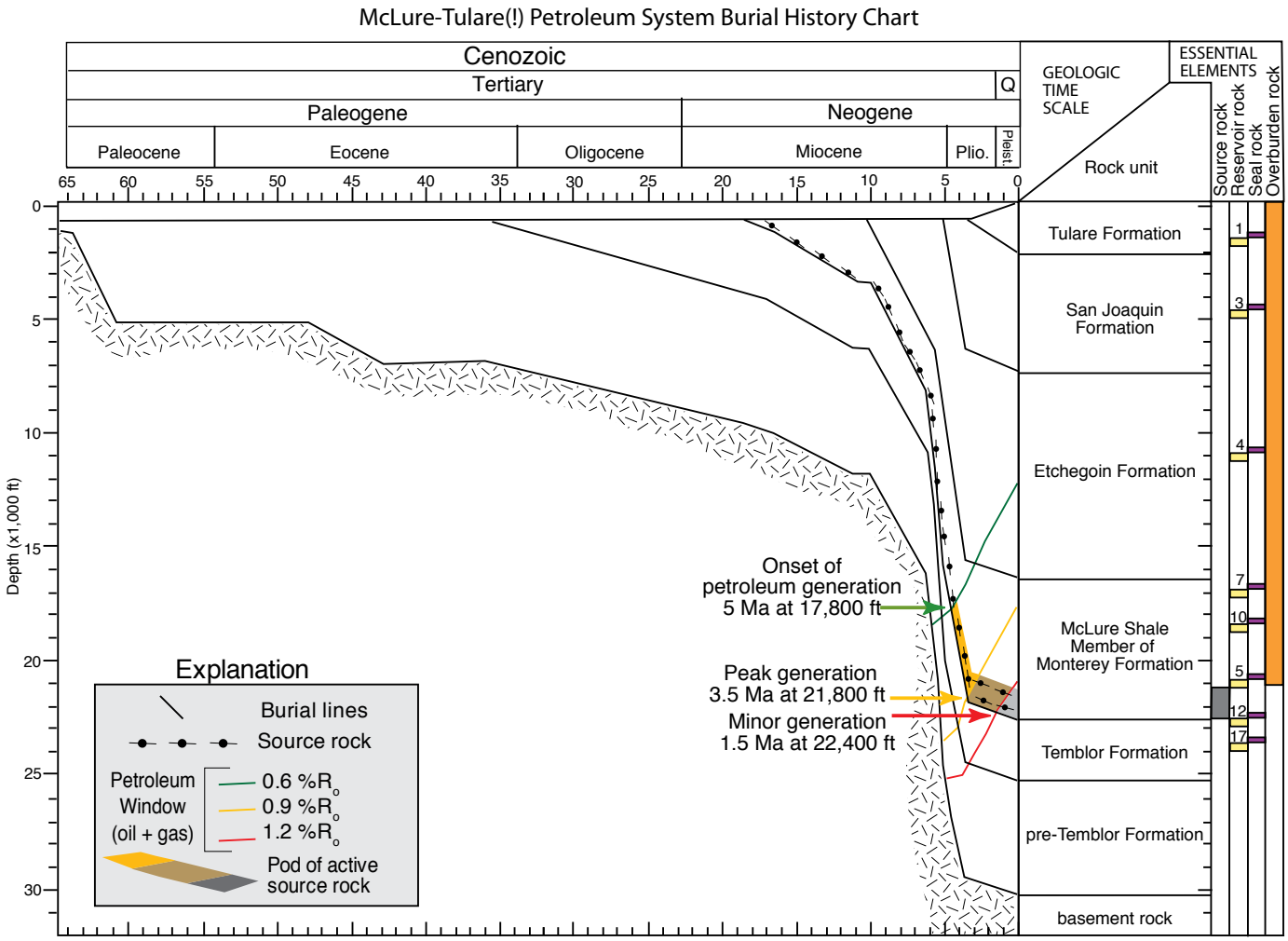

Figure 8.12. Burial history chart for the McLure-Tulare(!) petroleum system shows the onset of petroleum generation at 5 Ma, peak generation at 3.5 Ma, and source rock depletion at 1.5 Ma. The pod of active source rock is indicated by warm shading. The numbers overlying yellow rectangles in the reservoir rock column refer to the reservoir rock numbers in table 8.6 and appendix 8.2. Pleist., Pleistocene; Plio., Pliocene; Q, Quaternary; $\%R_o$, percent vitrinite reflectance.

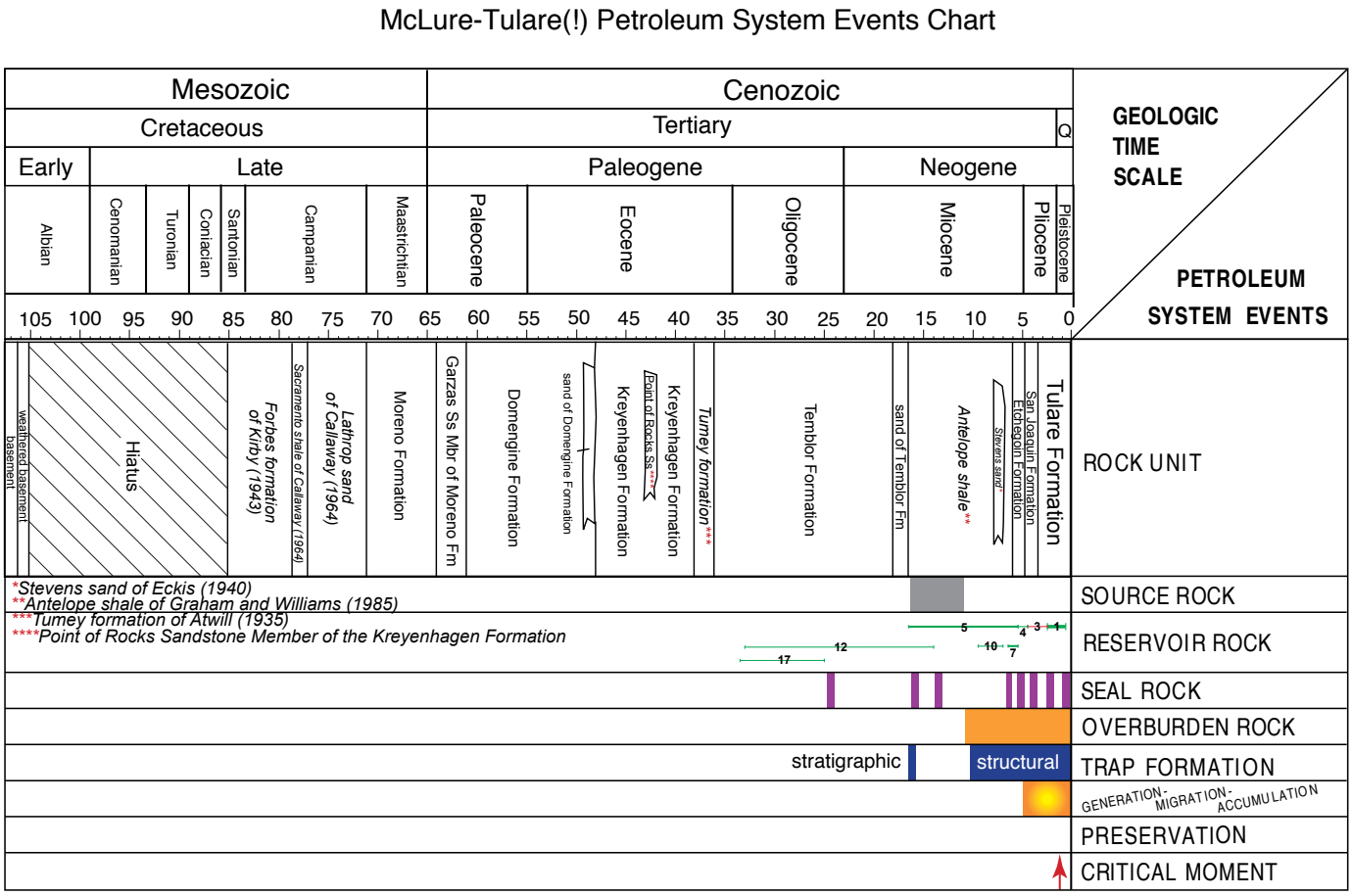

Figure 8.13. Events chart for the McLure-Tulare(!) petroleum system shows the timing of the essential elements and processes of this petroleum system. Note that trap development occurred before and during petroleum migration. The numbers on the lines in the reservoir rock item refer to the reservoir numbers in table 8.6; the relative thickness of the lines is proportional to the volume of gas (red) or oil (green) in known pools. Formation names in italics are informal. Fm, Formation; Mbr, Member; Q, Quaternary; Ss, Sandstone.

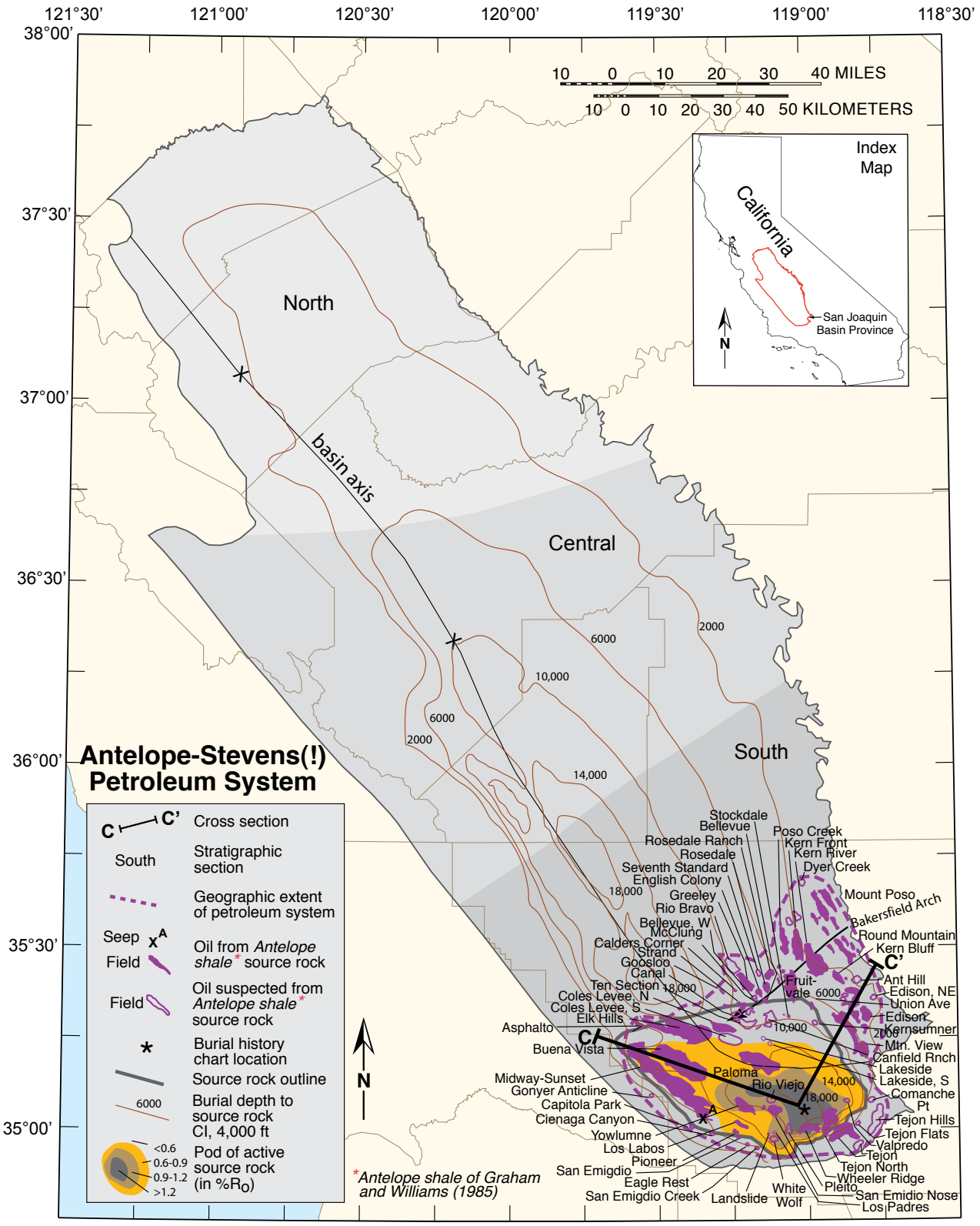

Figure 8.14. The Antelope-Stevens(!) petroleum system map shows the present-day burial depth of the known source rock—the Antelope shale (brown contours)—as well as the extent of the source rock thought to have good source rock qualities (such as facies, hydrogen index, and total organic carbon; gray line), location of cross section C-C', location(*) of burial history chart, and a purple dashed line indicating the geographic extent of the system. Petroleum accumulations in this system are shown in purple; solid polygons indicate accumulations based on geochemical analysis, whereas outlines indicate suspected accumulations based on stratigraphic proximity. Seep location is from Cole and others (1999). CI, contour interval; $\%R_o$, percent vitrinite reflectance.

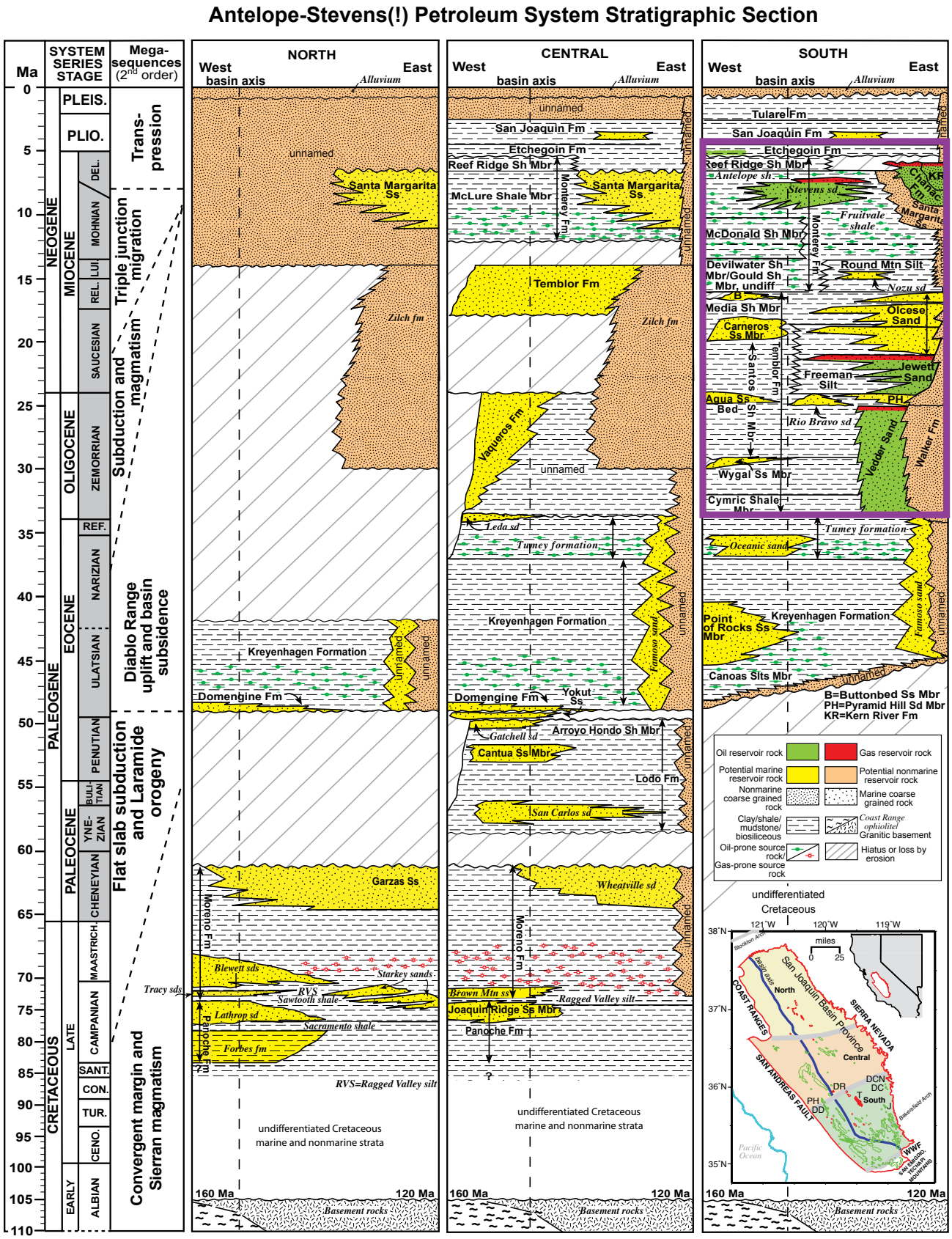

Figure 8.15. Stratigraphic column shown in figure 8.2, but with petroleum source rock and reservoir rocks for the Antelope-Stevens(!) petroleum system (purple outline) on the south region of the stratigraphic section.

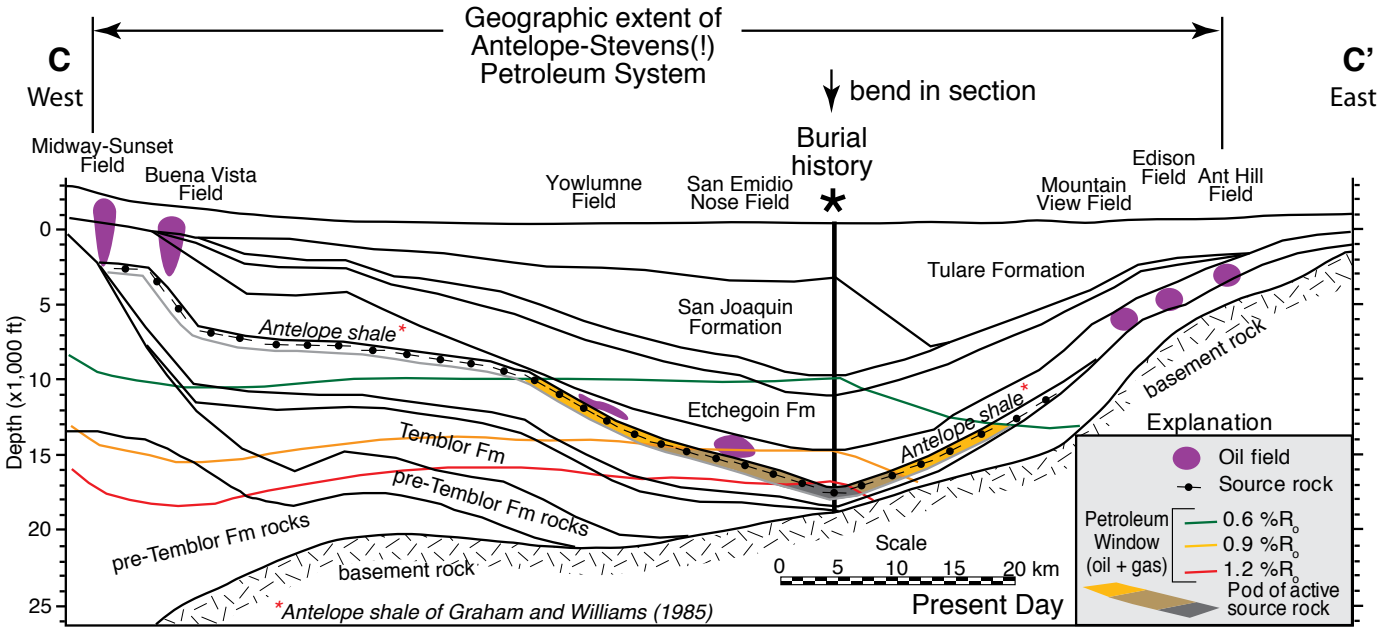

Figure 8.16. Cross section C-C' showing geographic extent of the Antelope-Stevens(!) petroleum system, the location of the burial history chart (vertical line; location also shown on map in fig. 8.14 and chart shown in fig. 8.17), the Antelope shale source rock interval (circle-bar pattern), the petroleum window, pod of active source rock (warm shading), and the stratigraphic units that contain the petroleum accumulations in known fields (purple blobs). Stratigraphic depth contours and vitrinite reflectance contours ($\%R_o$) are derived from the San Joaquin Basin model of Peters, Magoon, Lampe, and others (this volume, chapter 12). Fm, Formation.

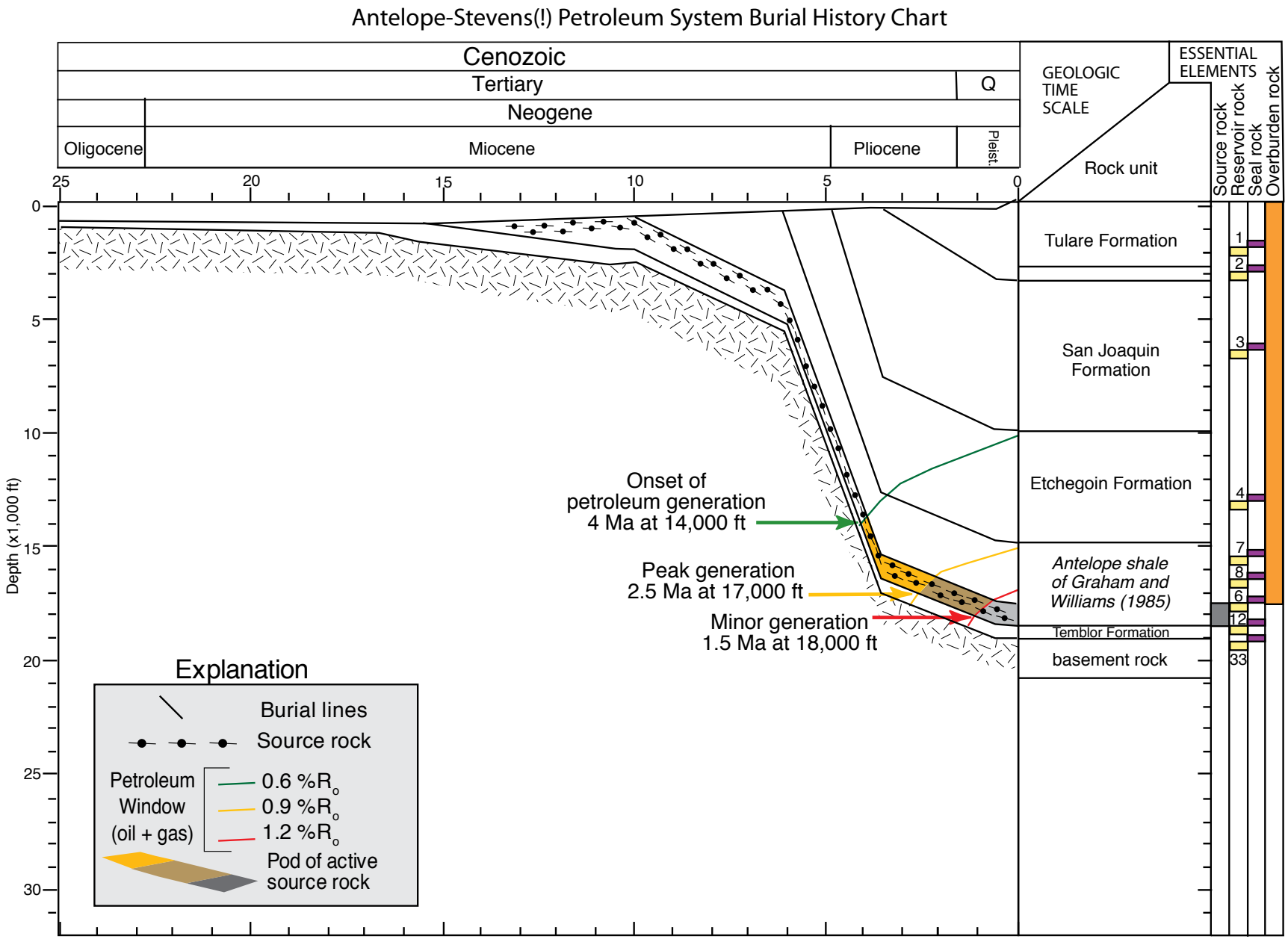

Figure 8.17. Burial history chart for the Antelope-Stevens(!) petroleum system shows the onset of petroleum generation at 4 Ma, peak generation at 2.5 Ma, and source rock depletion at 1.5 Ma. The pod of active source rock is indicated by warm shading. The numbers overlying yellow rectangles in the reservoir rock column refer to the reservoir rock numbers in table 8.7 and appendix 8.2. Pleist., Pleistocene; Q, Quaternary; $\%R_o$, percent vitrinite reflectance.

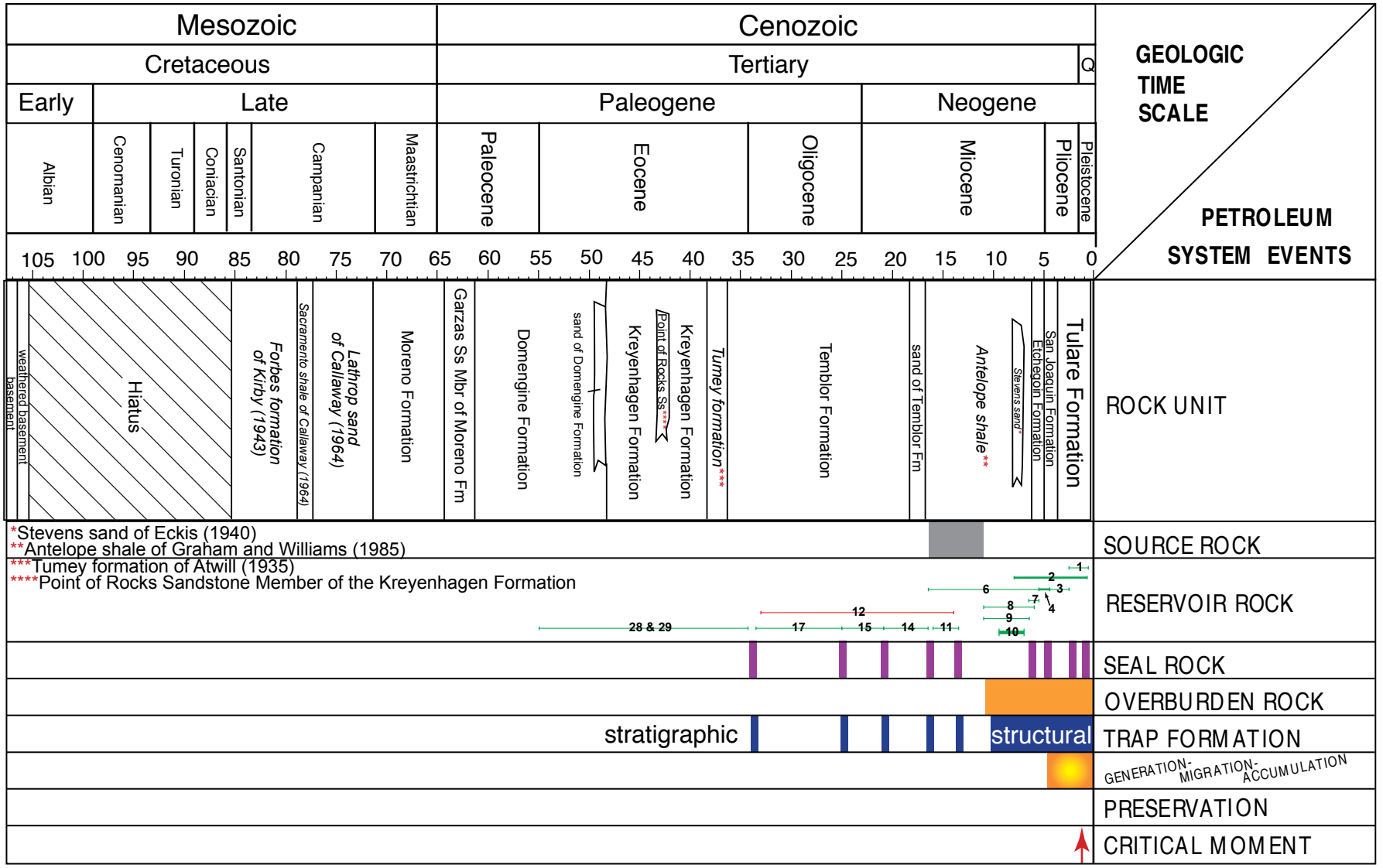

Figure 8.18. Events chart for the Antelope-Stevens(!) petroleum system shows the time of deposition of the essential elements and processes of this petroleum system. Note that trap development occurred before and during petroleum migration. The numbers on the lines in the reservoir rock item refer to the reservoir numbers in table 8.7; the relative thickness of the lines is proportional to the volume of gas (red) or oil (green) in known pools. Formation names in italics are informal. Fm, Formation; Mbr, Member; Q, Quaternary; Ss, Sandstone.

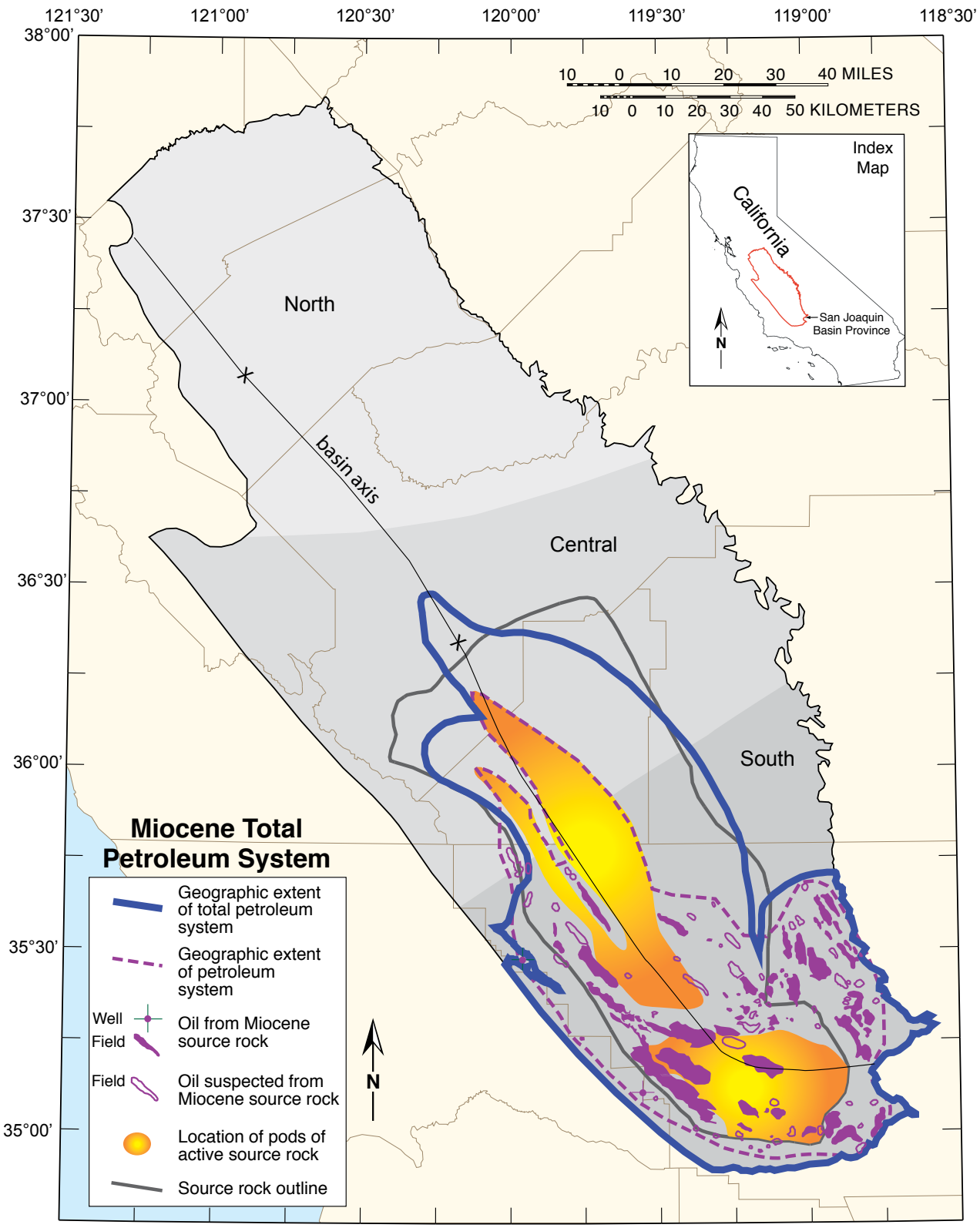

Figure 8.19. Miocene Total Petroleum System map combines the McLure-Tulare(!) and the Antelope-Stevens(!) petroleum systems for the purposes of assessment. Oil accumulations in this petroleum system are shown in purple; solid polygons indicate oil accumulations based on geochemical analysis, whereas outlines indicate suspected accumulations from stratigraphic proximity. Warm shading indicates location of pods of active source rock for the two systems.

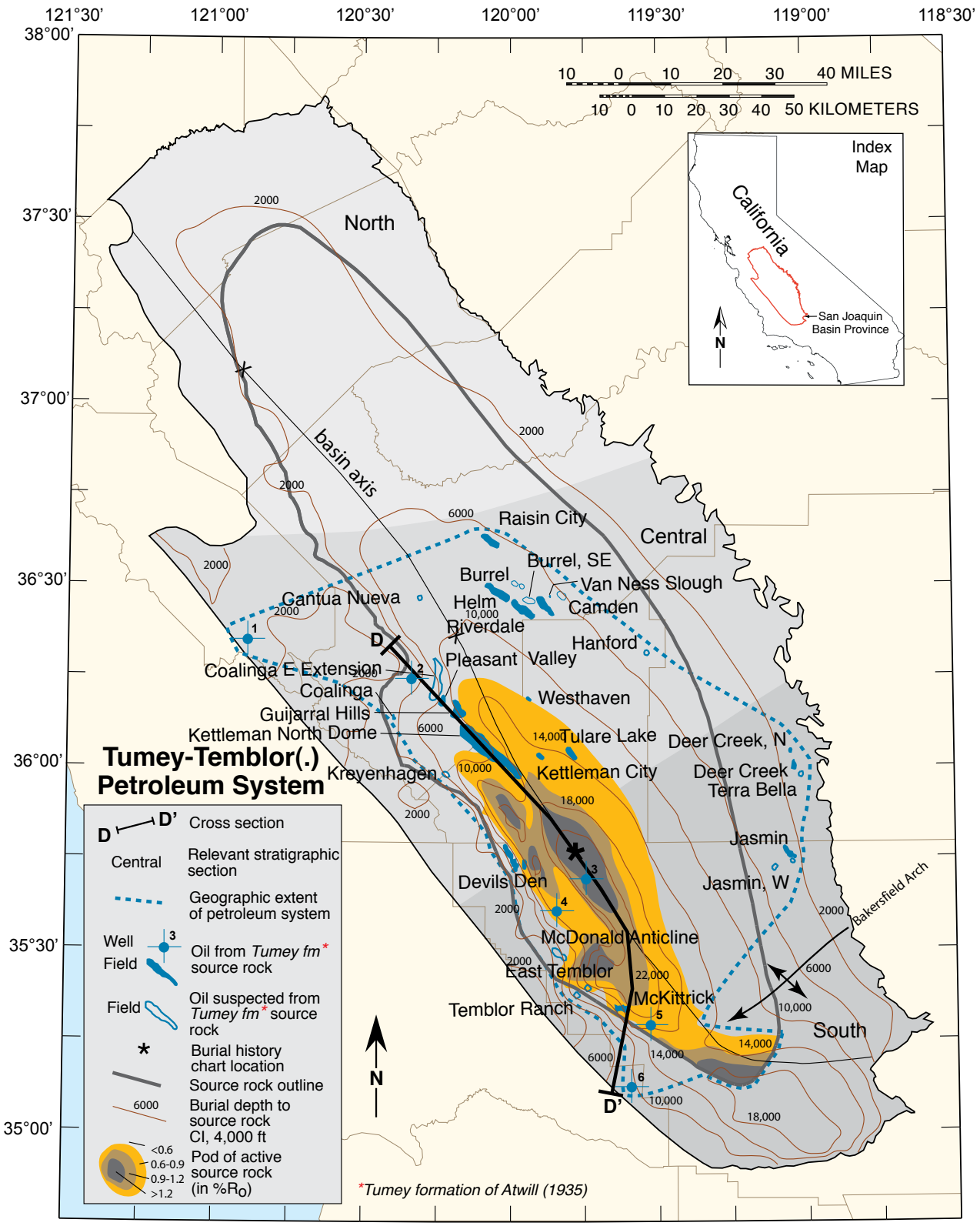

Figure 8.20. Tumey-Temblor(.) petroleum system map shows the present-day burial depth of the hypothetical source rock—the Tumey formation of Atwell (1935; brown contours)—as well as the extent of the source rock thought to have good source rock qualities (such as facies, hydrogen index, and total organic carbon; gray line), location of cross section D-D', location(*) of burial history chart, and a blue dashed line indicating the geographic extent of the system. Petroleum accumulations in this system are shown in blue; solid polygons indicate accumulations based on geochemical analysis, whereas outlines indicate suspected accumulations based on stratigraphic proximity. CI, contour interval; fm, formation; $\%R_o$, percent vitrinite reflectance.

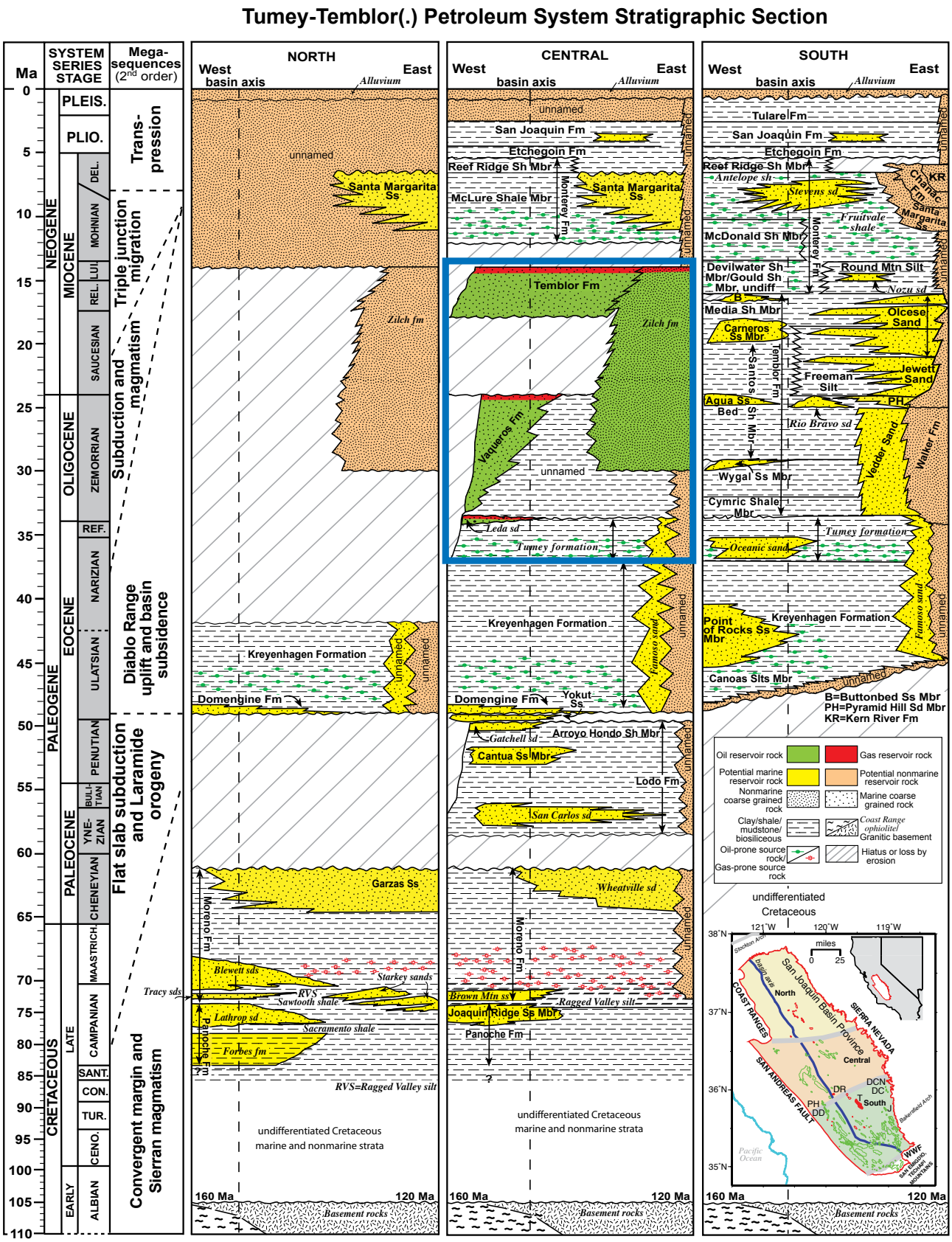

Figure 8.21. Stratigraphic column shown in figure 8.2, but with petroleum source rock and reservoir rocks for the Tumey-Temblor(.) petroleum system (blue outline) on the central region of the stratigraphic section.

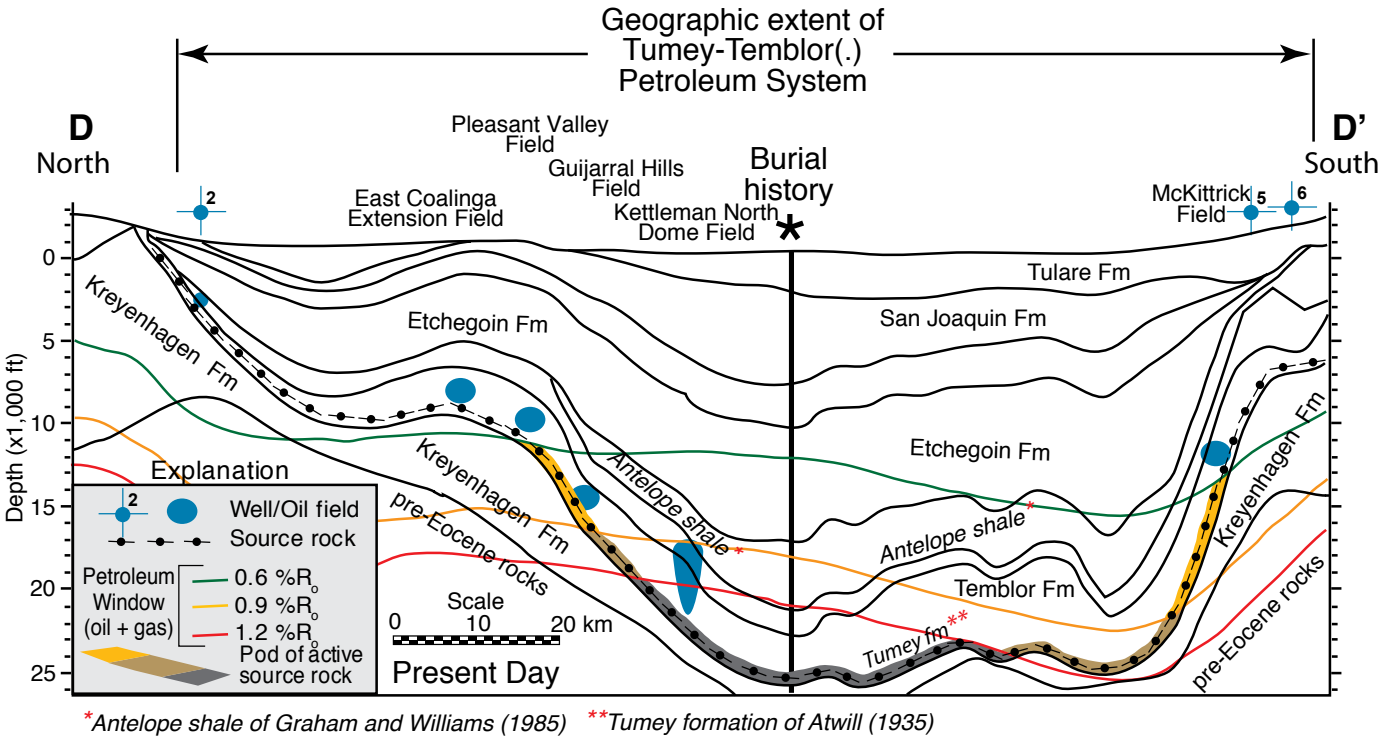

Figure 8.22. Cross section D-D' showing geographic extent of the Tumey-Temblor(.) petroleum system, the location of the burial history chart (vertical line; location also shown on map in fig. 8.20 and chart shown in fig. 8.23), the Tumey formation source rock interval (circle-bar pattern), the petroleum window, pod of active source rock (warm shading), and the stratigraphic units that contain the petroleum accumulations in known fields (blue blobs). Stratigraphic depth contours and vitrinite reflectance contours ($\%R_o$) are derived from the San Joaquin Basin model of Peters, Magoon, Lampe, and others (this volume, chapter 12). Fm, Formation; fm, formation.

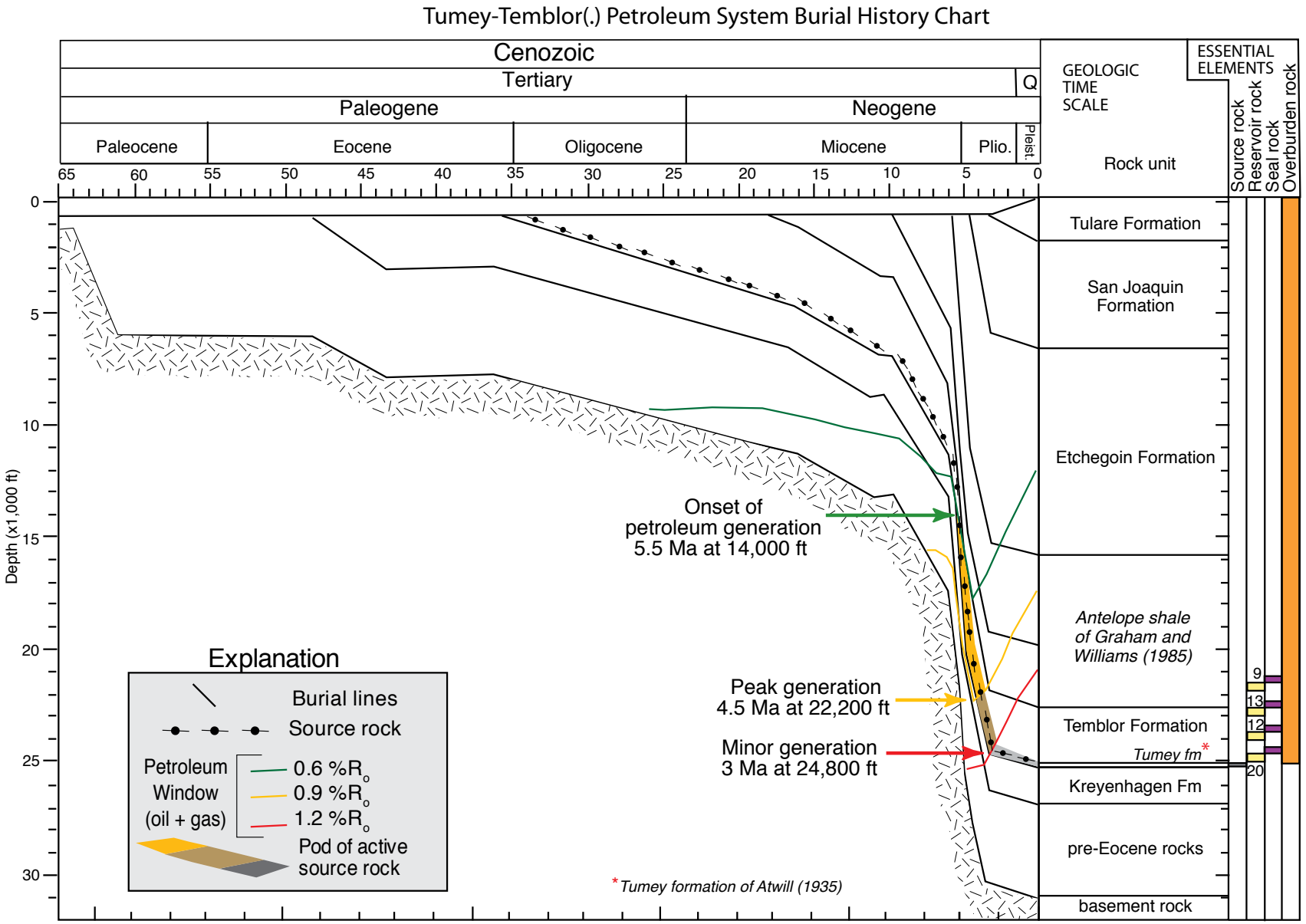

Figure 8.23. Burial history chart for the Tumey-Temblor(.) petroleum system shows the onset of petroleum generation at 5.5 Ma, peak generation at 4.5 Ma, and source rock depletion at 3 Ma. The pod of active source rock is indicated by warm shading. The numbers overlying yellow rectangles in the reservoir rock column refer to the reservoir numbers in table 8.8 and appendix 8.2. Fm, Formation; fm, formation; Pleist., Pleistocene; Plio., Pliocene; Q, Quaternary; $\%R_o$, percent vitrinite reflectance.

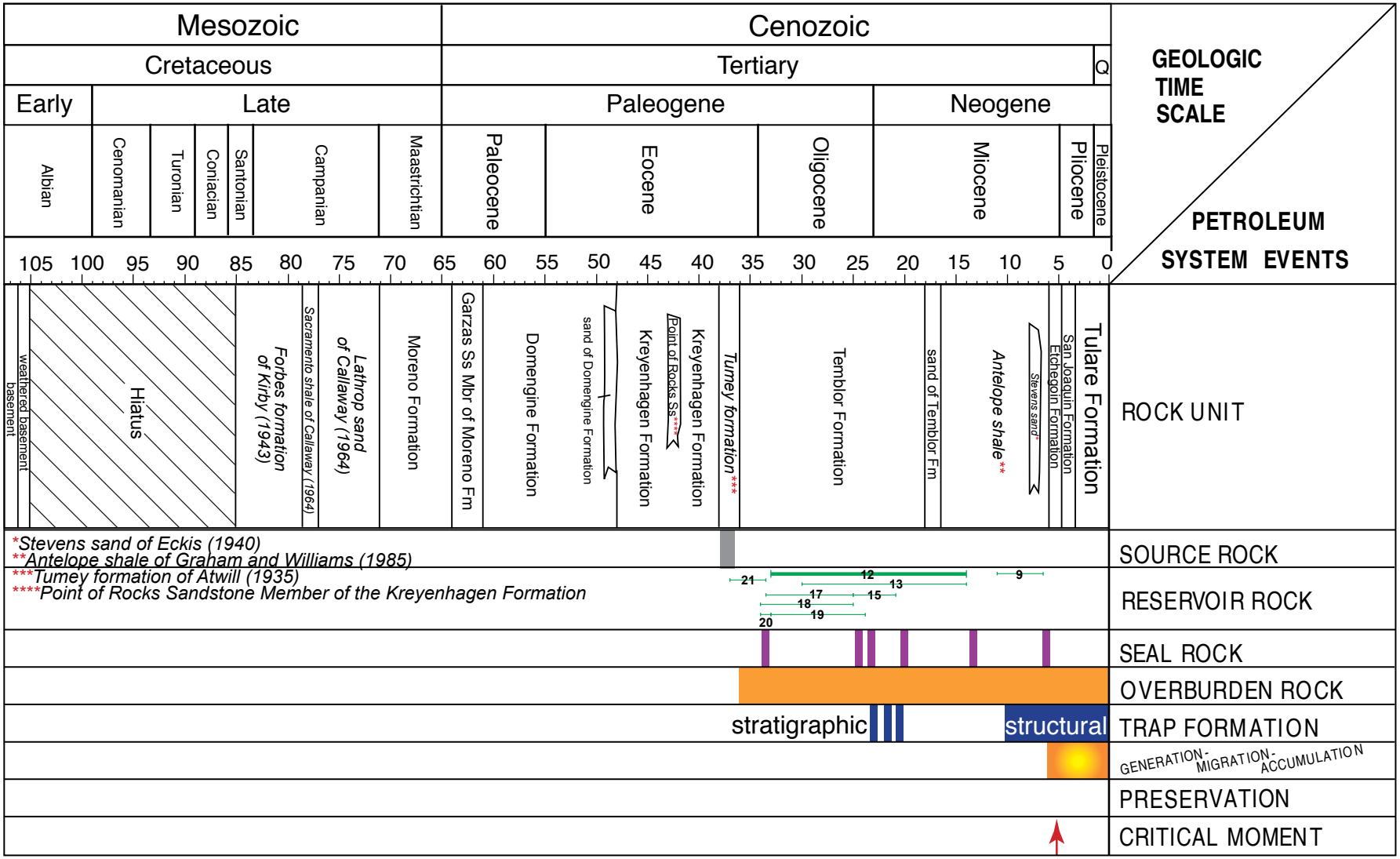

Figure 8.24. Events chart for the Tumey-Temblor(.) petroleum system shows the time of deposition of the essential elements and processes of this petroleum system. Note that trap development occurred before and during petroleum migration. The numbers on the lines in the reservoir rock item refers to the reservoir numbers in table 8.8; the relative thickness of the lines is proportional to the volume of oil (green) in known pools. Formation names in italics are informal. Fm, Formation; Mbr, Member; Q, Quaternary; Ss, Sandstone.

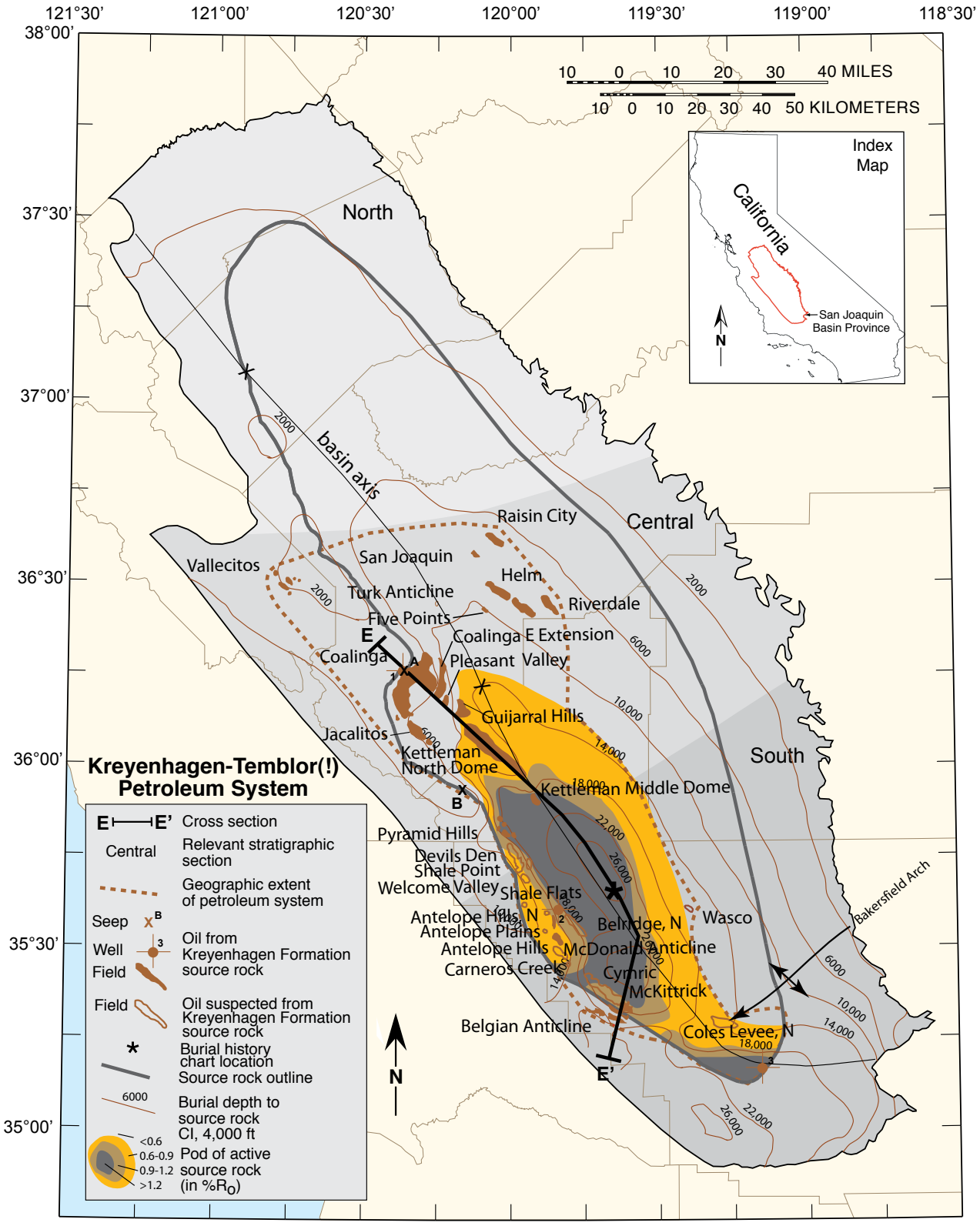

Figure 8.25. Kreyenhagen-Temblor(!) petroleum system map shows the present-day burial depth of the known source rock—the Kreyenhagen Formation (brown contours)—as well as the extent of the source rock thought to have good source rock qualities (such as facies, hydrogen index, and total organic carbon; gray line), location of cross section E-E', location(*) of burial history chart, and a brown dashed line indicating the geographic extent of the system. Petroleum accumulations in this system are shown in brown; solid polygons indicate accumulations based on geochemical analysis, whereas outlines indicate suspected accumulations based on stratigraphic proximity. Seep location is from Cole and others (1999). CI, contour interval; $\%R_o$, percent vitrinite reflectance.

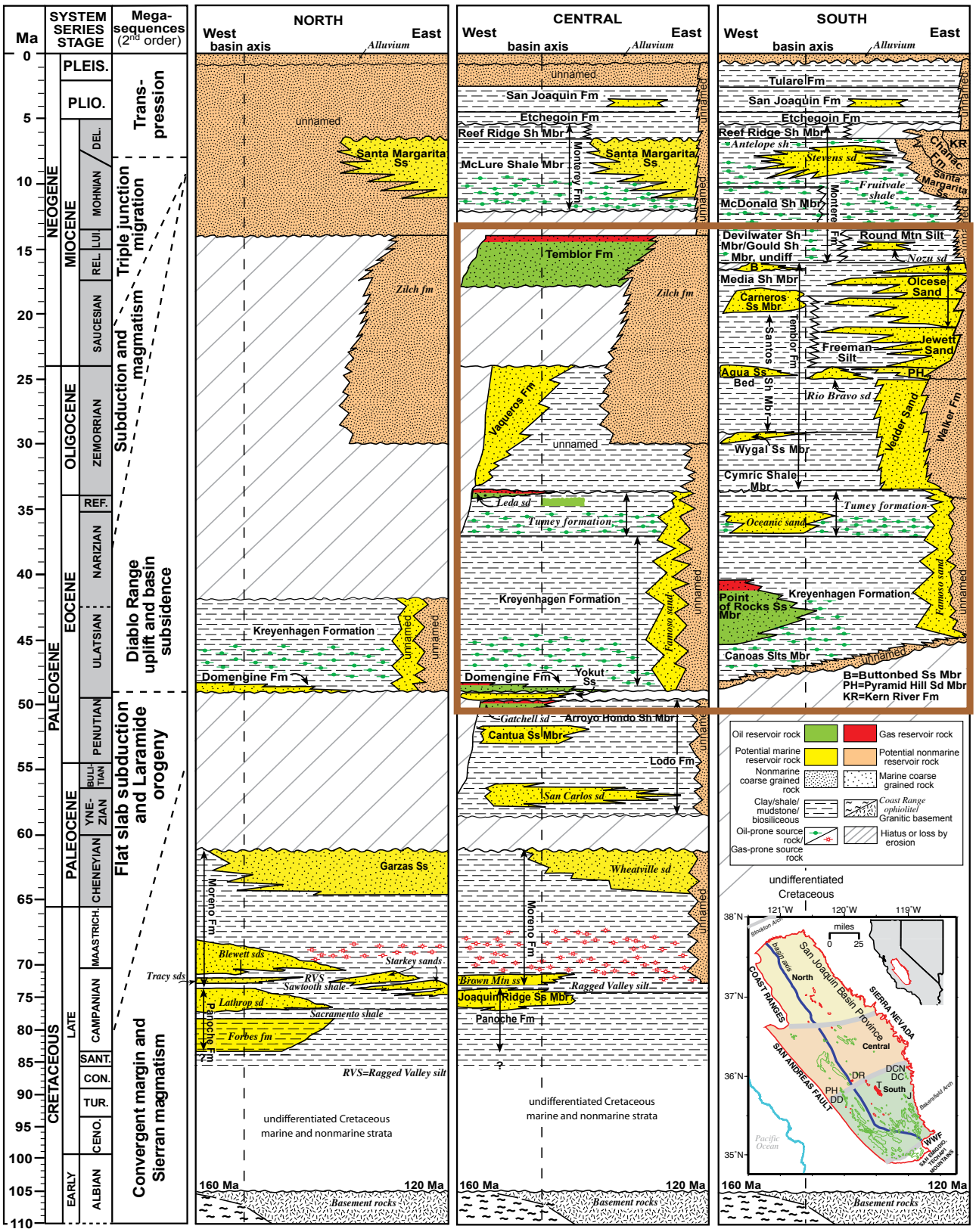

Figure 8.26. Stratigraphic column shown in figure 8.2, but with petroleum source rock and reservoir rocks for the Kreyenhagen-Temblor(!) petroleum system (brown outline) on the central and south regions of the stratigraphic section.

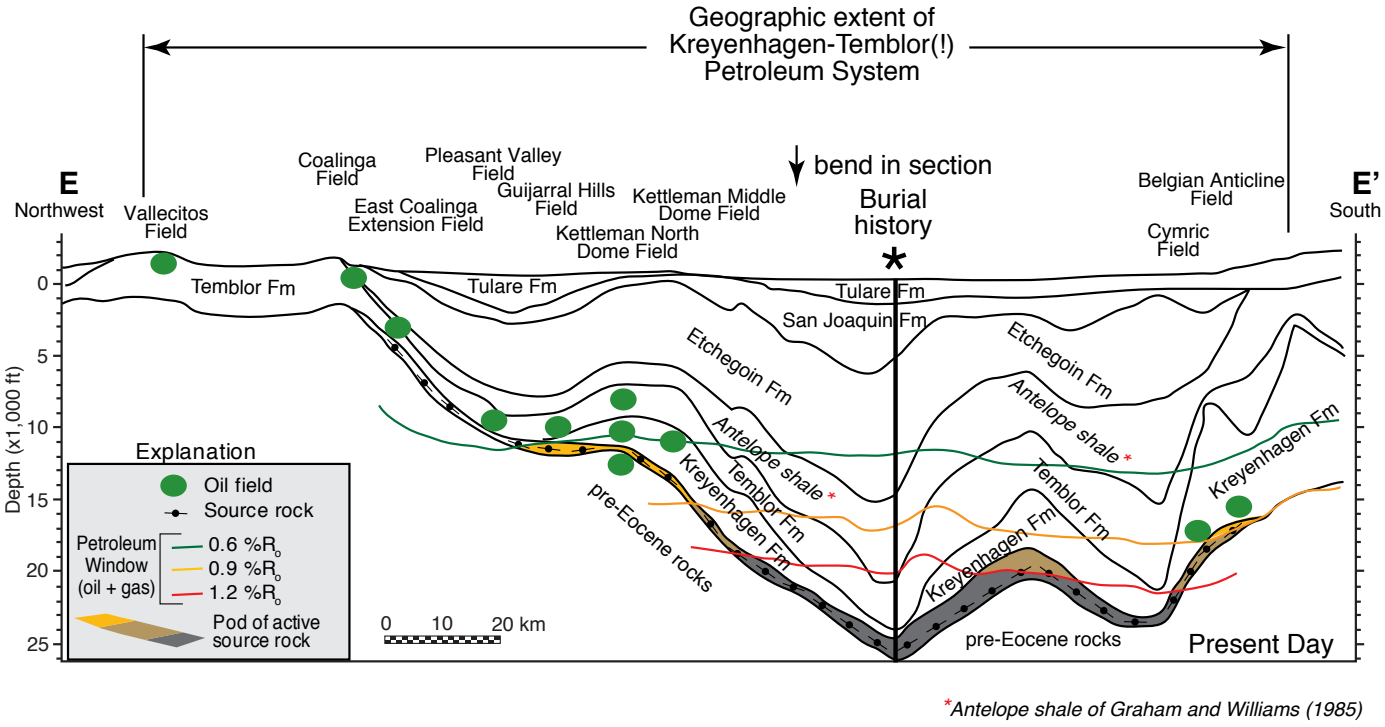

Figure 8.27. Cross section E-E′ showing geographic extent of the Kreyenhagen-Temblor(!) petroleum system, the location of the burial history chart (vertical line; location also shown on map in fig. 8.25 and chart shown in fig. 8.28), the Kreyenhagen Formation source rock interval (circle-bar pattern), the petroleum window, pod of active source rock (warm shading), and the stratigraphic units that contain the petroleum accumulations in known fields (green blobs). Stratigraphic depth contours and vitrinite reflectance contours (%R_o) are derived from the San Joaquin Basin model of Peters, Magoon, Lampe, and others (this volume, chapter 12). Fm, Formation.

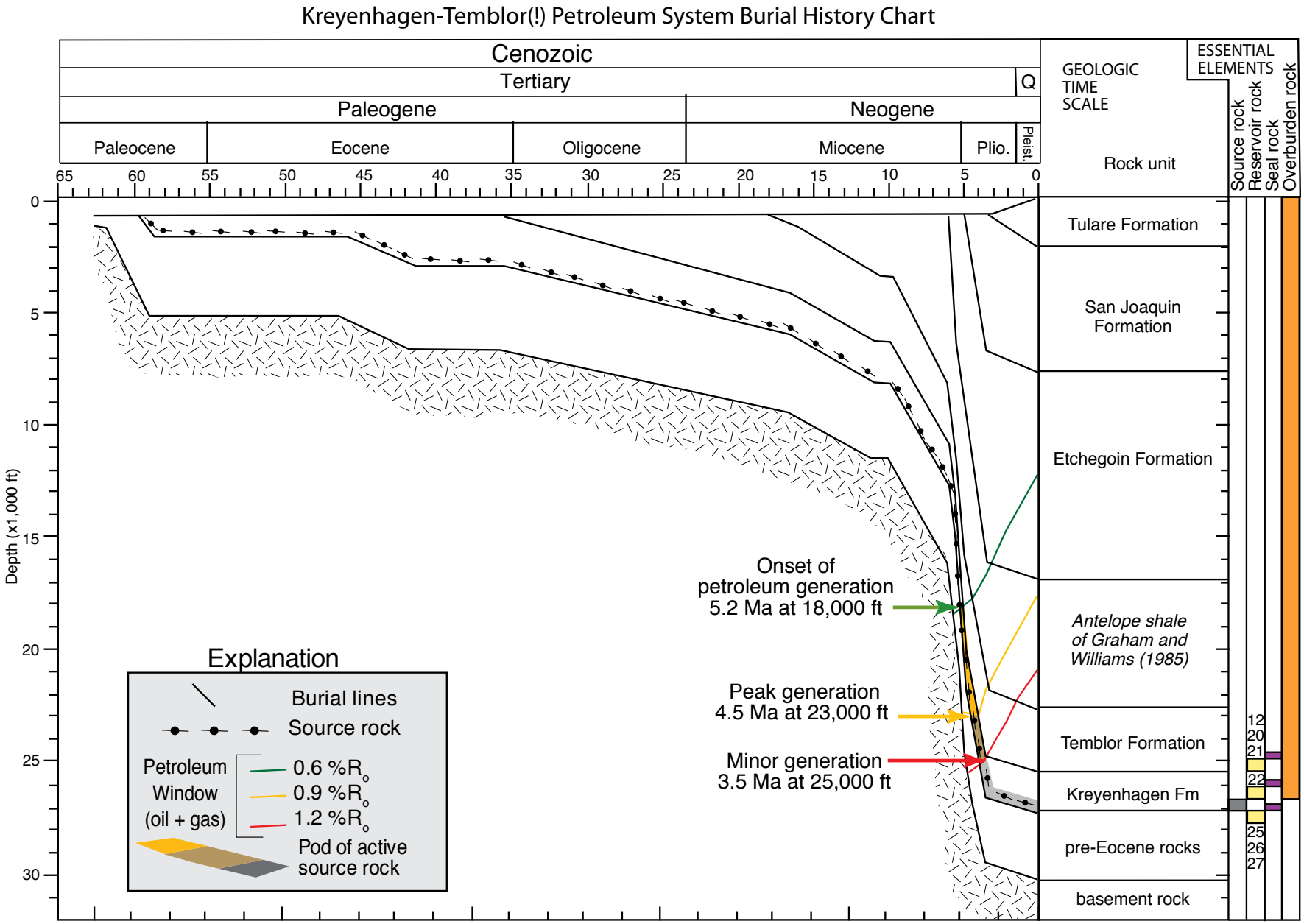

Figure 8.28. Burial history chart for the Kreyenhagen-Temblor(!) petroleum system shows the onset of petroleum generation at 5.2 Ma, peak generation at 4.5 Ma, and source rock depletion at 3.5 Ma. The pod of active source rock is indicated by warm shading. The numbers overlying yellow rectangles in the reservoir rock column refer to the reservoir numbers in table 8.9 and appendix 8.2. Fm, Formation; Pleist., Pleistocene; Plio., Pliocene; Q, Quaternary; $\%R_o$, percent vitrinite reflectance.

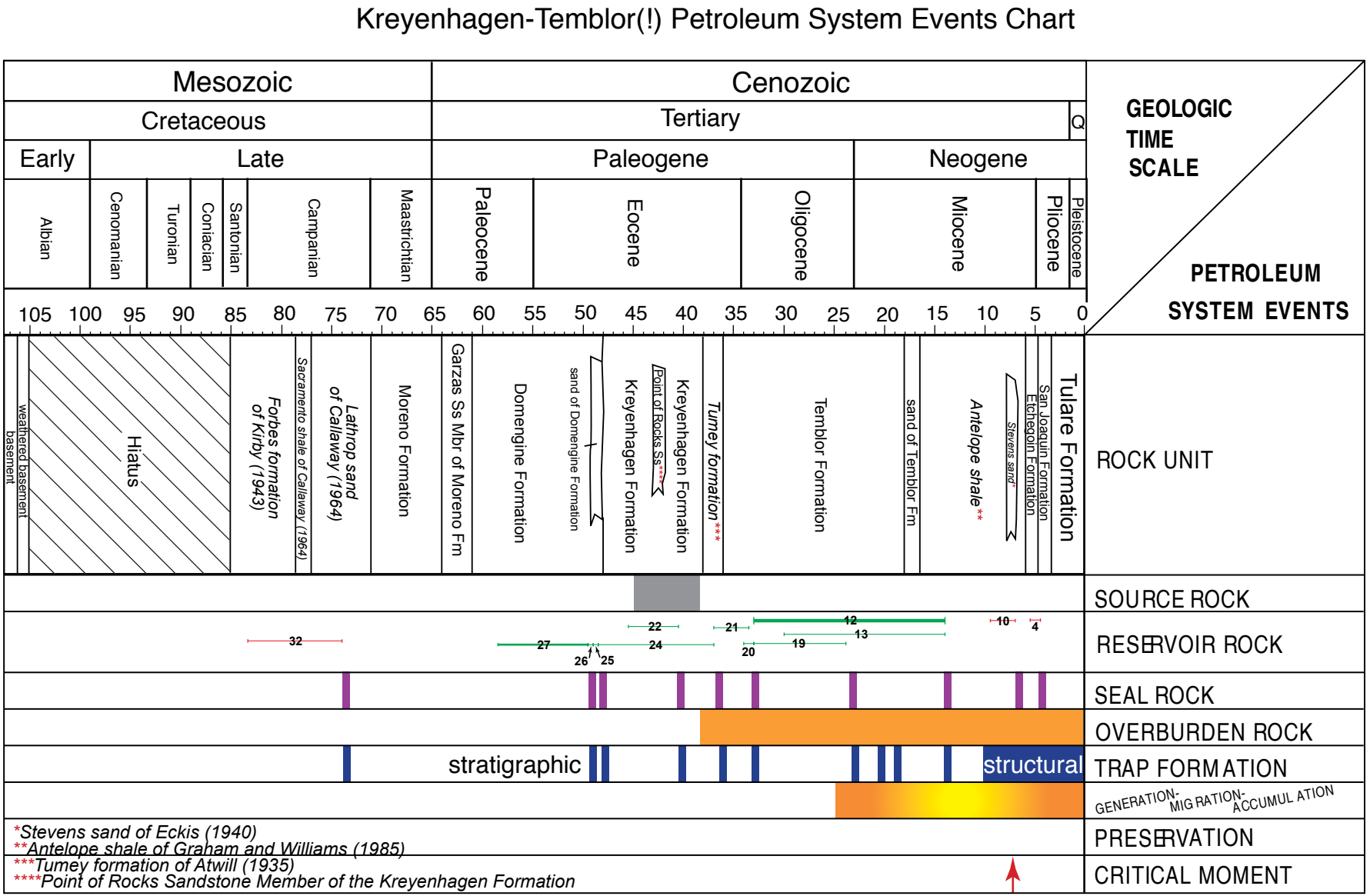

Figure 8.29. Events chart for the Kreyenhagen-Temblor(!) petroleum system shows the time of deposition of the essential elements and processes of this petroleum system. Note that trap development occurred before and during petroleum migration. The numbers on the lines in the reservoir rock item refers to the reservoir numbers in table 8.9; the relative thickness of the lines is proportional to the volume of oil (green) and gas (red) in known pools. Formation names in italics are informal. Fm, Formation; Mbr, Member; Q, Quaternary; Ss, Sandstone.

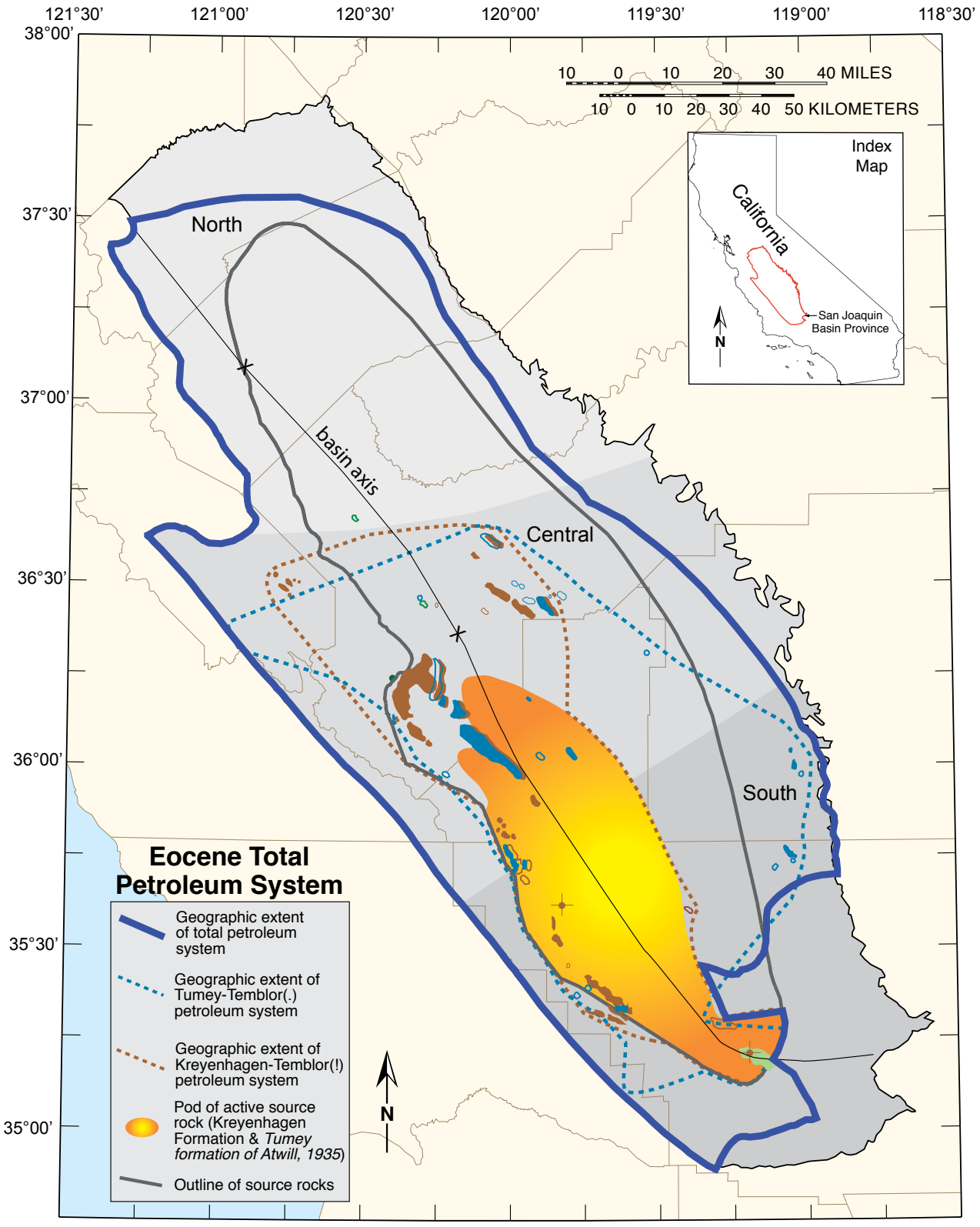

Figure 8.30. Eocene Total Petroleum System map combines the Tumey-Temblor(.) and the Kreyenhagen-Temblor(!) petroleum systems for the purposes of assessment. Oil accumulations in this petroleum system are shown in blue and brown; solid polygons indicate oil accumulations based on geochemical analysis, whereas outlines indicate suspected accumulations from stratigraphic proximity. Warm shading indicates location of pod of active source rock for the two systems.

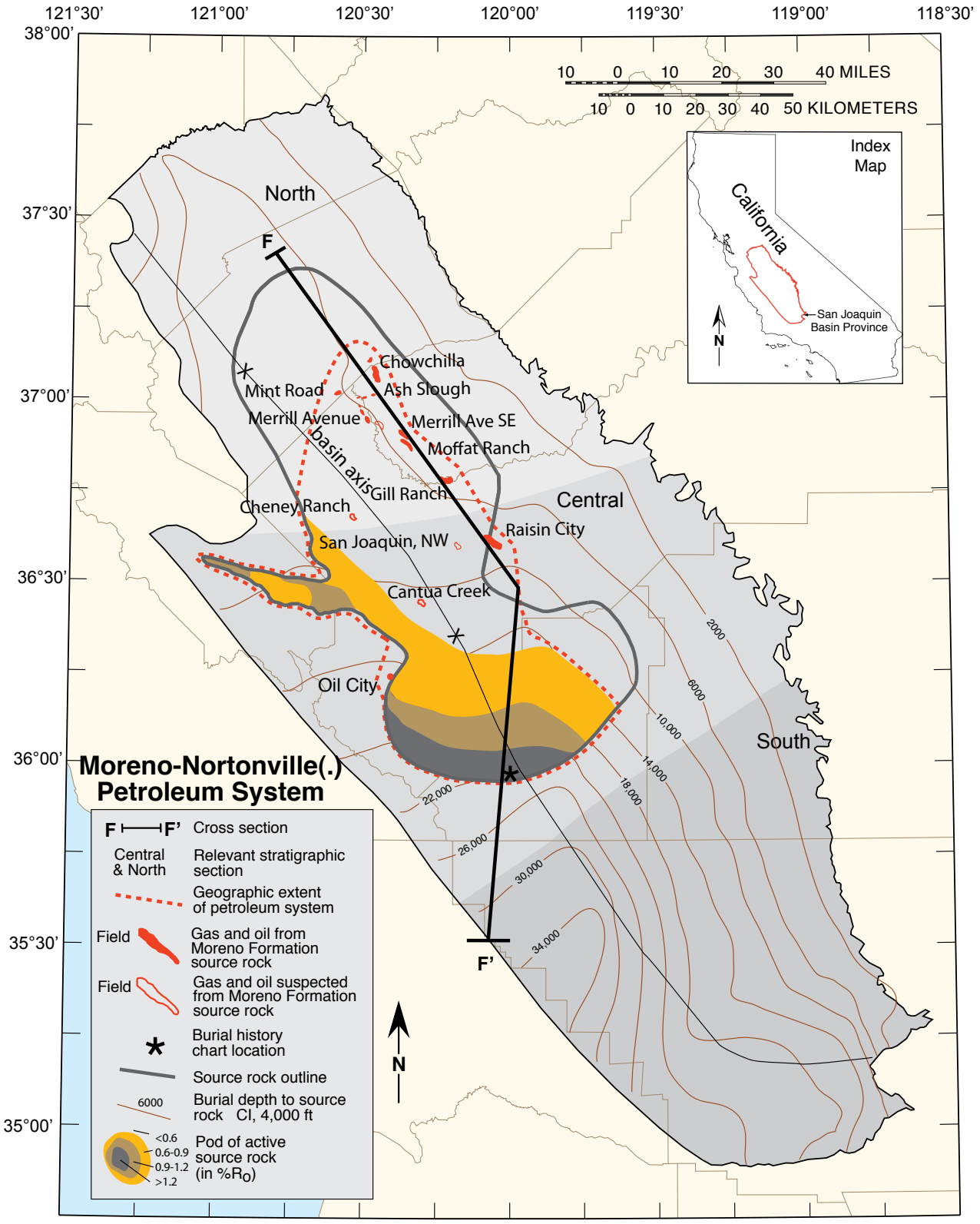

Figure 8.31. Moreno-Nortonville(.) petroleum system map shows the present-day burial depth of the hypothetical source rock—the Moreno Formation (brown contours)—as well as the extent of the source rock thought to have good source rock qualities (such as facies, hydrogen index, and total organic carbon; gray line), location of cross section F-F', location(*) of burial history chart, and a red dashed line indicating the geographic extent of the system. Petroleum accumulations in this system are shown in red; solid polygons indicate accumulations based on geochemical analysis, whereas outlines indicate suspected accumulations based on stratigraphic proximity. CI, contour interval; $\%R_o$, percent vitrinite reflectance.

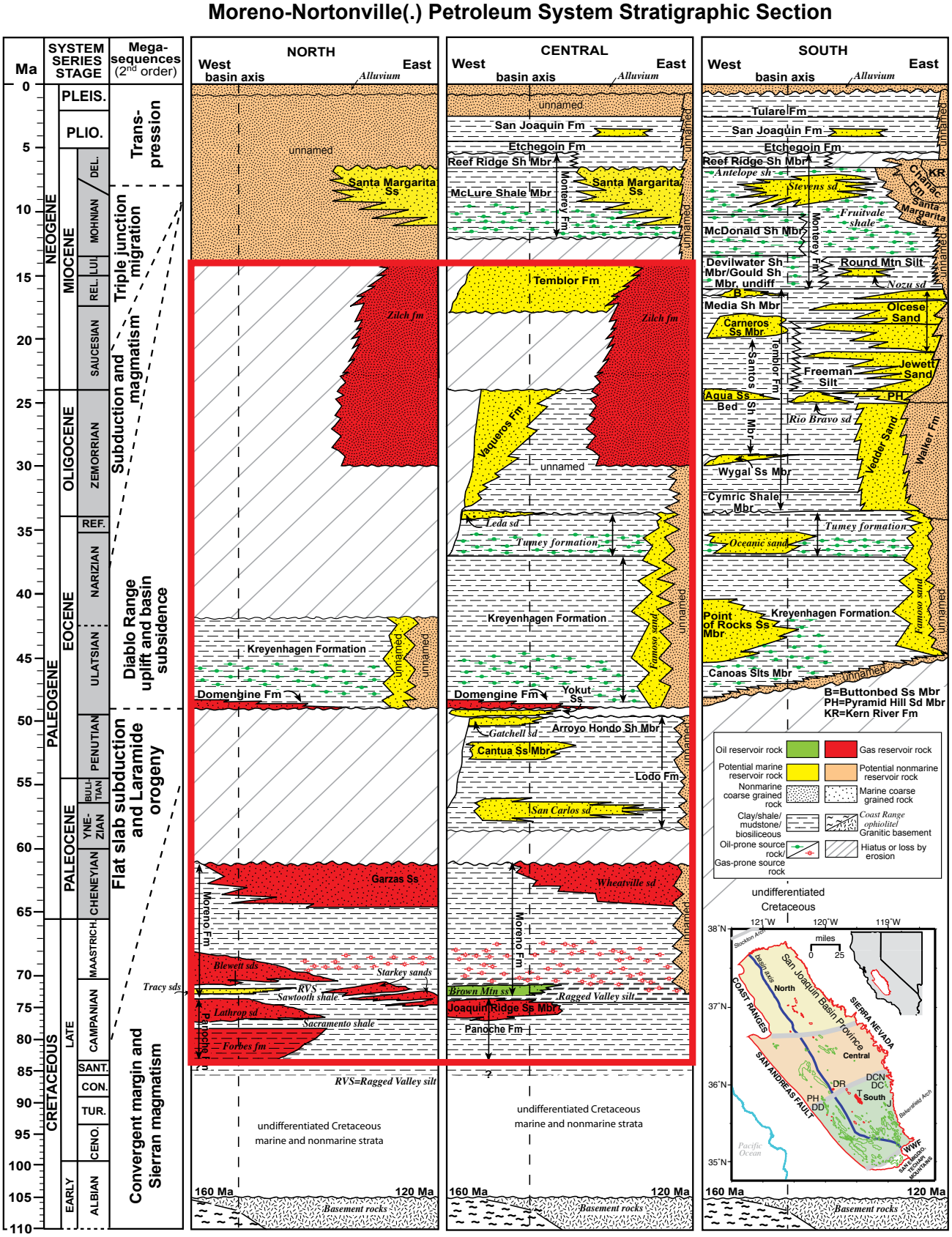

Figure 8.32. Stratigraphic column shown in figure 8.2, but with petroleum source rock and reservoir rocks for the Moreno-Nortonville(.) petroleum system (red outline) on the north and central regions of the stratigraphic section.

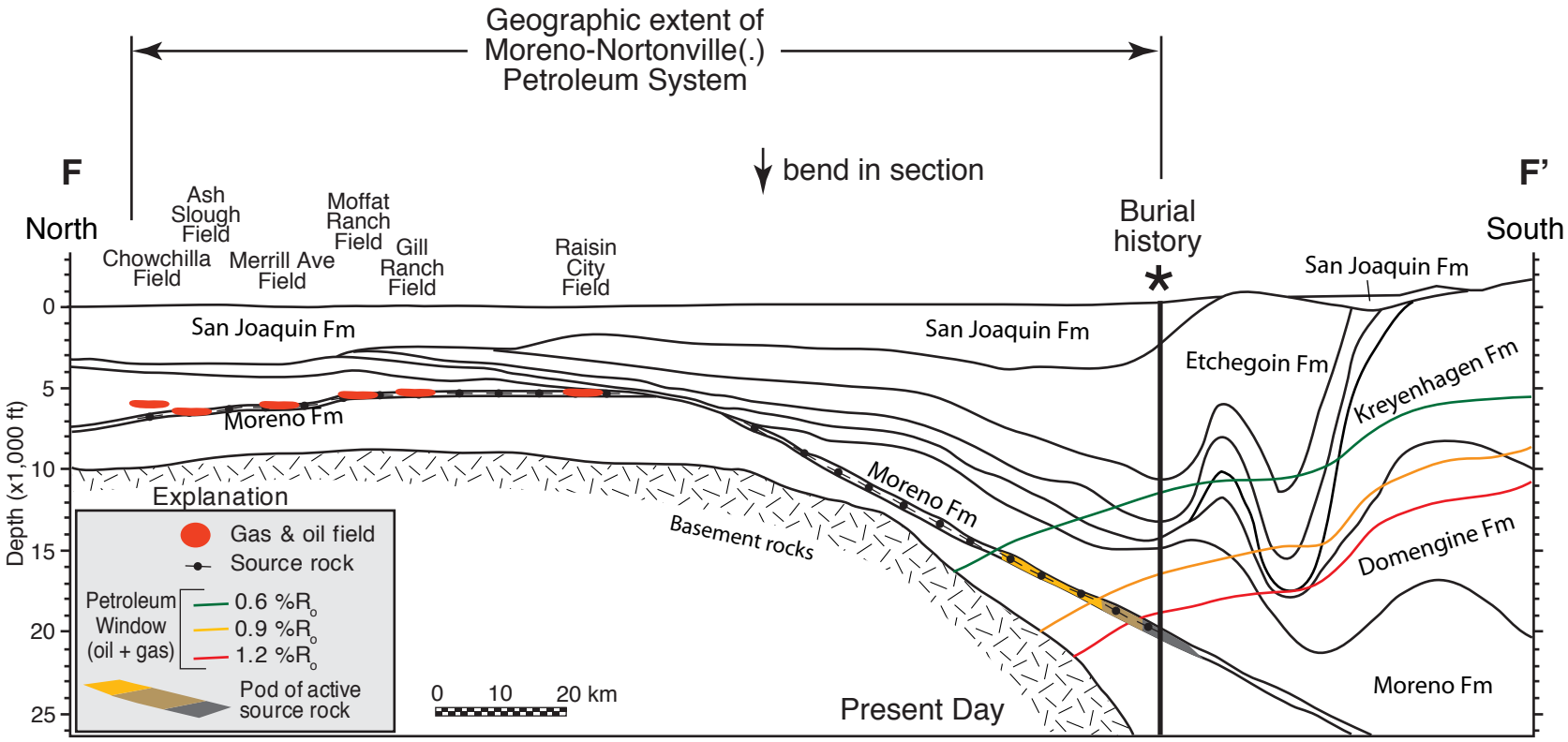

Figure 8.33. Cross section F-F' showing geographic extent of the Moreno-Nortonville(.) petroleum system, the location of the burial history chart (vertical line; location also shown on map in fig. 8.31 and chart shown in fig. 8.34), the Moreno Formation source rock interval (circle-bar pattern), the petroleum window, pod of active source rock (warm shading), and the stratigraphic units that contain the petroleum accumulations in known fields (red blobs). Stratigraphic depth contours and vitrinite reflectance contours ($\%R_o$) are derived from the San Joaquin Basin model of Peters, Magoon, Lampe, and others (this volume, chapter 12). Fm, Formation.

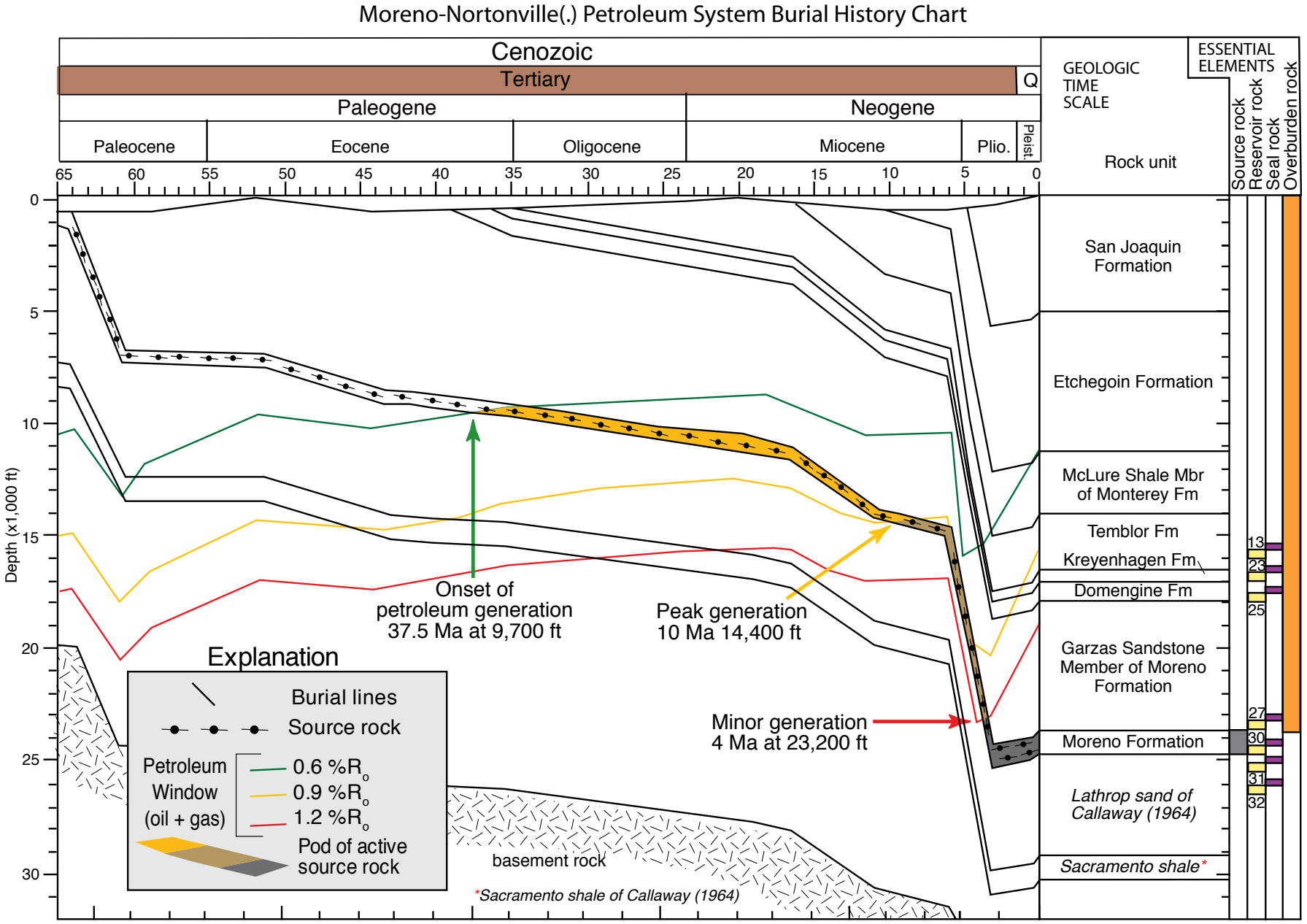

Figure 8.34. Burial history chart for the Moreno-Nortonville(.) petroleum system shows the onset of petroleum generation at 37.5 Ma, peak generation at 10 Ma, and source rock depletion at 4 Ma. The pod of active source rock is indicated by warm shading. The numbers overlying yellow rectangles in the reservoir rock column refer to the reservoir numbers in table 8.10 and appendix 8.2. Fm, Formation; Mbr, Member; Pleist., Pleistocene; Plio., Pliocene; Q, Quaternary; $\%R_o$, percent vitrinite reflectance.

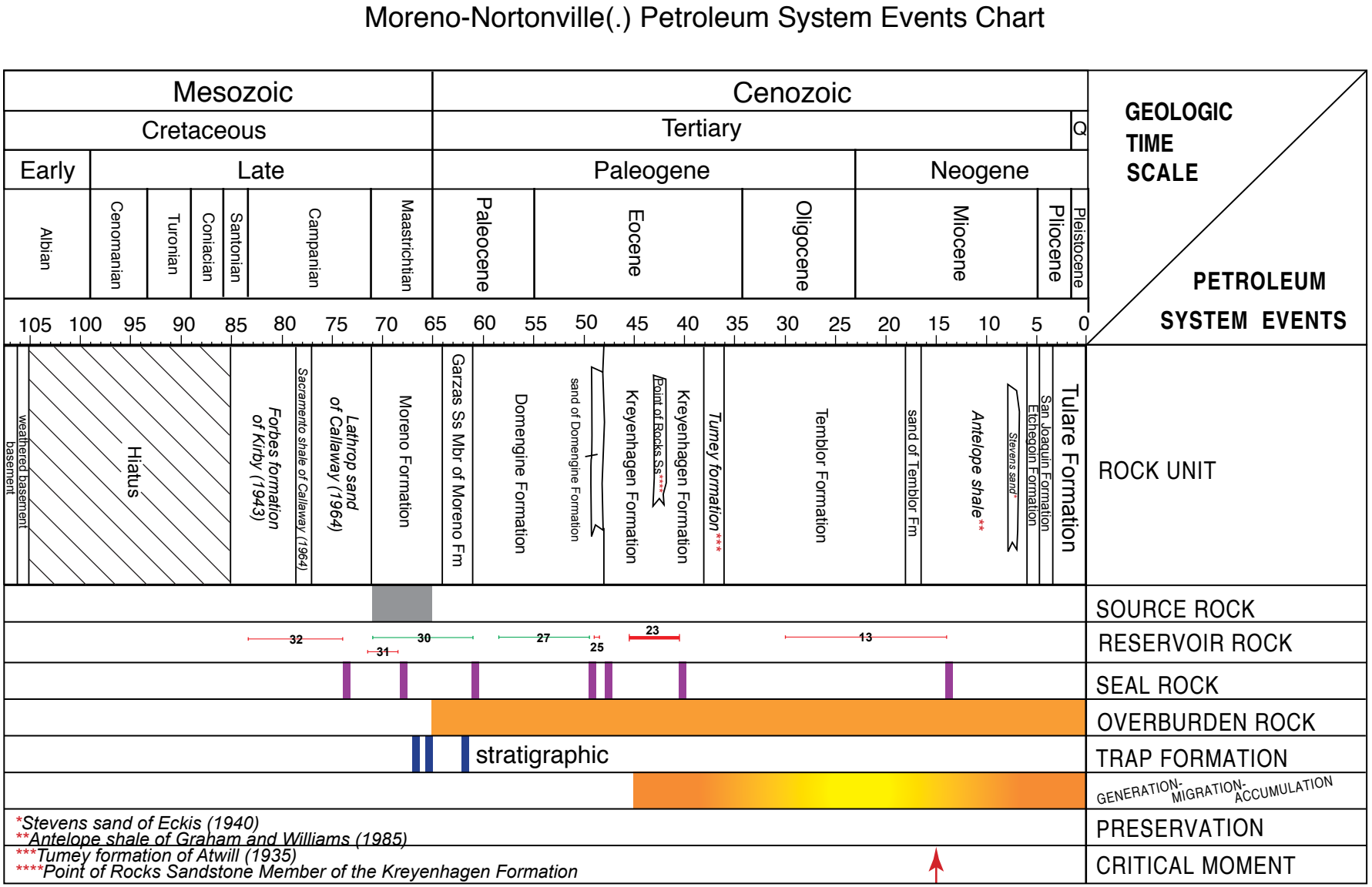

Figure 8.35. Events chart for the Moreno-Nortonville(.) petroleum system shows the timing of the essential elements and processes of this petroleum system. Note that the petroleum migrated after trap development. The numbers on the lines in the reservoir rock item refers to the reservoir numbers in table 8.10; the relative thickness of the lines is proportional to the volume of gas (red) or oil (green) in known pools. Formation names in italics are informal. Fm, Formation; Mbr, Member; Q, Quaternary; Ss, Sandstone.

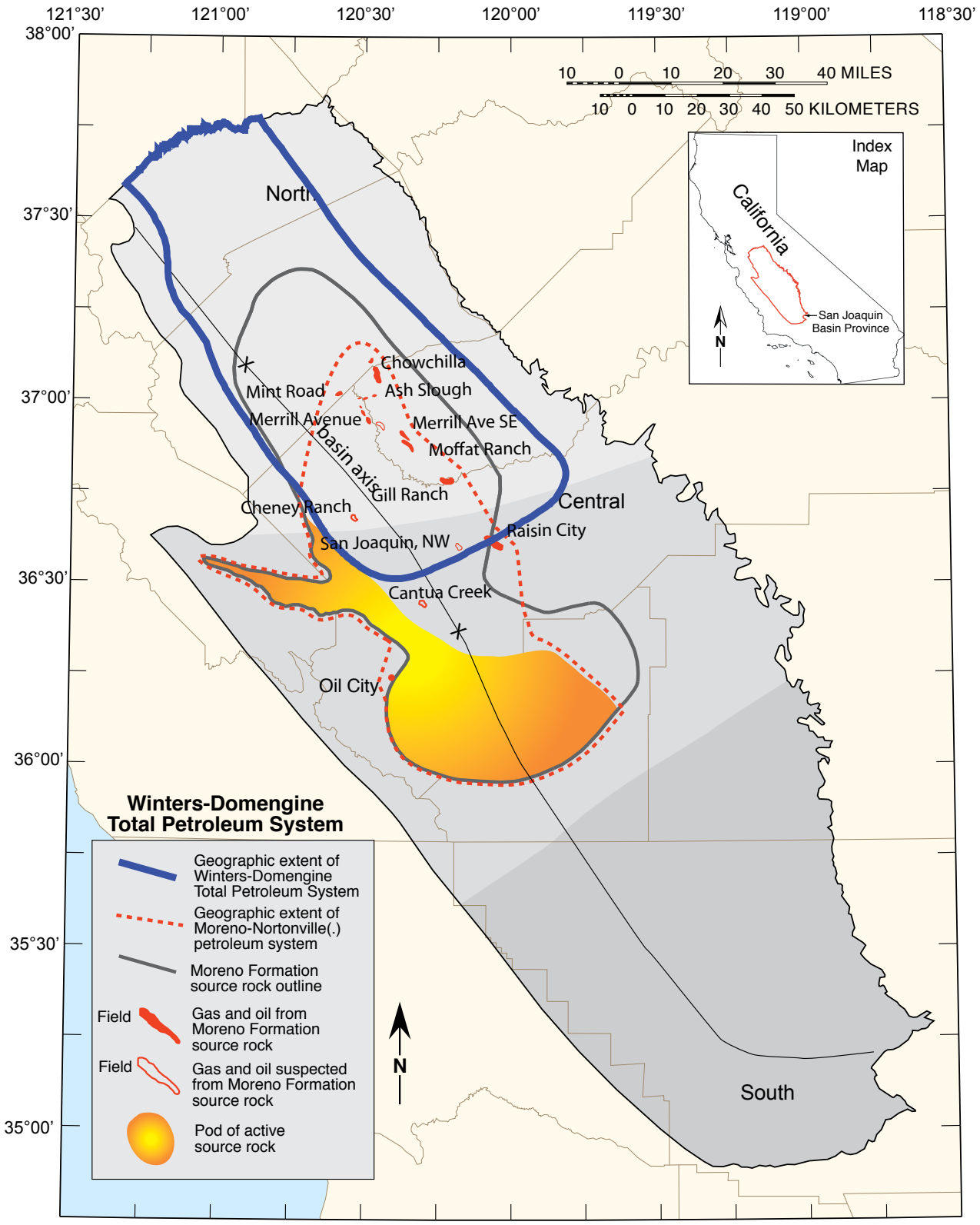

Figure 8.36. The Winters-Domengine Total Petroleum System, which comprises both discovered and undiscovered accumulations, includes a portion of the Moreno-Nortonville(.) petroleum system, which comprises only discovered accumulations (see text for more information). Gas accumulations in this petroleum system are shown in red; solid polygons indicate gas accumulations based on geochemical analysis, whereas outlines indicate suspected accumulations from stratigraphic proximity. Note that warm shading within Moreno-Nortonville(.) petroleum system indicates location of pod of active source rock, which lies entirely outside of the Winters-Domengine Total Petroleum System.

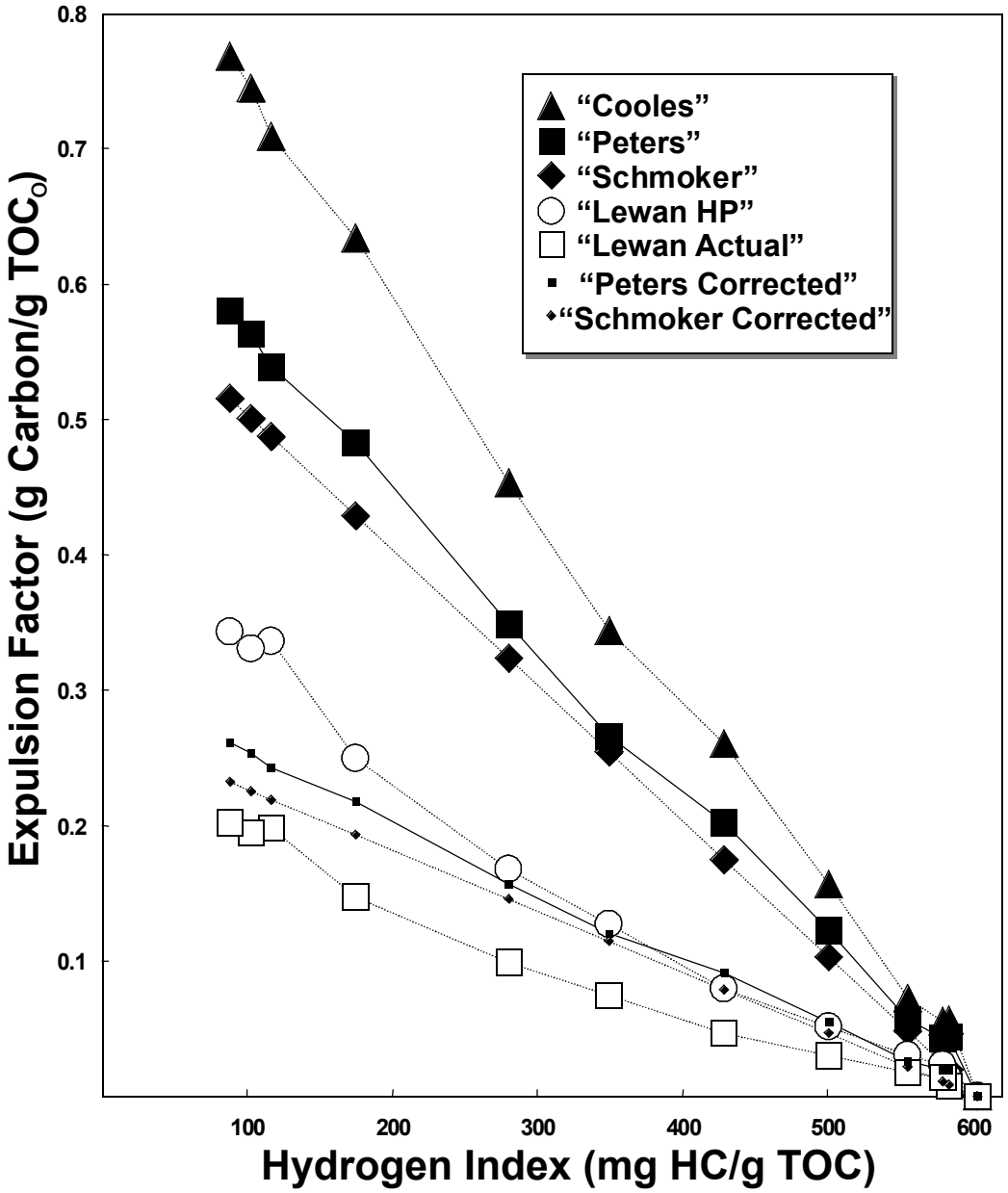

Figure 8.37. Expulsion factors calculated from the Rock-Eval and hydrous pyrolysis methods. The expulsion factor is the ratio of the grams of carbon expelled from a thermally mature source rock as petroleum compared to the original total organic carbon (TOC_o) of immature source rock. mg HC/g TOC, milligrams of hydrocarbon per gram of total organic carbon. Data sources are: "Cooles," Cooles and others (1986); "Peters," Peters and others (2006); "Schmoker," Schmoker (1994); "Lewan HP," Lewan and others (2002). "Lewan Actual," "Peters Corrected," and "Schmoker Corrected" data are explained in text.

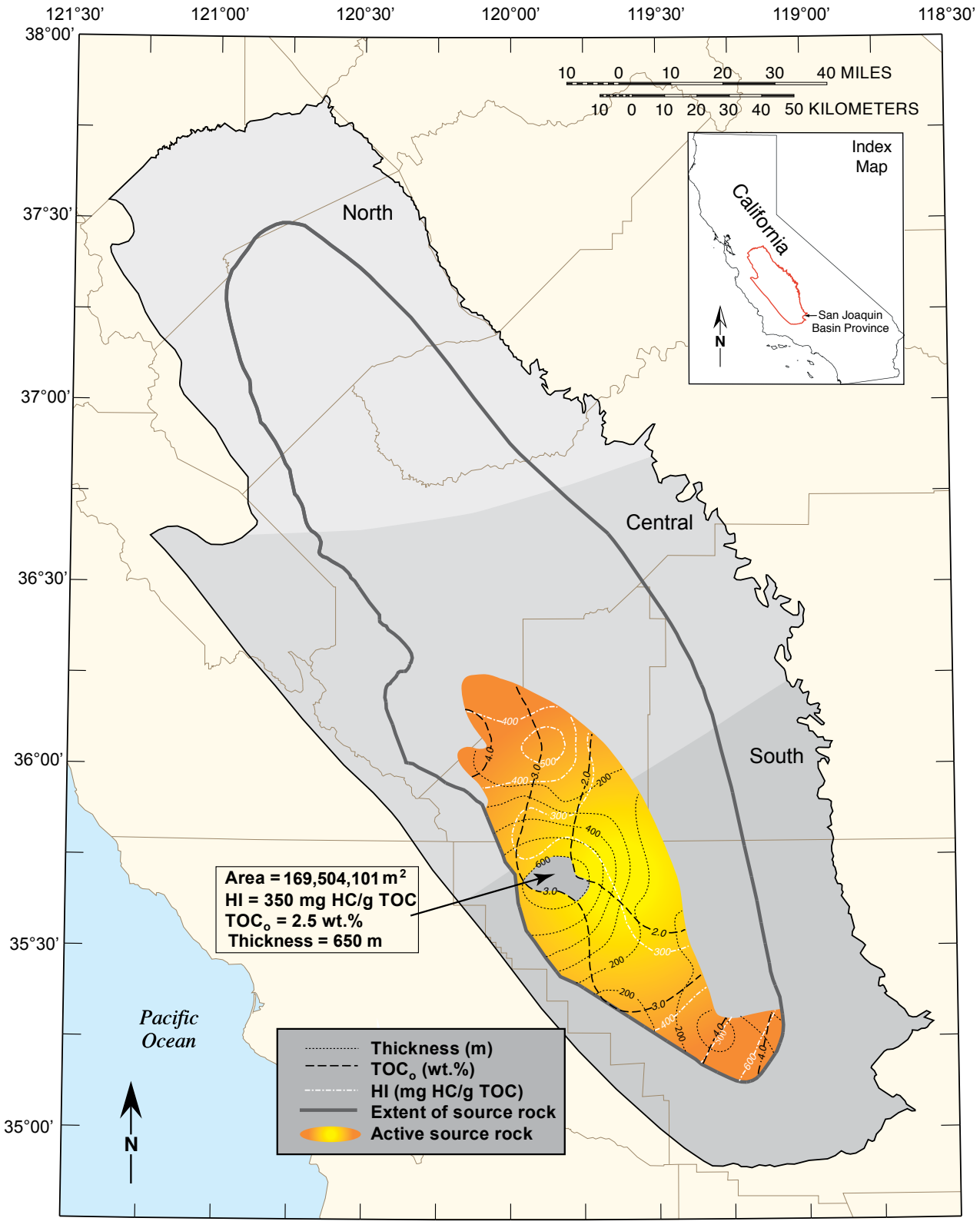

Figure 8.38. Example of a cell used to calculate volumes of generated petroleum from intersection of the hydrogen index (HI), original total organic carbon (TOC_o), and the thickness in meters (m). Example used is the pod of active source rock for the Kreyenhagen Formation. mg HC/g TOC, milligrams of hydrocarbon per gram of total organic carbon.

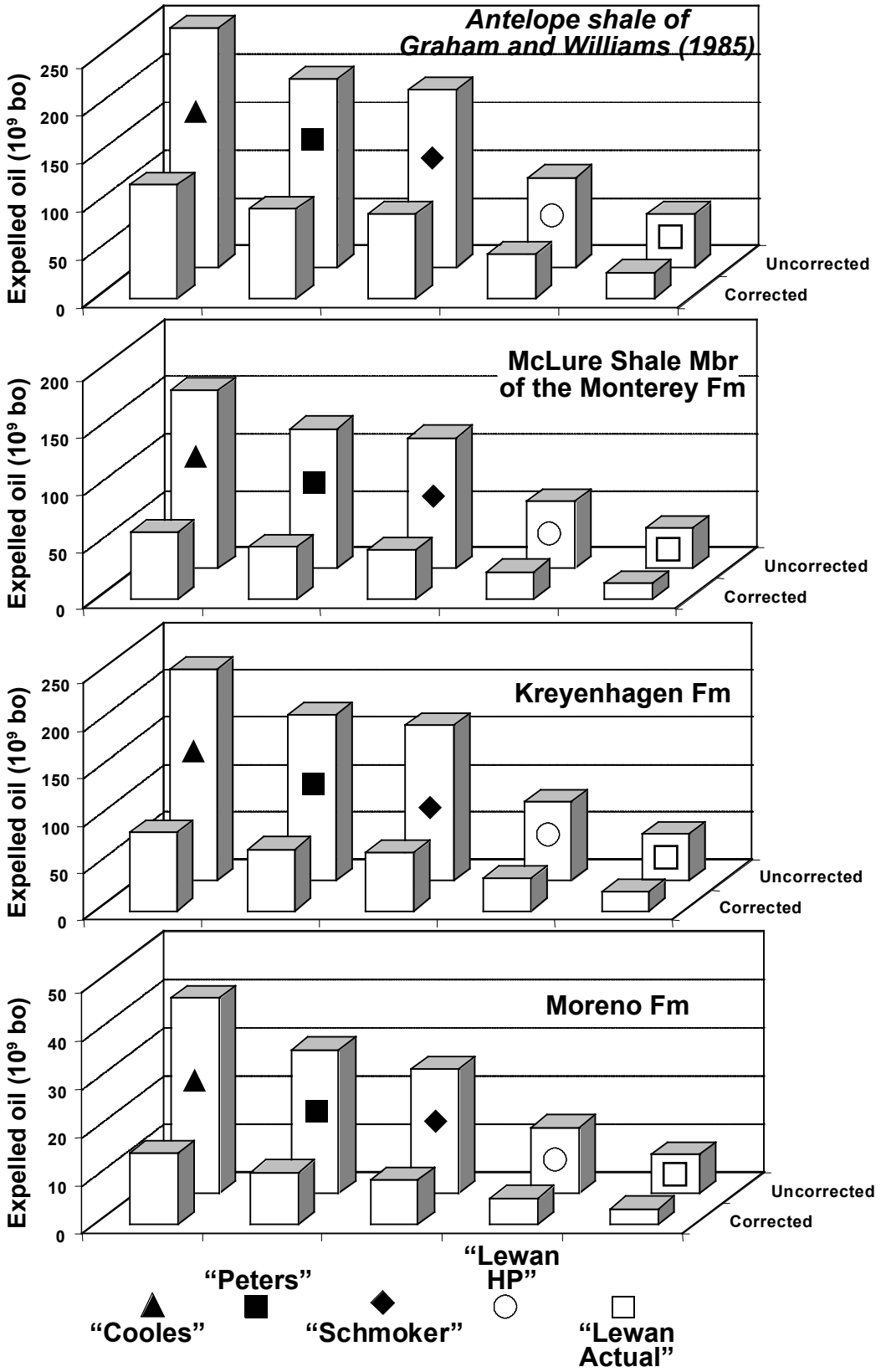

Figure 8.39. Volume of petroleum expelled from four thermally mature source rocks, determined by several methods. Data sources are: "Cooles," Cooles and others (1986); "Peters," Peters and others (2006); "Schmoker," Schmoker (1994); "Lewan HP," Lewan and others (2002); "Lewan Actual" and "Corrected" data refer to method explained in text. Formations in italics are informal. bo, barrel of oil; Fm, Formation; Mbr, Member.

Tables 8.1–8.13

Table 8.1. Relation of the total petroleum system to the petroleum system and assessment unit in the San Joaquin Basin Province.

[Petroleum system naming symbology is from Magoon and Dow (1994) and is explained in text]

Total Petroleum System (TPS)	Petroleum System (PS)						Assessment Unit									
	San Joaquin(?) PS	McLure-Tulare(!) PS	Antelope-Stevens(!) PS	Tumey-Temblor(.) PS	Kreyenhagen-Temblor(!) PS	Moreno-Nortonville(.) PS	Neogene Nonassociated Gas	Southeast Stable Shelf	Lower Bakersfield Arch	Miocene West Side Fold Belt	South of White Wolf Fault	Central Basin Monterey Diagenetic Traps	Eocene West Side Fold Belt	North and East of Eocene West Side Fold Belt	Deep Fractured Pre-Monterey	Northern Nonassociated Gas
Neogene Nonassociated Gas TPS	X						X									
Miocene TPS		X	X					X	X	X	X	X				
Eocene TPS				X	X								X	X		
Eocene-Miocene Composite TPS*		X	X	X	X										X	
Winters-Domengine TPS						X										X

*, no map provided for this TPS.

Table 8.2. Summary of oil and gas volume by petroleum system.

[Data from appendix 8.1 and appendix 8.2. EUR, estimated ultimate recovery; Mbo, thousands of barrels; MMcfg, millions of cubic feet of gas; GOR, gas-to-oil ratio; cfg/bo, cubic feet of gas per barrel of oil; Boe, Barrel of oil equivalent; NA, Not Applicable. World Scale Size, from Klemme (1994), is defined as: "Super Giant" Petroleum System (PS)>100x10^9 Boe; "Giant" PS=20x10^9 to 100x10^9 Boe; "Large" PS=5x10^9 to 20x10^9 Boe; "Significant" PS=0.2x10^9 Boe; and "Small" PS<0.2x10^9 Boe]

Petroleum System	EUR Oil (Mbo)	Oil (%)	EUR Gas (MMcfg)	Gas (%)	GOR (cfg/bo)	EUR Boe (Mbo)	Boe (%)	World Scale Size
San Joaquin(?)	0	0.0	367,897	2.0	NA	61,316	0.3	Small
McLure-Tulare(!)	2,606,588	17.9	1,804,291	9.6	692	2,907,303	16.4	Significant
Antelope-Stevens(!)	9,596,658	65.8	11,286,098	60.1	1,176	11,477,674	64.8	Large
Tumey-Temblor(.)	613,002	4.2	2,117,868	11.3	3,455	965,980	5.5	Significant
Kreyenhagen-Temblor(!)	1,776,710	12.2	3,020,627	16.1	1,700	2,280,148	12.9	Significant
Moreno-Nortonville(.)	158	0.0	182,774	1.0	1,156,797	30,620	0.2	Small
Total	14,593,116	100.0	18,779,555	100.0	1,287	17,723,042	100.0	

Table 8.3. Volume of petroleum on each flank of the San Joaquin Basin Province.

[Data from appendix 8.1 and appendix 8.2. EUR, estimated ultimate recovery; Mbo, thousands of barrels of oil; MMcfg, millions of cubic feet of gas; GOR, gas-to-oil ratio; cfg/bo, cubic feet of gas per barrel of oil; Boe, Barrel of oil equivalent; NA, Not Applicable]

Petroleum System	West Flank				East Flank				Basin
	EUR Oil (Mbo)	EUR Gas (MMcfg)	GOR (cfg/bo)	EUR Boe (Mbo)	EUR Oil (Mbo)	EUR Gas (MMcfg)	GOR (cfg/bo)	EUR Boe (Mbo)	EUR Boe (Mbo)
San Joaquin(?)	0	0	NA	0	0	367,897	NA	61,316	61,316
McLure-Tulare(!)	2,595,069	1,797,540	693	2,894,659	11,519	6,751	586	12,644	2,907,303
Antelope-Stevens(!)	5,718,703	9,103,445	1,592	7,235,944	3,877,955	2,182,653	563	4,241,731	11,477,674
Tumey-Temblor(.)	519,160	2,036,186	3,922	858,524	93,842	81,682	870	107,456	965,980
Kreyenhagen-Temblor(!)	1,752,235	2,944,872	1,681	2,243,047	24,476	75,755	3,095	37,102	2,280,148
Moreno-Nortonville(.)	158	3,859	24,424	801	0	178,915	NA	29,819	30,620
Total	10,585,325	15,885,902	1,501	13,232,975	4,006,792	2,893,652	722	4,489,067	17,723,043

Table 8.4. Trap type by petroleum system on each flank of the San Joaquin Basin Province.

[Data from appendix 8.1 and appendix 8.2. "Stratigraphic" traps include those involving truncation and asphalt; "Structure" traps include those involving anticlines, faults, or a combination. Data from State of California, Department of Conservation, CDOGGR (1998)]

Petroleum System	West Flank			East Flank			Basin			
	Structure	Stratigraphic	Unknown	Structure	Stratigraphic	Unknown	Structure	Stratigraphic	Unknown	Total
San Joaquin(?)	0	1	0	23	4	0	23	5	0	28
McLure-Tulare(!)	70	21	1	6	0	2	76	21	3	100
Antelope-Stevens(!)	97	45	2	84	88	0	181	133	2	316
Tumey-Temblor(.)	12	14	0	10	14	1	22	28	1	51
Kreyenhagen-Temblor(!)	48	40	0	7	3	0	55	43	0	98
Moreno-Nortonville(.)	0	3	0	13	0	5	13	3	5	21
Total	227	124	3	143	109	8	370	233	11	614
Percent	64	35	1	55	42	3	60	38	2	100

Table 8.5. San Joaquin(?) petroleum system gas volume by reservoir rock.

[Data from appendix 8.1 and appendix 8.2. Res No., Reservoir Number corresponding to column 8 in appendix 8.1; Ma, million years ago; EUR Oil, Estimated ultimate recovery of oil; Mbo, thousands of barrels of oil; EUR Gas, Estimated ultimate recovery of gas; MMcfg, millions of cubic feet of gas; GOR, gas-to-oil ratio; cfg/bo, cubic feet of gas per barrel of oil; Boe, Barrel of oil equivalent; NA, Not Applicable. ** and yellow shading highlight the major reservoir rock for the petroleum system]

Res No.	Reservoir Rock Unit	Age Range (Ma)	Number of Pools	EUR Oil (Mbo)	EUR Gas (MMcfg)	GOR (cfg/bo)	Oil (%)	Gas (%)	EUR Boe (Mbo)	Boe (%)
1	Tulare Formation	2.5-0.6	1	0	4,866	NA	0	1.3	811	1.3
3	**San Joaquin Formation****	**4.5-2.5**	**16**	**0**	**309,135**	NA	**0**	**84.0**	**51,523**	**84.0**
4	Etchegoin Formation	5.5-4.5	11	0	53,896	NA	0	14.6	8,983	14.6
		Total	28	0	367,897	NA	0	100.0	61,316	100.0

Table 8.6. McLure-Tulare(!) petroleum system petroleum volumes by reservoir rock.

[Data from appendix 8.1 and appendix 8.2. Res No., Reservoir Number corresponding to column 8 in appendix 8.1; Ma, million years ago; EUR Oil, Estimated ultimate recovery of oil; Mbo, thousands of barrels of oil; EUR Gas, Estimated ultimate recovery of gas; MMcfg, millions of cubic feet of gas; GOR, gas-to-oil ratio; cfg/bo, cubic feet of gas per barrel of oil; Boe, Barrel of oil equivalent; Fm, Formation; NA, Not Applicable; zz-undesignated, unknown reservoir rock. ** and yellow shading highlight the major reservoir rock for the petroleum system; * and green shading highlight source rock interval for the petroleum system]

Res No.	Reservoir Rock Unit	Age Range (Ma)	Number of Pools	EUR Oil (Mbo)	EUR Gas (MMcfg)	GOR (cfg/bo)	Oil (%)	Gas (%)	EUR Boe (Mbo)	Boe (%)
1	**Tulare Formation****	**2.5-0.6**	**12**	**1,343,167**	**838,769**	**624**	**51.5**	**46.5**	**1,482,962**	**51.0**
3	San Joaquin Formation	4.5-2.5	4	20	877	43,850	0.0	0.0	166	0.0
4	Etchegoin Formation	5.5-4.5	12	84,690	141,154	1,667	3.3	7.8	108,216	3.7
5	McLure Shale Member of Monterey Fm*	16.5-5.5	26	102,684	403,026	3,925	3.9	22.3	169,855	5.8
7	Reef Ridge Shale Member of Monterey Fm	6.5-5.5	11	876,004	119,277	136	33.6	6.6	895,884	30.8
10	Stevens sand of Eckis (1940)	9.5-7	5	121,979	164,827	1,351	4.7	9.1	149,450	5.1
12	Temblor Formation	33-14	26	72,495	132,973	1,834	2.8	7.4	94,657	3.3
17	Vedder Sand	33.5-25	3	5,189	3,354	646	0.2	0.2	5,748	0.2
34	zz-undesignated	NA	6	360	34	94	0.0	0.0	366	0.0
		Total	105	2,606,588	1,804,291	693	100.0	100.0	2,907,303	100.0

Table 8.7. Antelope-Stevens(!) petroleum system petroleum volumes by reservoir rock.

[Data from appendix 8.1 and appendix 8.2. Res No., Reservoir Number corresponding to column 8 in appendix 8.1; Ma, million years ago; EUR Oil, Estimated ultimate recovery of oil; Mbo, thousands of barrels of oil; EUR Gas, Estimated ultimate recovery of gas; MMcfg, millions of cubic feet of gas; GOR, gas-to-oil ratio; cfg/bo, cubic feet of gas per barrel of oil; Boe, Barrel of oil equivalent; Fm, Formation; NA, Not Applicable; zz-undesignated, unknown reservoir rock; ?, unknown age. ** and yellow shading highlight the major reservoir rock for the petroleum system; * and green shading highlight source rock interval for the petroleum system]

Res No.	Reservoir Rock Unit	Age Range (Ma)	Number of Pools	EUR Oil (Mbo)	EUR Gas (MMcfg)	GOR (cfg/bo)	Oil (%)	Gas (%)	EUR Boe (Mbo)	Boe (%)
1	Tulare Formation	2.5-0.6	2	20	1	50	0.0	0.0	20	0.0
2	Kern River Formation	8-0.7	4	2,076,205	19,308	9	21.6	0.2	2,079,423	18.1
3	San Joaquin Formation	4.5-2.5	11	2,313	44,191	19,105	0.0	0.4	9,678	0.1
4	Etchegoin Formation	5.5-4.5	34	734,882	459,986	626	7.7	4.1	811,546	7.1
6	Antelope shale of Graham and Williams (1985)*	16.5-5.5	4	9,646	49,800	5,163	0.1	0.4	17,946	0.2
7	Reef Ridge Shale Member of Monterey Fm	6.5-5.5	9	12,928	6,859	531	0.1	0.1	14,071	0.1
8	Chanac Formation	11-6	29	457,593	164,567	360	4.8	1.5	485,021	4.2
9	Santa Margarita Sandstone	11-6.5	25	52,002	15,453	297	0.5	0.1	54,578	0.5
10	**Stevens sand of Eckis (1940)****	**9.5-7**	**92**	**1,849,775**	**9,080,344**	**4,909**	**19.3**	**80.5**	**3,363,166**	**29.3**
11	Round Mountain Silt	16-13.5	12	8,556	5,219	610	0.1	0.0	9,426	0.1
12	Temblor Formation	33-14	10	5,558	165,509	29,779	0.1	1.5	33,143	0.3
14	Olcese Sand	21-16.5	14	25,160	20,948	833	0.3	0.2	28,651	0.2
15	Jewett Sand	25-21	19	442,058	56,505	128	4.6	0.5	451,476	3.9
16	Basalt formation(?)	?	1	1,384	18,742	13,542	0.0	0.2	4,508	0.0
17	Vedder Sand	33.5-25	28	282,779	459,535	1,625	2.9	4.1	359,368	3.1
18	Walker Formation	34-25	2	0	0	0	0.0	0.0	0	0.0
19	Vaqueros Formation	33-24	1	0	0	0	0.0	0.0	0	0.0
28	San Emigdio Formation	?	5	24,347	58,663	2,409	0.3	0.5	34,124	0.3
29	Tejon Formation	?	5	204	2,488	12,196	0.0	0.0	619	0.0
33	schist	NA	4	18	0	0	0.0	0.0	18	0.0
34	zz-undesignated	NA	6	3,611,230	657,980	182	37.6	5.8	3,720,893	32.4
		Total	317	9,596,658	11,286,098	1,176	100.0	100.0	11,477,674	100.0

Table 8.8. Tumey-Temblor(.) petroleum system petroleum volumes by reservoir rock.

[Data from appendix 8.1 and appendix 8.2. Res No., Reservoir Number corresponding to column 8 in appendix 8.1; Ma, million years ago; EUR Oil, Estimated ultimate recovery of oil; Mbo, thousands of barrels of oil; EUR Gas, Estimated ultimate recovery of gas; MMcfg, millions of cubic feet of gas; GOR, gas-to-oil ratio; cfg/bo, cubic feet of gas per barrel of oil; Boe, Barrel of oil equivalent; NA, Not Applicable; zz-undesignated, unknown reservoir rock. ** and yellow shading highlight the major reservoir rock for the petroleum system; * and green shading highlight source rock interval for the petroleum system]

Res No.	Reservoir Rock Unit	Age Range (Ma)	Number of Pools	EUR Oil (Mbo)	EUR Gas (MMcfg)	GOR (cfg/bo)	Oil (%)	Gas (%)	EUR Boe (Mbo)	Boe (%)
9	Santa Margarita Sandstone	11-6.5	3	3,352	7	2	0.5	0.0	3,353	0.3
10	Stevens sand of Eckis (1940)	9.5-7	1	0	0	0	0.0	0.0	0	0.0
12	**Temblor Formation****	**33-14**	**32**	**485,214**	**1,976,597**	**4,074**	**79.2**	**93.3**	**814,647**	**84.3**
13	Zilch formation of Loken (1959)	30-14	9	78,989	62,500	791	12.9	3.0	89,406	9.3
15	Jewett Sand	25-21	1	2	0	0	0.0	0.0	2	0.0
17	Vedder Sand	33.5-25	1	4,005	5	1	0.7	0.0	4,006	0.4
18	Walker Formation	25-34	1	71	0	0	0.0	0.0	71	0.0
19	Vaqueros Formation	33-24	3	27,339	49,114	1,796	4.5	2.3	35,525	3.7
20	Leda sand of Sullivan (1962)	34-33	2	10,240	22,758	2,222	1.7	1.1	14,033	1.5
21	Tumey formation of Atwill (1935)*	37-33.5	4	173	889	5,139	0.0	0.0	321	0.0
34	zz-undesignated	NA	1	3,617	5,998	1,658	0.6	0.3	4,617	0.5
		Total	58	613,002	2,117,868	3,455	100.0	100.0	965,980	100.0

Table 8.9. Kreyenhagen-Temblor(!) petroleum system petroleum volumes by reservoir rock.

[Data from appendix 8.1 and appendix 8.2. Res No., Reservoir Number corresponding to column 8 in appendix 8.1; Ma, million years ago; EUR Oil, Estimated ultimate recovery of oil; Mbo, thousands of barrels of oil; EUR Gas, Estimated ultimate recovery of gas; MMcfg, millions of cubic feet of gas; GOR, gas-to-oil ratio; cfg/bo, cubic feet of gas per barrel of oil; Boe, Barrel of oil equivalent; Ss, Sandstone; Mbr, Member; Fm, Formation; NA, Not Applicable; zz-undesignated, unknown reservoir rock. ** and yellow shading highlight the major reservoir rock for the petroleum system; * and green shading highlight source rock interval for the petroleum system]

Res No.	Reservoir Rock Unit	Age Range (Ma)	Number of Pools	EUR Oil (Mbo)	EUR Gas (MMcfg)	GOR (cfg/bo)	Oil (%)	Gas (%)	EUR Boe (Mbo)	Boe (%)
4	Etchegoin Formation	5.5-4.5	2	3	403	134,333	0.0	0.0	70	**0.0**
10	Stevens sand of Eckis (1940)	9.5-7	2	0	586	NA	0.0	0.0	98	0.0
12	**Temblor Formation****	**33-14**	**23**	**1,069,169**	**906,423**	**848**	**60.2**	**30.0**	**1,220,240**	**53.5**
13	Zilch formation of Loken (1959)	30-14	2	784	1,247	1,591	0.0	0.0	992	0.0
19	Vaqueros Formation	33-24	1	2	12	6,000	0.0	0.0	4	0.0
20	Leda sand of Sullivan (1962)	34-33	2	23,702	32,704	1,380	1.3	1.1	29,153	1.3
21	Tumey formation of Atwill (1935)	37-33.5	8	31,886	94,172	2,953	1.8	3.1	47,581	2.1
22	Point of Rocks Ss Mbr, Kreyenhagen Fm	45.5-40.5	26	15,069	82,994	5,508	0.8	2.7	28,901	1.3
24	Kreyenhagen Formation*	48.5-37	4	761	848	1,114	0.0	0.0	902	0.0
25	Domengine Formation	49-48.5	6	23,555	74,105	3,146	1.3	2.5	35,906	1.6
26	Yokut Sandstone	49.5-49	3	5,351	5,622	1,051	0.3	0.2	6,288	0.3
27	Lodo Formation	58.5-49.5	16	556,719	1,661,893	2,985	31.3	55.0	833,701	36.6
30	Moreno Formation	71-61	1	0	0	0	0.0	0.0	0	0.0
32	Panoche Formation	83.5-74	1	0	8	NA	0.0	0.0	1	0.0
34	zz-undesignated	NA	2	49,710	159,610	3,211	2.8	5.3	76,312	3.3
		Total	99	1,776,710	3,020,627	1,700	100.0	100.0	2,280,149	100.0

Table 8.10. Moreno-Nortonville(.) petroleum system gas and oil volumes by reservoir rock.

[Data from appendix 8.1 and appendix 8.2. Res No., Reservoir Number corresponding to column 8 in appendix 8.1; Ma, million years ago; EUR Oil, Estimated ultimate recovery of oil; Mbo, thousands of barrels of oil; EUR Gas, Estimated ultimate recovery of gas; MMcfg, millions of cubic feet of gas; GOR, gas-to-oil ratio; cfg/bo, cubic feet of gas per barrel of oil; Boe, Barrel of oil equivalent; NA, Not Applicable. ** and yellow shading highlight the major reservoir rock for the petroleum system; * and pink shading highlight source rock interval for the petroleum system]

Res No.	Reservoir Rock Unit	Age Range (Ma)	Number of Pools	EUR Oil (Mbo)	EUR Gas (MMcfg)	GOR (cfg/bo)	Oil (%)	Gas (%)	EUR Boe (Mbo)	Boe (%)
13	Zilch formation of Loken (1959)	30-14	3	0	5,968	NA	0.0	3.3	995	3.2
23	**Nortonville sand of Frame (1950)****	**45.5-40.5**	**4**	**0**	**74,067**	**NA**	**0.0**	**40.5**	**12,345**	**40.3**
25	Domengine Formation	49-48.5	2	0	2435	NA	0.0	1.3	406	1.3
27	Lodo Formation	58.5-49.5	1	40	801	20,025	25.3	0.4	174	0.6
30	Moreno Formation*	71-61	4	118	4742	40,186	74.7	2.6	908	3.0
31	Blewett sands of Hoffman (1964)	71.5-68.5	4	0	34905	NA	0.0	19.1	5,818	19.0
32	Panoche Formation	83.5-74	3	0	59,856	NA	0.0	32.7	9,976	32.6
		Total	21	158	182,774	1,156,797	100.0	100.0	30620	100.0

Table 8.11. Oil samples analyzed from surface seeps and wells.

[Figure refers to map in chapter where well or seep is shown; Map Abb., abbreviation of well or seep on that particular map; Sec-Twn-Rng, location of sample in notation of public land survey system; Fm, Formation; fm, formation; Mbr, Member. Reservoir rock and source rock names are modified to comply with USGS geologic name standards. "Outlier" in source rock column refers to classification scheme of Lillis and Magoon (this volume, chapter 9). Shading in Petroleum System column corresponds to colors used in same column of appendix 8.1]

Figure	Map Abb.	Seep or Well	Well or Seep Name	Sec-Twn-Rng	Longitude	Latitude	Depth	Reservoir Rock[1]	Source Rock[2]	Age	Sample No.[3]	Petroleum System
8.9	1	well	EKHO 1	3-27S-22E	-119.58714	35.60267	~17000	None given	Antelope shale	Miocene	92	McLure-Tulare(!)
8.9	2	well	Great Basins 31X-10	10-27S-22E	-119.59196	35.59988	17248-17728	None given	Antelope shale-outlier	Miocene	117	McLure-Tulare(!)
8.9	3	well	Gene Reid 53-36	36-28S-18E	-119.99065	35.44851	1674-1692	None given	Antelope shale	Miocene	250, 251	McLure-Tulare(!)
8.9	4	well	SMUG 528-7X	7-29S-22E	-119.64833	35.41397	10412-10852	McLure Shale Mbr, Devilwater Shale Mbr, & Gould Shale Mbr of Monterey Fm	Antelope shale	Miocene	119	McLure-Tulare(!)
8.9	5	well	SEC 4Z 385X	4-30S-22E	-119.60703	35.34586	8750-8995	None given	Antelope shale	Miocene	118	McLure-Tulare(!)
8.14	A	seep	Midway-Sunset 4-21A	20-11N-23W	-119.35487	35.03143	0	None given	Antelope shale	Miocene	91	Antelope-Stevens(!)
8.20	1	well	Tully 1	21-18S-10E	-120.89189	36.34791	1670-1678	None given	Tumey fm-outlier	Eocene	252	Tumey-Temblor(.)
8.20	2	well	Coalinga 45-27	27-19S-15E	-120.33549	36.24122	1122-1724	Temblor Formation	Tumey fm-outlier	Eocene or Miocene	24	Tumey-Temblor(.)
8.20	3	well	Berkeley 1	6-26S-21E	-119.74449	35.69133	19370-19698	Gibson sand (Temblor Fm)	Tumey fm or Antelope shale	Eocene or Miocene	67	Tumey-Temblor(.)
8.20	4	well	BLC 2 (DST 3)	5-27S-20E	-119.8443	35.60342	~12200	Gibson sand (Temblor Fm)	Tumey fm	Eocene	255	Tumey-Temblor(.)
8.20	5	well	BLC 2 (DST 3)	5-27S-20E	-119.8443	35.60342	~11,400	Temblor Formation	Tumey fm	Eocene	256	Tumey-Temblor(.)
8.20	5	well	934-29R (DST 4)	29-30S-23E	-119.52946	35.29009	17400-17500	Oceanic sand (Tumey fm)	Tumey fm-outlier	Eocene	155	Tumey-Temblor(.)
8.20	6	well	Frank Short Melinda 2	22-32S-22E	-119.59417	35.12083	1598-1604	Temblor Formation	Tumey fm	Eocene	254	Tumey-Temblor(.)
8.25	A	seep	Coalinga	20-19S-15E	-120.36361	36.25775	0	Lodo Formation (?)	Kreyenhagen Fm	Eocene	27	Kreyenhagen-Temblor(!)
8.25	B	seep	Big Tar Canyon	18-23S-16E	-120.16646	35.93245	0	Kreyenhagen Formation	Kreyenhagen Fm	Eocene	129, 130, 131, 132	Kreyenhagen-Temblor(!)
8.25	1	well	Coalinga Rock	20-19S-15E	-120.36785	36.2576	shallow	Kreyenhagen Formation (?)	Kreyenhagen Fm	Eocene	23	Kreyenhagen-Temblor(!)
8.25	2	well	BLC 2 (DST 1)	5-27S-20E	-119.8443	35.60342	~13000	Kreyenhagen Formation	Kreyenhagen Fm	Eocene	253	Kreyenhagen-Temblor(!)
8.25	3	well	Paloma 28X-2	2-32S-26E	-119.16267	35.16687	~18300	Carneros Sandstone Mbr of Temblor Fm	Kreyenhagen Fm	Eocene	79	Kreyenhagen-Temblor(!)

[1]Informally described reservoir rocks are: Gibson sand of Williams (1938), Tumey formation of Atwill (1935), and Oceanic sand of McMasters (1948).
[2]Informally described source rocks are: Antelope shale of Graham and Williams (1985), and Tumey formation of Atwill (1935).
[3]Samples are provided in Lillis and Magoon (this volume, chapter 9).

Table 8.12. Averaged Rock-Eval pyrolysis/total organic carbon data for core and drill cuttings samples of hydrocarbon source rocks in the San Joaquin Basin Province.

[Well number refers to labeled red triangles in fig. 11.3 of Peters, Magoon, Valin, and Lillis (this volume, chapter 11); table data come from table 11.5 of that chapter. TOC_o, original total organic carbon of immature source rock; HI_o, original hydrogen index; mg HC/g TOC, milligrams of hydrocarbon per gram of total organic carbon]

Well Number	Well Name	Longitude	Latitude	Number of analyses	TOC_o (weight %)	HI_o (mg HC/g TOC)
McLure Shale Member of Monterey Formation						
4	Furtado 55-36	-119.85807	36.23955	2	2.27	126
9	Van Sicklen 45	-119.66325	35.53545	4	4.57	455
10	Mobil (GP) 2-110	-119.7515	35.65538	1	4.19	347
13	Univ. Consolidated 44	-119.73196	35.62241	3	5.64	314
20	Monte Christo 163	-119.71218	35.58257	8	4.36	500
21	Gulf 142 (4-16)	-119.7164	35.58427	2	5.24	597
23	Chevron 9-3X	-119.71512	35.59923	4	4.29	428
24	Arco 801	-119.70753	35.56033	2	2.56	413
25	Arco 901	-119.72554	35.57124	2	1.86	689
28	Chevron 678X	-119.82556	36.0218	3	0.71	111
29	J.G. Boswell 31-1	-119.73999	36.06124	2	1.95	148
31	Chevron Morris 1	-119.44473	35.79634	45	3.16	303
44	Chevron 7-26Q	-120.00212	35.98059	20	2.11	181
55	Camp West Lowe 1	-119.10948	35.41884	18	2.62	269
56	Sheep Springs 1	-119.71045	35.33025	40	2.72	389
59	Hellman 13-1X	-119.89165	35.78794	18	2.55	356
61	Richardson 46	-119.75656	35.41906	7	2.78	413
63	Tenneco 73-12	-119.43928	35.59627	24	3.13	351
65	Howe 1-2	-119.88098	35.95074	22	1.97	317
66	Malley 1	-120.00877	35.82034	15	2.22	263
67	Haven 44X-6	-119.95057	36.22078	11	1.92	205
68	Geyer 1	-120.09526	35.84787	12	1.7	153
74	Shafter C-1	-119.29611	35.54405	7	3.49	301
75	Shafter B-1	-119.26759	35.52228	8	3.3	236
76	Kernco 11-34	-119.27669	35.45534	20	2.55	314
Antelope shale of Graham and Williams (1985)						
12	Arco KCLD-26-29	-119.04277	35.00983	3	4.78	265
22	Getty 9D-523	-119.40683	35.16054	8	3.55	407
45	Midway Sunset 801	-119.58421	35.27017	166	3.46	468
57	Union Avenue 1	-119.01176	35.34403	21	2.68	322
77	N. Coles Levee 26-29	-119.32004	35.28647	15	3.06	306
78	Paloma 81X-3	-119.16403	35.17935	4	2.39	303
79	Santiago A 72-30	-119.26237	35.01537	11	3.37	506
80	Pioneer 1	-119.25645	34.99837	13	3.87	364
81	Maricopa Flats 47X-7	-119.27071	35.049	18	2.7	464
82	Texaco 21X-13	-119.18495	35.04625	7	2.67	391
83	Channel 38X-6	-119.1651	35.06332	13	2.44	350
84	Tenneco 27X-26	-119.09727	35.0927	9	1.6	413
85	Gen. American 81-4K	-119.33165	35.07536	16	2.74	347
88	Bear Valley 1	-119.56737	35.28079	79	1.86	429
89	Fairfield Fee D48-38	-119.56285	35.26828	68	2.33	357
90	White Wolf 205-5	-119.15196	34.98685	75	4.18	480
91	653Z-26B	-119.47267	35.19515	98	2.24	295

Table 8.12. Averaged Rock-Eval pyrolysis/total organic carbon data for core and drill cuttings samples of hydrocarbon source rocks in the San Joaquin Basin Province—Continued.

[Well number refers to labeled red triangles in fig. 11.3 of Peters, Magoon, Valin, and Lillis (this volume, chapter 11); table data come from table 11.5 of that chapter. TOC_o, original total organic carbon of immature source rock; HI_o, original hydrogen index; mg HC/g TOC, milligrams of hydrocarbon per gram of total organic carbon]

Well Number	Well Name	Longitude	Latitude	Number of analyses	TOC_o (weight %)	HI_o (mg HC/g TOC)
Kreyenhagen Formation						
1	Chevron 4-18J	-120.18022	36.10254	9	4.38	446
3	Hanneman 83-30	-120.1512	36.59958	2	2.96	53
6	Aqueduct 1-14	-119.98513	36.18994	17	3.11	297
26	West. Cont. BLC #2	-119.8443	35.60342	17	3.71	388
27	Chevron 73-30V	-119.95322	35.90116	30	3.06	311
29	J.G. Boswell 31-1	-119.73999	36.06124	18	2.02	277
30	Conoco W. Lake 36-1	-119.87068	36.05965	4	2.84	578
34	Union Bravo 1	-120.30113	36.58513	1	4.11	451
39	Ferry 1-2	-120.09575	36.38788	4	3.54	505
43	61X-17A	-120.36112	36.28139	2	1.37	25
46	Cheney Ranch 1	-120.58321	36.68315	10	2.56	247
58	KCL G-1	-119.1395	35.36286	3	4.7	552
60	Beer 5	-119.91242	35.65666	21	2.91	327
67	Haven 44X-6	-119.95057	36.22078	16	2.73	341
63	Tenneco 73-12	-119.43928	35.59627	5	1.58	224
86	Jacalitos 67	-120.36621	36.09563	9	2.79	342
87	Williamson 33	-119.78958	35.68265	10	2.03	345
Moreno Formation						
8	Bravo Oil 1-35	-120.19988	36.23955	27	2.95	342
34	Union Bravo 1	-120.30113	36.58513	4	1.57	140
36	Shell 363X	-120.32388	36.27841	1	2.8	304
39	Ferry 1-2	-120.09575	36.38788	3	2.43	382
46	Cheney Ranch 1	-120.58321	36.68315	191	1.99	169
47	Magnet Fearon 2	-120.38205	36.18628	16	3.69	270
48	Helm Unit 31-34	-120.11	36.5012	7	0.7	114
49	Russ Hewitt 1	-120.76998	36.85642	29	1.99	74
50	Ponte 1	-120.16376	36.77382	4	1.17	23
51	Lillis 85-36	-120.60589	36.58309	14	2.61	259
52	Henderson 66-22	-120.31988	36.60749	2	1.02	99
53	Cerini 1	-119.90267	36.47505	6	1.84	121
67	Haven 44X-6	-119.95057	36.22078	9	2	225
73	Dos Palos corehole 3	-120.68403	36.64375	13	2.08	143

Table 8.13. Volumes of petroleum (in units of 10^9 barrels of oil) within the San Joaquin Basin Province predicted using equation 8.1 compared to in-place petroleum assigned to the corrected volume for each source rock.

[EUR Boe, Estimated ultimate recovery of barrel of oil equivalent; GAE, generation-accumulation efficiency; HP, Hydrous Pyrolysis. See text for discussion of "HP" versus "Actual" results. *Corrected volumes of expelled petroleum determined by the Rock-Eval pyrolysis method assume that (1) at least 2.0 weight percent TOC is required for expulsion (Lewan, 1987; Peters and others, 2005), and that (2) 55 weight percent of the pyrolyzate consists of NSO-compounds (Behar and others, 1997) swept out of the rock by carrier gas that would otherwise cross-link to form pyrobitumen and thus not contribute to expelled petroleum. Volumes of expelled petroleum determined by hydrous pyrolysis were corrected using a factor of 0.5 as recommended by Lewan and others (1995; 2002) and discussed in the text]

Source Rock	Rock-Eval Pyrolysis Method			Hydrous Pyrolysis Method		EUR Boe (10^9)	In-place Boe (10^9)
	Cooles and others (1986)	Peters and others (2006)	Schmoker (1994)	Lewan and others (2002) HP	Lewan and others (2002) Actual	Magoon and others (this study)	Magoon and others (this study)
McLure Shale Member of Monterey Formation pod of active source rock							
Uncorrected	157	123	115	59	35	2.91	-
Corrected*	58	46	43	24	14		
GAE (%)	20.0	25.2	27.0	48.3	82.6	-	11.6
Antelope shale of Graham and Williams (1985) pod of active source rock							
Uncorrected	250	196	185	94	55	11.48	-
Corrected*	123	96	91	47	28		
GAE (%)	37.3	47.8	50.4	97.7	163.9(?)	-	45.9
Kreyenhagen Formation pod of active source rock							
Uncorrected	223	175	164	83	49	2.28	-
Corrected*	82	65	61	34	20		
GAE (%)	11.1	14.0	14.9	26.8	45.5	-	9.1
Moreno Formation pod of active source rock							
Uncorrected	40	30	26	14	8.1	0.031	-
Corrected*	15	11	9.2	5.5	3.3		
GAE (%)	0.8	1.1	1.3	2.3	3.8	-	0.124